TÉCNICO LISBOA

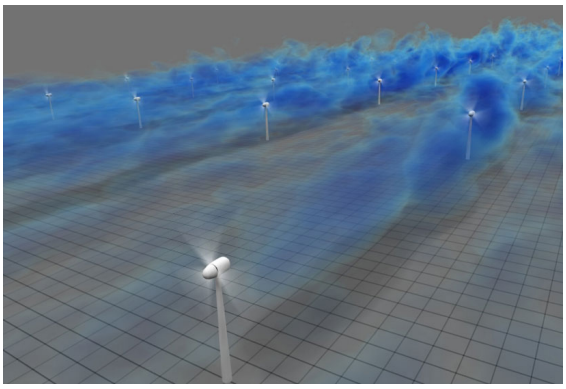

Empirical modelling of flow through a wind farm for comparison with wake model

Davide Liviero

Thesis to obtain the Master of Science Degree in

Energy Engineering and Management

Supervisors: Prof. Gareth Erfort
Prof. Gil Domingos Marques

Examination Committee

Chairperson: Prof. José Alberto Caiado Falcão de Campos
Supervisor: Prof. Gil Domingos Marques
Member of the Committee: Prof. Ricardo Balbino dos Santos Pereira

September 2017

Dedicated to my late grandfather, who instilled in me the passion for engineering.

Acknowledgments

First and foremost, I would like to thank my two supervisors Gareth Erfort and Gil Domingos Marques for helping me throughout the whole project any time I needed. Thanks to their help I was able to conclude his work that at the beginning I doubted I could.

Special thanks also to Louis Jestin for helping me in finding the thesis topic and to the wind farm management team for allowing me to use their measurement data.

Many thanks also to Duarte de Mesquita e Sousa and César Valderrama for being always available to help, especially (but not only) concerning the software licences.

I also want to thank Prof. Pedro Sebastião for his willingness to help in the last part of the thesis.

I would like also to thank my family and friends for the moral support during these last years of university.

A special thanks to my coursemates from both the Bachelor and the Master because of their constant help and because they had to undergo similar work loads.

Last but not least, I would like to thank Robin Gracie and João Santos and their respective teams for helping me free my mind with their trainings.

Resumo

O objetivo desta tese de mestrado é criar um modelo, baseado em dados reais, capaz de prever a potência de saída de um parque eólico. Inicialmente, foi adoptada uma metodologia baseada em conceitos físicos, usando modelos de modelação do efeito esteira disponíveis na literatura. Os resultados obtidos não foram aceitáveis. Foram estudadas as razões da falha deste modelo na produção de resultados fiáveis e apresentam-se sugestões de possíveis melhorias para trabalhos futuros. A criação de um segundo modelo, o modelo empírico, é então descrita. Os novos resultados são apresentados e analisados de modo a compreender as suas vantagens e inconvenientes e sugere-se aonde atuar de modo a obter-se um modelo mais preciso. Como passo seguinte, sugere-se um número de equações capazes de prever a potência de saída de uma turbine isolada baseado na velocidade e direção do vento. Os resultados desta abordagem são depois discutidos. Finalmente, numa tentativa de diminuição do erro de predição, apresenta-se uma terceira abordagem que permite determinar diretamente a potência de saída usando apenas a velocidade e direção do vento. Este modelo é comparado com o modelo empírico.

Palavras-chave: Modelo para efeito de esteira, parque eólico, previsão, energia eólica, modelo empírico.

Abstract

The goal of this Master's thesis project is to create a model that is able to predict the power output of the wind farm based on actual measurements. Initially, a physical approach was used by studying and implementing wake models available in literature. Then, its results and reasons why it failed to produce an accurate prediction are studied, trying to suggest possible improvements for future work on similar topics. Afterwards, the creation of a second model based on empirical data is described. The new results are subsequently uncovered and described in order to understand its pros and cons and suggest where to act in order to possibly obtain a more accurate model. As a next step, a number of approaches for the creation of a set of equations able to predict the power output of a single turbine using only wind speed and direction as inputs are suggested. The results of each single approach are then exposed. Finally, a third model predicting directly the power output based on the wind speed and direction is formulated in an attempt to decrease the error in the prediction. The outcome of this last model is finally shown and compared with the results from the empirical one.

Keywords: wake model, wind farm, prediction, wind energy, empirical model

Contents

List of Tables

List of Figures

Nomenclature

Greek symbols

σ	Standard deviation
ε	Turbulence

Roman symbols

Δu_{acc}	Accumulated velocity difference
A	Rotor area
a	Axial induction factor
C_p	Power coefficient
C_T	Thrust coefficient
D	Rotor diameter
E	Energy
N_{turb}	Number of turbines
P	Power
R	Rotor radius
r	Radial direction
s	Axial distance normalised by the diameter (x/D)
U_∞	Undisturbed wind speed
x	Axial direction
$\Delta\overline{U}$	Speed deficit
u, v	Velocity Cartesian components

Subscripts

∞	Free-stream condition

opt	Optimal conditions
w	Relative to the wake

Glossary

5PL	Five Parametre Logistic
CFD	Computational Fluid Dynamics
DWM	Dynamic Wake Meandering
MAPE	Mean Absolute Percentage Error
MPE	Mean Percentage Error
NWP	Numerical Weather Prediction
TKE	Turbulent Kinetic Energy

Chapter 1

Introduction

1.1 Motivation

Wind energy is continuously increasing its share of installed power and energy produced worldwide. However, because of the stochastic nature of the wind resource, it results difficult to predict the power output of a wind farm. This element creates problems to the management teams when they have to sell their energy in the market. Creating a model that predicts the output of the wind farm would help them in this aspect and consequently give additional stability to the grid.

1.2 Topic Overview

Extensive effort was put into determing the wake effect of adjacent turbines within the farm. The existing wake models estimate a normalised velocity deficit ($\Delta\overline{U}$) which is later subtracted from the value of the undisturbed wind speed (U_∞), according to equation (1.1). Using one of these wake models, the wind velocity profile in the wind farm is studied and used to predict the overall power output.

$$u = U_\infty \cdot (1 - \Delta\overline{U}) \tag{1.1}$$

The layout of the wind farm on which the model is employed is shown in Figure 1.1, where the North is upwards. Afterwards, a new model based on a statistical analysis of empirical data is created. Also, the reasons that brought to the creation of this second model are analysed. Finally, in an attempt to decrease the error of the prediction a third and final model is proposed. The results of these two other models represent the best results of the project and therefore its core part. In Figure 1.2, the wind rose relative to the data available and therefore relative to 2016 is shown.

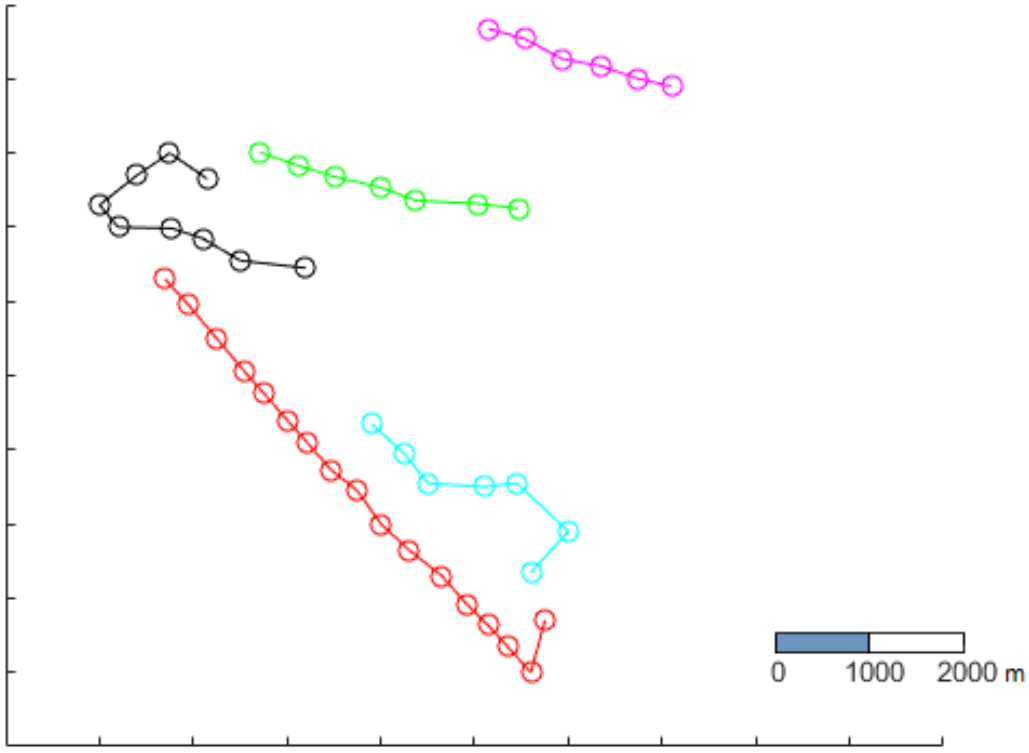

Figure 1.1: Layout of the wind farm where the models are employed

1.3 Data

The data used for the calculations were provided by the management team of the wind farm. The data covered the 12 months of 2016 in 10 minute increments. For each time slot and for each physical quantity described, the maximum, minimum and mean values were provided, together with the relative standard deviation. The data was from sensors placed on each turbine within the farm and 2 met masts also on site. The met masts were used mainly in an attempt to improve the second model (as explained in Section 5.10) because their data was deemed unrealible to describe the incoming wind (Section 3.5.1). The characteristics coming from the anemometers of the wind turbines that were mainly used were the wind speed and direction. The direction was described starting from North (which is therefore indicated as $0°$) and going clockwise (consequently, East is $90°$). The data from any single turbine was deemed realiable since it matched fairly well with turbines within close proximity. As such the farm provided enough individual data sets to ensure the overall validity of the data provided. However, one year is not enough to properly describe the behaviour of the wind in the site. In fact, the data coming from a single year might be affected from particular and unique conditions verified during it.

1.4 Objectives

The objective of this project is to create a model that is able to predict the power output according to the conditions of the wind entering the wind farm. In order to create this model, 9 out of the 12 months of

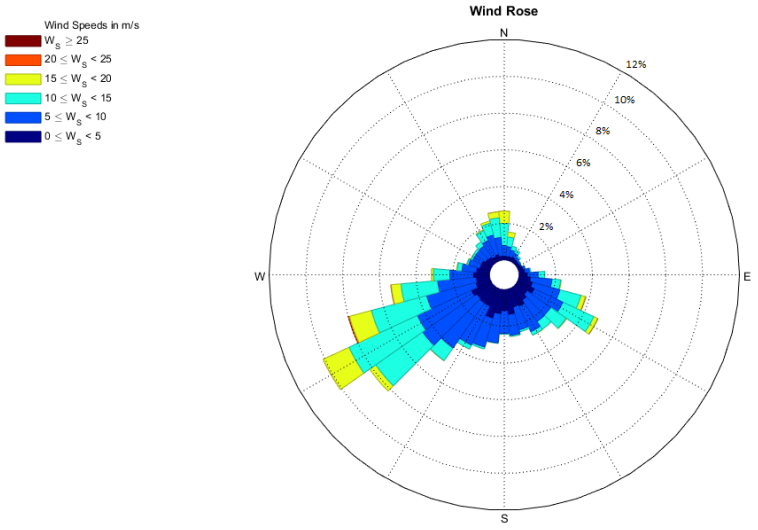

Figure 1.2: Wind rose relative to the data provided by the wind farm management

data available will be used for the training, while the remaining 3 will be predicted with the model itself to verify its validity. Different approaches are used in order to obtain this model, e.g. both a physical and a statistical path are followed. The physical approach models the effects of the wake based on equations, while the statistical one uses real world data to determine an underlying relationship. Among the approaches used, two managed to produce some results and were able to predict the power output of the 3 simulated months. The second model (uncovered in Chapter 5) produced a prediction for each month which Mean Absolute Errors relative to the time slot of 10 minutes (in which the data is organised) vary between $1153.73kWh$ and $1821.21kWh$. On the other hand, the third model (exposed in Chapter 7), simulated the three months with Mean Absolute Errors ranging between $1051.10kWh$ and $1585.75kWh$. After creating the model, the goal was to create a way for the wind farm management team to easily implement the model and to use its results. This way has initially thought to be a set of equations that would reproduce the behaviour of each wind turbine. Having an equation for each wind turbine would allow for implementation even when nearby turbines were out of order. Eventually, given the last approach proposed, the results are simply represented in a table indicating the power output depending on wind speed and direction.

1.5 Thesis Outline

The thesis is organised in 8 chapters overall, including the introduction and the conclusions. In Chapter 2, the theory behind the wake models and the wake models themselves are explained. In Chapter 3 and Chapter 4 the creation of the model based on the analysis of the wake and its results (and shortcomings) are exposed, respectively. Given the lack of consistency in the results, a second model and the new results are displayed in Chapter 5. Subsequently, the creation of the set of the equations reproducing the power output of the turbines is uncovered in Chapter 6. In order to decrease the error in

the prediction phase, a third model predicting directly the power output of the whole wind farm is created. The rationale behind this final model is exposed in Chapter 7. Finally, the conclusions of all the work carried out are explained in Chapter 8.

Chapter 2

Background

An extremely important aspect that influences the power output and the layout of a wind farm is the wake effect. When wind is converted into electricity, a wake characterised by a lower wind speed is created behind the rotor, there is therefore a speed deficit within this wake. As the downwind distance from the turbine increases, the deficit decreases and the wind speed reaches values extremely near, if not equal, to the one measured in the undisturbed air. Through the years, several models have been studied so that it would be possible to predict such a deficit. As usual, the complexity of the model increased with every new model.

2.1 Wake Models

2.1.1 Jensen Model

The first approach to the creation of a wake model was proposed by N.O. Jensen [1]. His model was then further studied and improved by I. Katic [2], bringing it to its present form. The Jensen model is also known as PARK model [3] and it is still widely used. In fact, WAsP (a software used for several purposes in the wind energy industry) uses the Jensen model for the wake estimations [4] [5].

The Jensen model aims to calculate the deficit inside of the wake based only on the downwind distance, once that the turbine characteristics have been determined. This is possible thanks to the assumption of axial symmetry within the wake. Therefore, the deficit is constant with the distance from the centreline of the wake and is consequently defined as a "top hat" model. Because of that, the Jensen model is defined as a one-dimensional ($1D$) model if we consider only the space aspect. Jensen proposed a linear expansion of the wake, based on the wake decay coefficient k. The value of the wake decay coefficient k varies with the turbulence and with the atmospheric stability, but generally the values used are 0.075 for onshore sites and 0.04 for offshore ones [4]. These values are also used in WAsP. However, further studies have been carried out and other formulations for k have been found (e.g. [4]). Yet, there are still doubts whether in large wind farm the value of the wake decay coefficient must be higher or not. Figure 2.1 below and equation (2.1) describe the expansion of the wake behind the rotor.

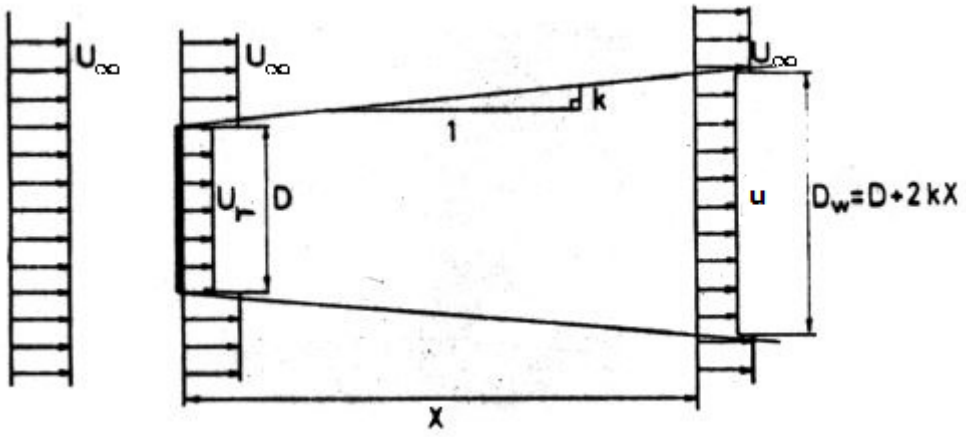

Figure 2.1: Expansion of the wake behind the turbine according to the Jensen model (modified from [2])

$$D_w = D \cdot (1 + 2 \cdot k \cdot s) \tag{2.1}$$

$s = x/D$ is the distance from the rotor normalised by the diameter.

The wake is divided in two different regions according to the downstream distance from the rotor. The two regions are called near wake region and far wake region. The distance at which the transition from the near to the far one varies depending on the publication. Usually, its value ranges between 2 and 4 rotor diameters. For example, in [6] the far wake region is defined as the part of the wake which is further than 3 rotor diameters. The Jensen model is used to describe the wind speed in the far wake region. Using the notation shown in Figure 2.1, the speed within the wake is represented by equation (2.2):

$$u = U_\infty \cdot \left[1 - \frac{1 - \sqrt{1 - C_T}}{(1 + 2 \cdot k \cdot s)^2}\right], \tag{2.2}$$

where C_T is the thrust coefficient of the turbine.

2.1.2 Ainslie Model

Another attempt to describe the wake created by a wind turbine was made by J. F. Ainslie in 1988 [8]. This model (known both as the Ainslie model and as the Eddy Viscosity model) is a two-dimensional field model, which means that it is able to describe the wind field of a regular wind farm by assuming axial symmetry inside the wake. Thanks to this assumption, the model is simplified because the number of equations needed to be solved using this assumption decreases compared to the case without axial symmetry. The Ainslie model is based on time averaged Navier-Stokes equations for an incompressible flow. Other important assumptions made were a stationary and fully turbulent wake with circumferential velocity equal to zero and negligible pressure gradient within the wake. The approximation of the Navier-Stokes equation used in this model is reported in (2.3).

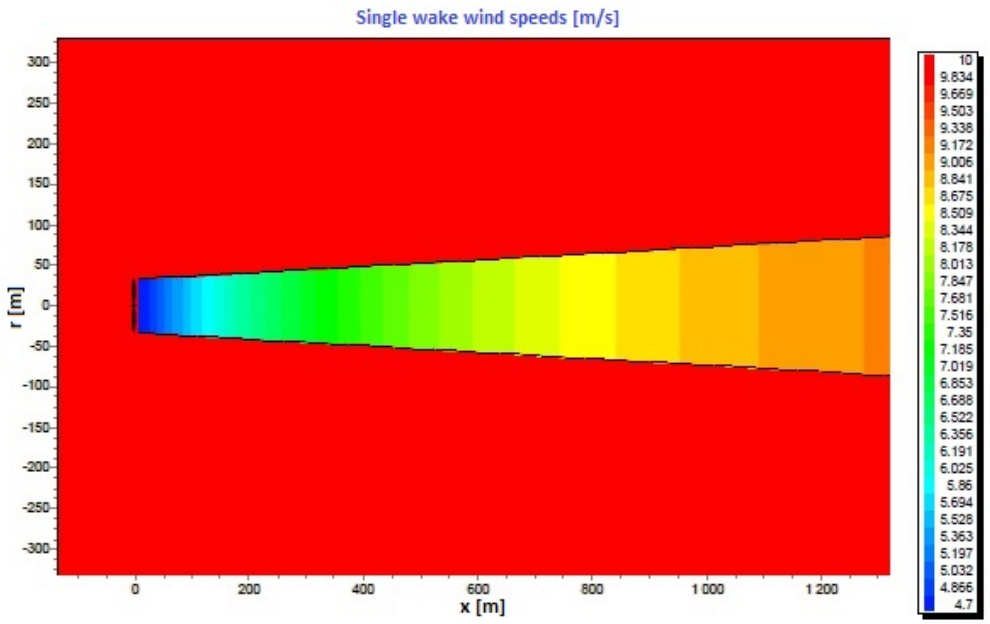

Figure 2.2: Speed deficit behind the rotor according to the Jensen model (modified from [7])

$$u\frac{\partial u}{\partial x} + v\frac{\partial u}{\partial r} = -\frac{1}{r}\frac{(r\overline{u'v'})}{\partial r}\,, \tag{2.3}$$

where:

- u is the downstream velocity
- x is the downstream distance from the rotor
- v is the radial velocity
- r is the radial distance
- $\overline{u'v'}$ is the Reynolds stress and defined as in (2.4)

$$-\overline{u'v'} = \varepsilon(x)\frac{\partial u}{\partial r}\,, \tag{2.4}$$

where ε is the eddy viscosity, found as the sum of the eddy viscosity of the atmospheric flow ε_a and the one produced by the wind shear in the wake ε_w.

$$\varepsilon(x) = \varepsilon_a + \varepsilon_w(x)\,, \tag{2.5}$$

with:

$$\varepsilon_w(x) = k_l \cdot b \cdot (U_\infty - u_c(x))\,, \tag{2.6}$$

where k_l is a constant equal to 0.015, b is the wake width and $(U_\infty - u_c(x))$ is the velocity deficit along the centreline.

Just like the Jensen model, the Ainslie model is studied in order to be used in the far-wake region, which according to Ainslie himself begins between 2 and 4 rotor diameters behind the turbine [8].

The main objective of this model is not to provide an easily-applicable model (like the Jensen model), but to thoroughly describe the behaviour of the wake behind a turbine [9]. A representation of this behaviour is shown in Figure 2.3.

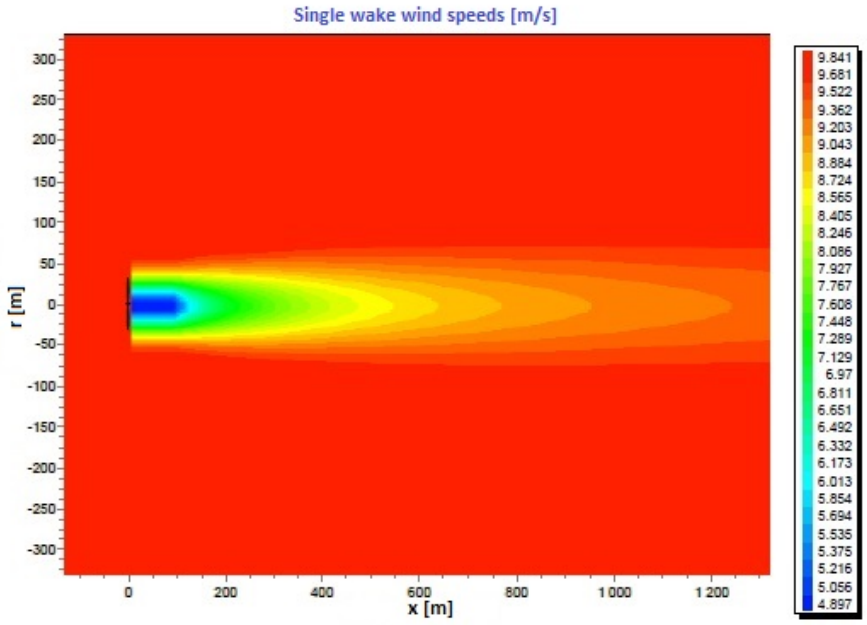

Figure 2.3: Speed deficit behind the rotor according to the Ainslie model (modified from [7])

2.1.3 Larsen Model

The Larsen model was proposed in different stages: the first version was published in 1988 [10], then an improved version was presented at the European Wind Energy Conference and Exhibition of 1996 [11] and eventually the present version was revealed in 2009 [12]. This model is implemented into the software WindPRO in two different versions.

The radius of the wake at a specific downstream distance x is defined in equation (2.7).

$$R_w(x) = \left(\frac{105c_1^2}{2\pi}\right)^{1/5} \cdot (C_T \cdot A(x + x_0))^{1/3}\,, \tag{2.7}$$

with:

$$x_0 = \frac{9.6D}{\left(\frac{2R_{9.6}}{kD}\right)^3 - 1}\,, \tag{2.8}$$

$$c_1 = \left(\frac{kD}{2}\right)^{5/2} \left(\frac{105}{2\pi}\right)^{-1/2} (C_T \cdot A \cdot x_0)^{-5/6}\,, \tag{2.9}$$

where:

$$k = \sqrt{\frac{m+1}{2}}\,, \tag{2.10}$$

$$m = \frac{1}{\sqrt{1-C_T}}\,, \tag{2.11}$$

$R_{9.6}$ is the radius of the wake at 9.6 diameters of downstream distance from the rotor and is empirically defined as:

$$R_{9.6} = a_1 \cdot exp\Big(a_2 \cdot C_T^2 + a_3 \cdot C_T + a_4\Big) \cdot (b_1 \cdot \varepsilon + 1) \cdot D\,, \tag{2.12}$$

with ε representing the ambient turbulence and a_1, a_2, a_3, a_4 and b_1 are numerical coefficients obtained in an empirical way.

The speed deficit $\Delta\overline{U}$ is given by the sum of two terms of the first and second order, respectively $\Delta\overline{U}_1$ and $\Delta\overline{U}_2$, as shown in equation (2.13).

$$\Delta\overline{U}(x,r) = \Delta\overline{U}_1(x,r) + \Delta\overline{U}_2(x,r) \tag{2.13}$$

However, the second term can be neglected and the speed deficit will be:

$$\Delta\overline{U}(x,r) = \Delta\overline{U}_1(x,r) = -\frac{\overline{U}}{9}\cdot\Big(C_T\cdot A\cdot(x+x_0)^{-2}\Big)^{1/3}\cdot\left[r^{3/2}\cdot\Big(3\cdot c_1^2\cdot C_T\cdot A(x+x_0)\Big)^{-1/2} - \left(\frac{35}{2\pi}\right)^{3/10}\Big(3\cdot c_1^2\Big)^{-1/5}\right]^2 \tag{2.14}$$

The Larsen model tries also to describe the near-wake region with two possible approaches, one of the first order (Figure 2.4(a)) and one of the second order (Figure 2.4(b))

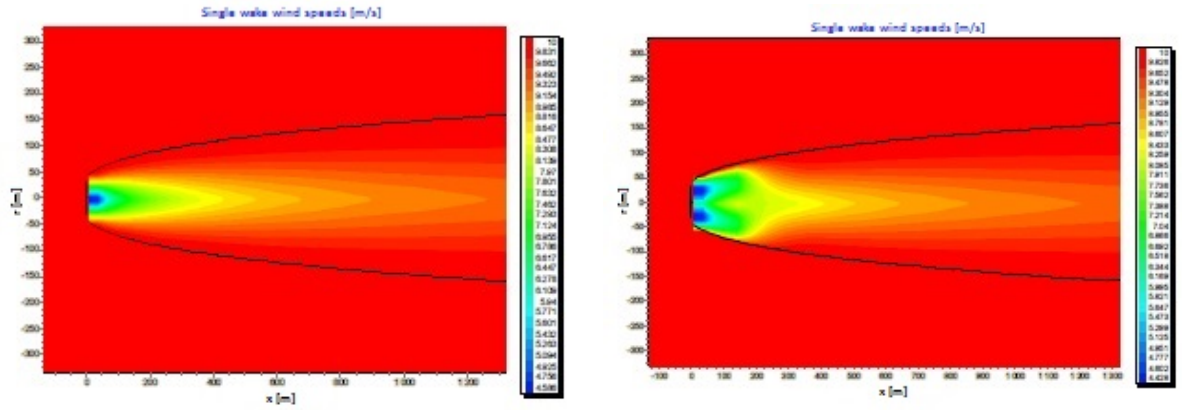

(a) First order approximation

(b) Second order approximation

Figure 2.4: Speed deficit behind the rotor according to the Larsen model (modified from [7])

2.1.4 Frandsen Model

Another model that can be used for the study of the wake behind a wind turbine is the Frandsen model, presented in 2006 [13]. This model has been studied to predict the overall behaviour of large offshore

wind farms with rectangular shape and constant distance between rows. Just like the Jensen model, the Frandsen model is also characterised by a top-hat profile, as it can be seen in Figure 2.5.

In the original article the diameter of the wake is defined as shown in equation (2.15). However, following further studies it has been found that it is better described by equation (2.17).

$$D_w(x) = D \cdot \left(\beta^{n/2} + \alpha \cdot s\right)^{1/n}, \tag{2.15}$$

with $n = 2$, $\alpha = 0.7$ and β defined by:

$$\beta = \frac{1 + \sqrt{1 - C_T}}{2 \cdot \sqrt{1 - C_T}}. \tag{2.16}$$

The more recent definition for the wake diameter however is the following one [14]:

$$D_w(x) = D \cdot max[\beta, \alpha \cdot s]^{1/2} \tag{2.17}$$

The parametre β is also used to describe the area of the wake just after the expansion through the rotor ($A_{w,0}$).

$$A_{w,0} = A \cdot \beta \tag{2.18}$$

The wind speed within a single wake is assumed constant with the radius and is defined in equation (2.19) and shown in Figure 2.5.

$$u = \frac{U_\infty}{2} \cdot \left(1 \pm \sqrt{1 - 2 \cdot \frac{A}{A_w} \cdot C_T}\right) \tag{2.19}$$

Where $+$ is used when $C_T \leq 0.75$ and $-$ when $C_T > 0.75$.

2.1.5 Gaussian Wake Model

This very recent model was formulated in 2014 and uses a new approach to the problem [15]. This new approach was used because in the far-wake region the speed deficit inside the wake is similar to a Gaussian curve in the radial direction [3]. The Gaussian Wake Model (sometimes indicated as GWM) has its foundations in the laws of mass and momentum conservation. The speed deficit is calculated with the following equation:

$$\Delta\overline{U} = C(x) \cdot exp\left(\frac{-r^2}{2 \cdot \sigma^2}\right). \tag{2.20}$$

In equation (2.20), σ is the standard deviation of the speed deficit at the downstream distance x, while $C(x)$ is estimated with equation (2.21):

$$C(x) = 1 - \sqrt{1 - \frac{C_T}{8 \cdot (\sigma/D)^2}} \tag{2.21}$$

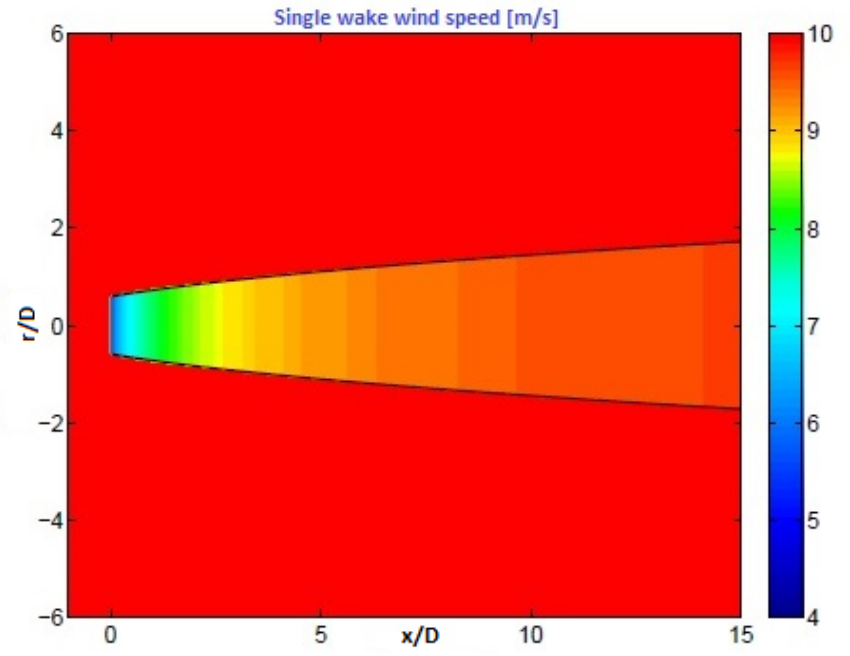

Figure 2.5: Speed deficit behind the rotor according to the Frandsen model (modified from [14])

$$\frac{\sigma}{D} = k^* s + \epsilon \tag{2.22}$$

where $k^* = \delta\sigma/\delta x$ is the expansion rate of the wake, assumed to be linear, and ϵ is the value of σ/D when x tends to 0.

By substituting (2.21) and (2.22) in (2.20), the final formulation of the speed deficit is obtained:

$$\Delta\overline{U} = \left(1 - \sqrt{1 - \frac{C_T}{8(k^* s + \epsilon)^2}}\right) \cdot exp\left(-\frac{1}{2(k^* s + \epsilon)^2}\left[\left(\frac{z - z_h}{D}\right)^2 + \left(\frac{y}{D}\right)^2\right]\right) \tag{2.23}$$

where z and y are respectively the vertical and horizontal coordinates and z_h is the height of the hub of the turbine. Therefore, the deficit purely depends on k^*, a site-dependent parametre that varies with the surface roughness and the turbulence intensity.

The behaviour of the deficit inside the wake is graphically shown in Figure 2.6

2.2 Wake Combination Models

The majority of the wake models available are single wake models, which means that further calculations are needed in order to apply them in case of a wind farm. One of the difficulties to overcome when combining single wake models is that the deficit created by the wakes of the turbines in front varies with the distance from the centreline of the wake, r. This problem can also happen with single wake models (e.g. Larsen model). In case the deficit is not constant with r, the wind speed passing through the rotor has to be averaged in order to estimate the power output using the power curve. In order to obtain this average speed value the equation (2.24) [16] can be used:

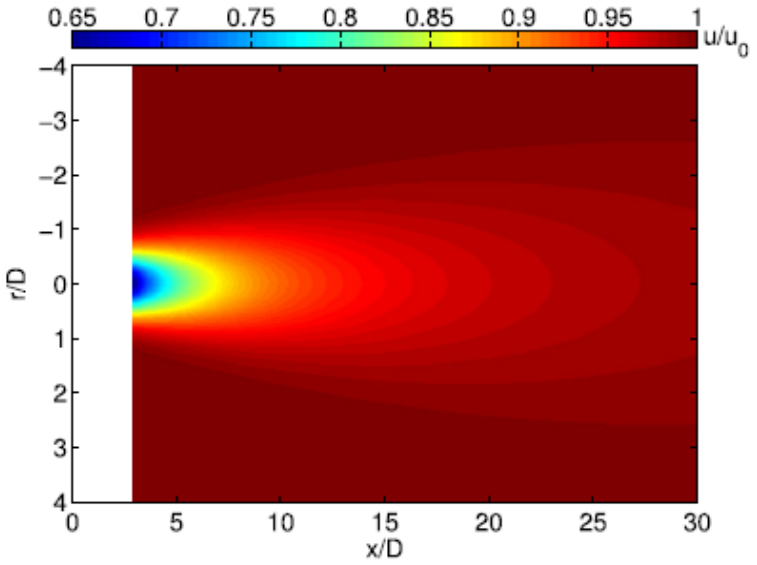

Figure 2.6: Speed deficit behind the rotor according to the GWM [3]

$$(U_\infty - u_{rotor})^2 = \frac{1}{A} \int_{rotor} (U_\infty - u_w)^2 dA \tag{2.24}$$

Where u_w is the non-uniform wake velocity, which depends on the magnitude and the sense of the vector $\vec{r}$.

2.2.1 Merging of Multiple Wakes

The main issue that is encountered when a single wake model is used for a whole wind farm is merging multiple wakes in order to obtain a single global deficit. There are four different models that have been tested and therefore can be used to merge multiple wakes: simple linear superposition, quadratic superposition, superposition within the Dynamic Wake Meandering (DWM) approach and the Larsen wake superposition approach [17]. In addition to these, there is also the approach of considering only the largest deficit among the ones produced by the wakes [18].

Linear Superposition

With this model, the total deficit at the $n^{th}+1$ rotor is found from the linear superposition of the previous n wakes at that location (indicated as $x(n+1)$). Such a concept is expressed in equation (2.25):

$$\Delta\overline{U}_{n+1} = \sum_{j=1}^{n} \left(\Delta\overline{U}_j|_{x(n+1)}\right) \tag{2.25}$$

Quadratic Superposition

The quadratic superposition is widely used and was proposed by Katic to improve the Jensen model [2]. This model is also suggested in several different articles (e.g. [19]) and it is used in the PARK program.

The quadratic superposition is defined as follows:

$$\Delta\overline{U}_{n+1} = \sqrt{\sum_{j=1}^{n} \left(\Delta\overline{U}_j|_{x(n+1)}\right)^2} \tag{2.26}$$

Superposition Within the Dynamic Wake Meandering Approach

The superposition within the Dynamic Wake Meandering approach (phenomenon exhaustively explained in [20]) assumes that the wakes intercepting the rotor are independent of each other. Consequently, they are defined using the same inflow conditions, which are the mean wind speed and turbulence field. The overall deficit according to this model is estimated using equation (2.27):

$$\Delta\overline{U}_{n+1}(t) = max\big(\Delta\overline{U}_i(t)\big)|_{x(n+1)} \tag{2.27}$$

In equation (2.27), i varies between 1 and n and represents an upstream turbine, while t is the time instant.

Larsen Wake Superposition Approach

In the Larsen wake superposition approach, the contribution of each single wake is calculated under unsteady inflow conditions, which means that the upstream wakes are considered [21]. The flow field at the location of a given turbine (indicated as x) is estimated using a linear summation of the contributions of each single wake. The instantaneous flow field $U(t)$ at the location of the $n^{th}+1$ turbine is estimated with the following equation:

$$U_{n+1}(t) = \overline{U}_0 + \sum_{j=1}^{n} \left(U_j(t)|_{x(n+1)}^{\tilde{U}_j(t)} - \tilde{U}_j(t)\right) \tag{2.28}$$

Every single contribution $U_j(t)$ is calculated at the same location $x(n+1)$. $\tilde{U}_j(t)$ represents the inflow condition at the instant t and is calculated according to equation (2.29):

$$\tilde{U}_j(t) = \overline{U}_0 + \sum_{i=1}^{j-1} (U_i(t)|_{x(j)} - \overline{U}_0) \tag{2.29}$$

2.3 Forecast Models

Since the power output of a wind turbine depends purely on the wind conditions, wind forecasts are an extremely important aspect for a wind farm. Knowing the wind conditions in advance allows for a better prediction of the future output and consequently, it can help the stability of the grid. Generally speaking, the forecasting methods used to predict the wind conditions can be divided into six groups [22]:

- Persistence method
- Physical method

- Statistical method
- Spatial correlation method
- Artificial intelligence method
- Hybrid approach.

Forecasting models can also be categorised depending on the time-scale they work with. In this case they can be divided into 4 additional classes [22]:

- Ultra-short-term: the time-scale varies between few minutes and 1 hour
- Short-term: it varies between 1 hour and several hours
- Medium-term: between several hours and 1 week
- Long-term: between 1 week and 1 year or more.

2.3.1 Persistence Method

The persistence method is the simplest method of the ones listed above. It is based on the assumption that the wind conditions will be the same of the moment in which the forecast is made. This assumption is therefore considered valid also for the power output, not only for the wind. Mathematically speaking, this model is easily defined in (2.30) and (2.31):

$$U_\infty(t + \Delta t) = U_\infty(t) \tag{2.30}$$

$$P(t + \Delta t) = P(t) \tag{2.31}$$

This model is surprisingly very accurate in the ultra-short term and because of its extremely low cost it is used as a benchmark in comparison of the new forecasting models to check their validity [23] [24]. However, the accuracy of the persistence method decreases rapidly when the time-scale of forecasting increases [25].

2.3.2 Physical Methods

Physical methods have been studied to improve Numerical Weather Prediction (NWP), so that more accurate forecasts could be reached. NWPs use weather and site-dependent data to obtain weather forecasts on large areas [26]. In order to run these methods supercomputers are needed.
The goal of physical models is to obtain the forecasts by using several parametres depending on an accurate description of the atmosphere.

2.3.3 Statistical Methods

Statistical methods use historical data in order to find correlations among some of the variables able to describe the atmospheric conditions. Obviously, in this case the objective is to find the wind speed and direction at a certain moment in the future. Statistical models are easy and cheap to create, if compared with the other possible methods. A typical negative aspect for these models is that their precision decreases as the time-scale increases [22]. It can happen that even with a prediction time of more than two days, the results from a sophisticated time series model are matched by using the mean of the wind data for the same day in each of the previous five years [27].

The methods that are most widely used for wind forecasts are the auto regressive (AR), the auto regressive moving average (ARMA), the auto regressive integrated moving average (ARIMA), Bayesian approach and gray predictions, These methods can also be integrated with additional ”functionalities”, for example the generalised autoregressive conditional heteroskedasticity (GARCH) [27]. GARCH components allow the variance to evolve in an autoregressive way over time. In the same article an approach for the prediction is also proposed, the esemble prediction. This different approach gives an evaluation of the weather uncertainty by creating an estimate of the probability density function for the weather variables.

2.3.4 Other Methods

The remaining methods listed in 2.3 are less used than the ones that have just been mentioned and therefore are collected into a single section.
Spatial correlation models use the measurements from other sites to find the wind conditions at the site studied. This method has been tested and produced solid results [28].

Artificial intelligence models have been created following the development of the artificial intelligence. Some of the models created make use of artificial neural network (ANN), adaptive neuro-fuzzy inference system (ANFIS), evolutionary optimisation algorithms, support vector machine (SVM), fuzzy logic methods and neuro-fuzzy network [22].

Finally, the hybrid models have been created in order to fix the weak points of a certain method by merging such a method with another one. This way it is possible to take advantage of the pros of each of the models [25]. Hybrid models can be used to merge models based on the approach (e.g. physical and statistical methods) or on the time-scale (e.g. short- and medium-term models) [24]. Some examples of hybrid methods are the combinations of artificial intelligence methods and any of following three: physical, statistical or another artificial intelligence approach [22].

2.4 Conclusions to the Chapter

At the beginning of this chapter, five possible wake models to implement in the physical model that will be formulated in Chapter 3 are exposed. The models exposed are the Jensen [1], the Ainslie [8], the Larsen [12], the Fradsen [13] and to conclude, the Gaussian [3] wake models. Afterwards, some possible ways

to consider multiple wakes are explained. To conclude, the forecast models commonly used by wind farms are exposed. The one that is used as a benchmark to prove the validity of the new models is the persistence method, which considers the wind conditions equal to the ones of the previous time interval. The other models included in the chapter are mainly part of two families, physical and statistical models.

Chapter 3

Physical Model

As reported in Chapter 2, there are several models that could be implemented in order to create a model that would allow to predict the power output of the wind farm. The choice on the wake and combination models to be used was made considering complexity, time of computation and other information found in the articles.

3.1 Choice of the models

As far as the wake model goes, the Jensen model [1] was chosen. This choice was made for several reasons:

- The deficit created by the wake is considered constant with the distance from the rotor, creating the top-hat profile that has already been mentioned
- As it can be seen from Equation (2.2), the model works with a limited amount of inputs, of which C_T and s depend on the turbine and the wake decay coefficient k can be found in literature
- The wake expands linearly with expansion rate equal to the wake decay coefficient; this characteristic will be very useful in Section 3.4, where the interceptions between wakes and rotors will be detected
- It is used in commercial softwares, which means that it is a reliable model that produces solid results, if working under the correct conditions
- In case of complex wind scenario, category under which the analysed wind farm falls, using improved wake models does not lead to significantly better results [3]
- In relation to what has just been mentioned, the limited computational time becomes an advantage as spending more time would not lead to better results.

For the Jensen model, the suggested combination model is the quadratic superposition method exposed in Section 2.2.1. This method in particular was formulated for the first time for the Jensen

model itself by Katic [2], which assures that the two models can work well together. The Jensen model also fits this case as the minimum distance between turbines is above 3 diameters, which means that we are only interested in the far wake region.

Given the complexity of the calculations relative to the prediction of the wind speed and the instrumentation needed (as explained in Section 2.3), it was chosen not to consider the aspect. Even though there was the possibility of using the persistence method (reported in Section 2.3.1), it was preferred not to consider it as the wind farm might have a prediction method of its own.

3.2 Creation of Custom Power Curves

After studying the layout of the wind farm, the validity of the power curve provided by the manufacturer was tested. This verification was made by comparing the power output estimated by using the power curve and the 10-minute average wind speed provided by the wind farm and the actual output according to the data. It was found that the power outputs were different and therefore the power curve of the manufacturer was deemed as unreliable. Creating custom power curves is a practice that is used by wind farms. They are used because the manufacturer power curve is usually valid only under idealised conditions (i.e. isolated single turbine, surrounded by flat terrain). Also, the manufacturer power curve best works when there is no interference among turbines [31]. Because of these reasons, four sets of power curves were produced and tested. Cutler et al. [31] initially suggested the use of a power curve for the whole wind farm. However, the creation of such a power curve would not allow to predict the output in case of shutdown of one or more turbines. Therefore, similarly to what is later suggested in the same article, direction-dependent power curves will be studied further on. The article proposes direction-dependent power curves and then finds a relationship between the speeds at the different turbines and the met mast measurements. In the model here proposed, instead of using the met mast measurements, at the end of the work the wind speeds at the turbines are found in relation to the undisturbed wind speed.

The first set was created using the wind speed and the power output data. Therefore, each point was characterised by the mean wind speed experienced by that turbine during those 10 minutes on the x-axis and by the average power output during the same time gap on the y-axis. In this first approach, only the time gaps in which the wind speed was between $2.5m/s$ and $11.5m/s$ were used, which means almost only the part of power curve where $P \propto u^3$. The curve itself was then obtained using the Curve Fitting app present in MATLAB. The results found using this new set were better than the previous results, therefore these new power curves were considered more reliable than the manufacturer one. However, there were some bad results at low speeds.

In the second approach, only data with wind speed between the cut-in wind speed ($3m/s$) and the rated wind speed ($11m/s$) were considered. The curve obtained was slightly better, but in some cases weak results were still attained.

In the third array of power curves, the wind speed interval considered was between $3.5m/s$ and $11m/s$. In addition to this, the outliers were not considered. In MATLAB, the outliers are defined as the

points which are greater than $q_3 + w \cdot (q_3 - q_1)$ or lower than $q_1 - w \cdot (q_3 - q_1)$. The parametres q_1 and q_3 represent respectively the 25^{th} and 75^{th} percentiles of the data, while the default value of w is 1.5. In this case, no negative values were found, making this new set of curves more reliable than the previous ones. Nevertheless, according to these curves, the power output for low wind speeds (near to the cut-in wind speed) is very high. When the wind speed is between $4m/s$ and $7m/s$ all these series of power curves yield power coefficients (C_p) that are too high.

The final procedure is based on the use of box plots and their medians. The data was divided into bins according to the wind speed and then the relative box plots were plotted. Two different sizes of bins were used: initially, the bins collected data within a gap of $1m/s$, while later bins of $0.5m/s$ were preferred. Also, both the case with and the case without outliers were considered. Eventually, the approach that was considered the best one was the one with bins of $0.5m/s$ and without outliers. In fact, the curves obtained using the bins of $0.5m/s$ led to results closer to the data when the wind speeds predicted by the model were compared with the measured ones. An example of the results of such a method is showed in Figure 3.1.

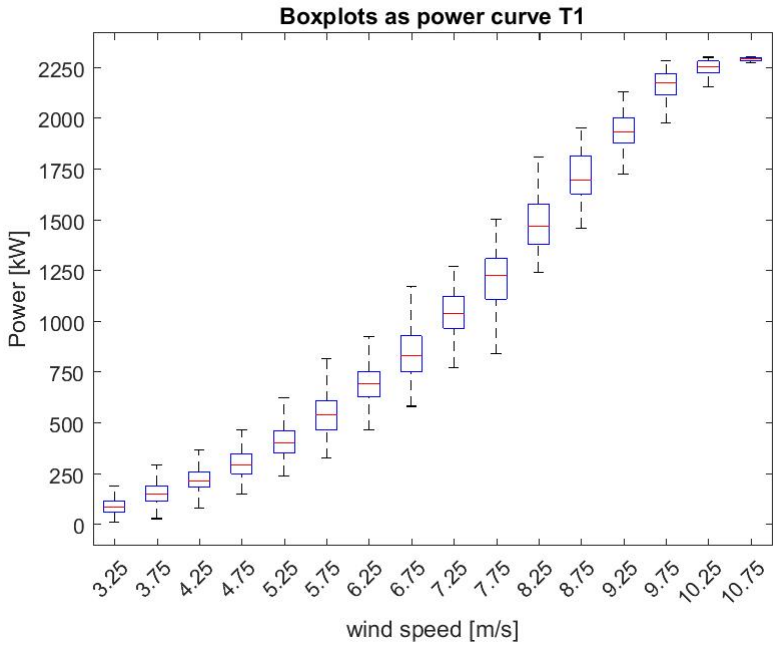

Figure 3.1: Disposition of the box plots used for the custom power curve

Once again, for wind speeds near to the cut-in wind speed, the estimated power output is very high. This most probably happens because of the variability of the wind and the use of the 10-minute intervals. In fact, during those 10 minutes the wind can vary significantly even though for a limited amount of time. This would lead to an increase in the value of the mean power output. Even though the mean wind speed value would grow, the increase cannot be of the same size because the power output increases with u^3. In addition to this aspect, if the wind speed reaches an elevated value for a very limited time, the power output will vary even faster [30]. The comparison among the manufacturer power curve, the power curve obtained with wind speeds between $3,5m/s$ and $11m/s$ and without outliers (in the graph defined as "Custom power curve") and the one obtained using the boxplots is shown in Figure 3.2.

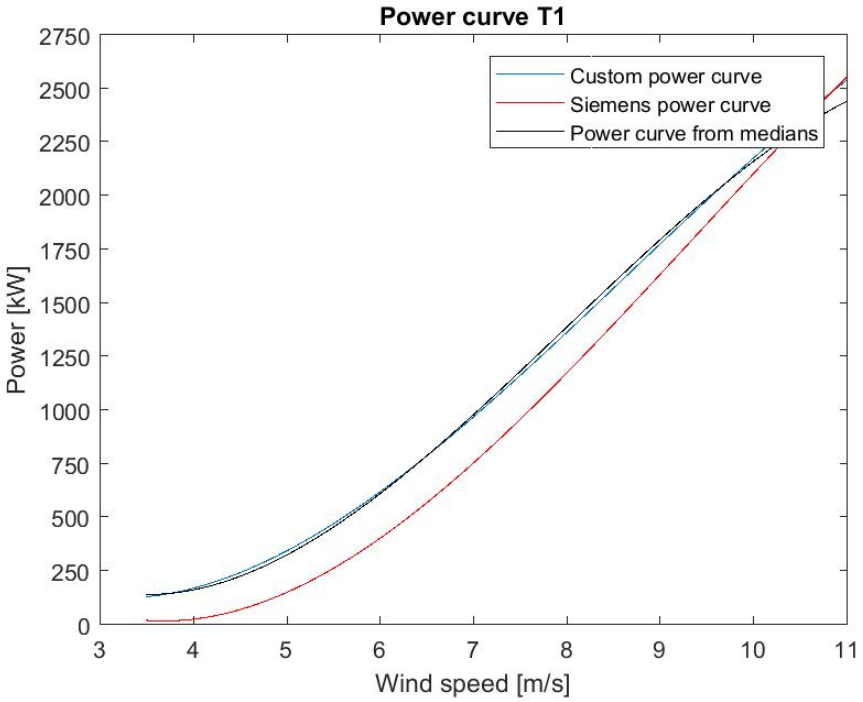

Figure 3.2: Comparison among the three possible power curves

Finally, the power curve was chosen among the different sets. The power curves obtained using the box plots of $0.5m/s$ and without outliers were considered the best ones mainly because they were the only ones that flattened near the rated wind speed.

The study of the power curves allowed also to identify two turbines whose data were not reliable. In fact, when calculating the C_p from the chosen power curve, its value was often above the Betz limit. This problem probably derives from a malfunctioning in their anemometers. In Figure 3.3, the comparisons among the different power curves for the two unreliable turbines are shown. By comparing the two images in Figure 3.3 with Figure 3.2, it is possible to notice the difference of the power curves and that the ones in Figure 3.3 produce higher power at the same wind speed than the one in Figure 3.2.

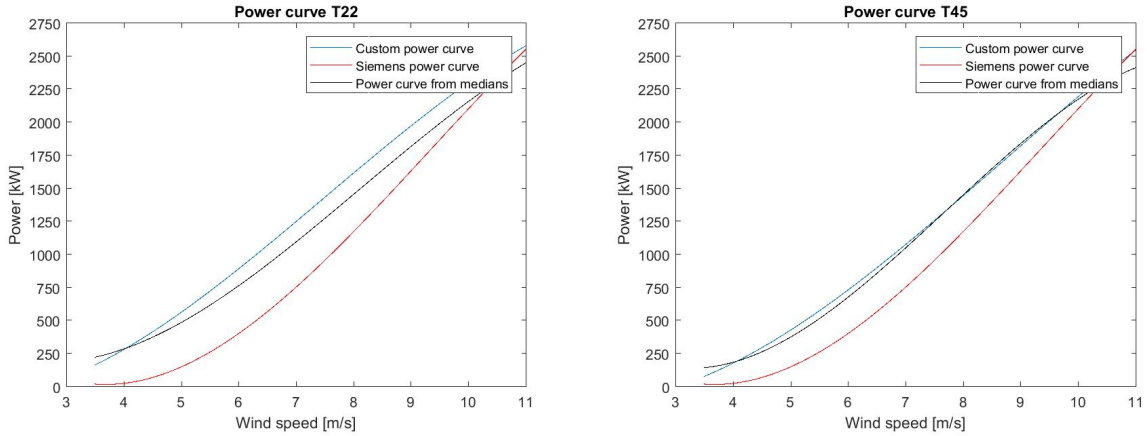

(a) Turbine 22

(b) Turbine 45

Figure 3.3: Comparisons among the power curves for the unreliable turbines

During the calculations, the power estimations relative to these two turbines have been carried out considering the manufacturer power curve, as it was the only one certainly reliable among the different sets considered.

3.3 Study of the Wind Field

As a next step, the evolution of the wind field within the wind farm was studied. This operation allowed to see how the wind behaves in the area and therefore, to detect the presence of any particular conformation or obstacle. The development of wind conditions was represented using sequences of quiver plots for several dates throughout the year. Each of the quivers was plotted using the average data of the 10-minute time slot. A quiver plot perfectly fits the representation of a vector field. In this particular case, the vector is the wind speed, with the sense of the vector indicating the direction in which the wind is blowing and its magnitude proportional to the value of the wind speed. An example of the plots obtained is shown in Figure 3.4. Because of the demeanour of some of the turbines, it was thought that there might be a hill eastern than the farm. However, no turbine suggested the presence of significant obstacles inside the wind farm and therefore, no further wake had to be considered in order to determine the wind field of the area.

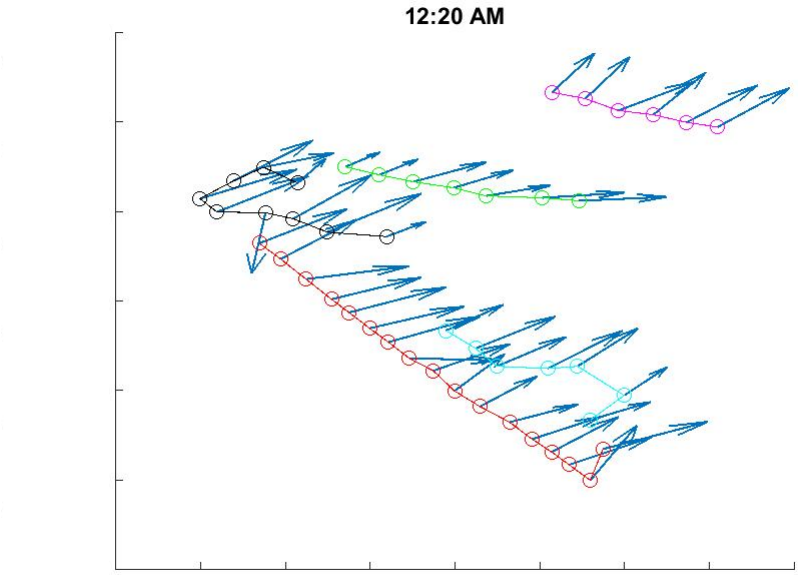

Figure 3.4: Quiver plot representing the wind field on $01/04/2016$ at $00:20$

The use of the quivers helped in discovering further unreliable turbines. In fact, some of the vectors were often pointing in directions that did not agree with the one that the nearby vectors were indicating. In order to be sure that these discrepancies were created by a malfunctioning in the anemometer and not by a real difference in the wind direction, the disparities in direction between the unreliable turbines and the averages of the nearby ones were calculated. It was found that in all the cases in which the possibility of a problem was detected these disparities were almost constant through time. Therefore, it could be

realistically assumed that the origin of the differences in direction was the anemometer. Consequently, this group of turbines was added to the two previous ones that had already been labelled as unreliable. Overall, the turbines classified as inaccurate were 6. In the quivers, sometimes it was also possible to notice the turbines that could not measure the wind speed properly. This happened because the vectors were significantly shorter than the adjacent ones, without the possibility that the reason was the wake of another turbine.

3.4 Detection of the Interceptions

In order to find the degradation of the wind along different directions thanks to the deficit that each turbine experiences, it was necessary to find when wakes intercept one or more rotors. To be able to detect these interceptions it was supposed that all the rotors face the same wind direction (a brief explanation of the reasons behind this assumption is included in Appendix A). This assumption is not completely true as the wind direction varies in space and time, especially considering 10-minute time gaps. However, it is reasonable to consider that near turbines experience similar wind directions. Thanks to the assumption of the Jensen model of linear expansion of the wake it was possible to check when the interception happened. Such an operation was carried out considering situations like the one shown in Figure 3.5.

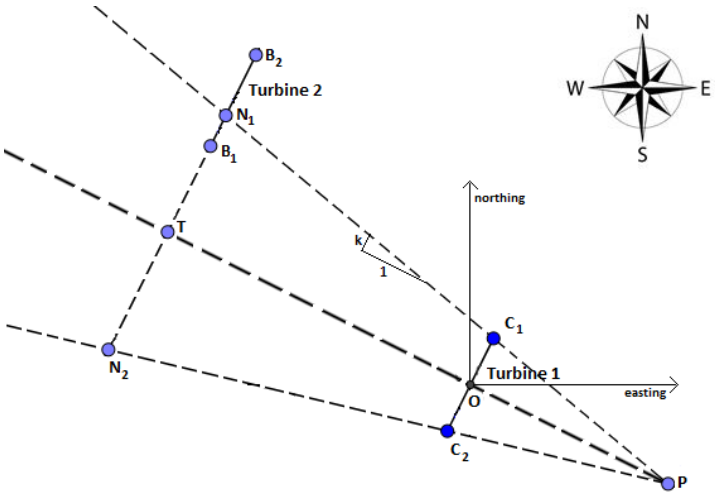

Figure 3.5: Graphical simplification of the interception between wake and rotor

Making the additional assumption that there are only complete interceptions, it was then possible to find the degradation of the wind along the different directions. The consequence of this assumption is that every time an interception happens, it is considered a full one and therefore the deficit is overestimated. In particular, the interception was detected by checking if either B_1 or B_2 was in the triangle formed by P, N_1 and N_2.

Using the scheme of Figure 3.5 as an example, the calculations needed to find the key points are listed below. The origin of the cartesian coordinate system has been taken in correspondence of the nacelle of turbine 1. In order to find point P, the equations reported in (3.1) must be calculated.

$$\begin{cases} x_P = \sqrt{\frac{R^2}{k^2 \cdot (1+m^2)}} \\ y_P = m \cdot x_P \end{cases} \tag{3.1}$$

The coordinates of point T can be found with the equations in (3.2).

$$\begin{cases} x_T = \frac{\frac{x_2}{m}+y_2}{m+\frac{1}{m}} \\ y_T = m \cdot x_T = m \cdot \frac{\frac{x_2}{m}+y_2}{m+\frac{1}{m}} \end{cases} \tag{3.2}$$

The explanation on the finding of the system of equations (3.2) is included in Appendix A. The points x_2 and y_2 in (3.2) are the difference in the GPS coordinates between the two turbines considered. These coordinates were provided by the wind farm in the format of cartesian corrdinates where x is denominated easting and y northing. After finding point T, it is possible to find the two most external points of the wake at distance $\overline{OT}$ from turbine 1, represented by points N_1 and N_2. The coordinates of these points are given by the two possible solutions to the system of equations reported in (3.3).

$$\begin{cases} (x - x_T)^2 + (y - y_T)^2 = -r^2 \\ y - y_T = -\frac{1}{m} \cdot (x - x_T) \end{cases} \tag{3.3}$$

In system (3.3), the variable r stands for the radius of the wake at distance $\overline{OT}$ from the origin of the coordinate system. Finally, the two extremities of the rotor of turbine 2, which are B_1 and B_2, are found by solving the system (3.4).

$$\begin{cases} (x - x_2)^2 + (y - y_2)^2 = -R^2 \\ y - y_2 = -\frac{1}{m} \cdot (x - x_2) \end{cases} \tag{3.4}$$

When the interception happens, for a given wind speed the value of the deficit depends only on the downstream distance from the upstream rotor. If there is no interception, the deficit will be considered equal to zero. The value of the deficit depends only on the distance from the rotor because the wake decay coefficient k has been considered equal to 0.075, as used also in WAsP [4]. The deficit varies with the wind speed because the thrust coefficient C_T has not been considered a constant characteristic of the turbine, but dependent on the C_p, according to (3.5):

$$C_T = \frac{C_p}{1 - a} \tag{3.5}$$

where a is the axial induction factor and is estimated from C_p following equation (3.6):

$$C_p = 4a \cdot (1 - a)^2 \tag{3.6}$$

The deficit was then estimated according to the Jensen model using equation (2.2). However, two conditions were set in order for the deficit to be valid: 1) the distance between the rotor creating the wake and the one intercepted must be lower than 40 diameters ($x < 40 \cdot D$) and 2) the deficit has to be

Table 3.1: Matrix containing the deficits for a wind speed of $5.5m/s$ for the physical model

	$0°$	$22.5°$	$45°$	$67.5°$	$90°$	$112.5°$	$135°$	$157.5°$	$180°$	$202.5°$	$225°$	$247.5°$	$270°$	$292.5°$	$315°$	$337.5°$
$T1$	0	0	0	0	0	0	0	0	0	0	0.021	0	0.172	0.185	0	0
$T2$	0	0	0	0	0.173	0.172	0	0	0	0	0.020	0.017	0	0.182	0	0
$T3$	0	0	0	0	0	0.162	0	0	0	0.023	0	0.016	0.164	0.184	0	0
$T4$	0	0	0	0	0.162	0.172	0	0	0	0.023	0.025	0.012	0	0.071	0.135	0
$T5$	0	0	0	0	0	0.090	0.135	0	0.021	0	0.015	0.012	0	0.164	0	0
$T6$	0	0	0	0	0	0.164	0	0	0.017	0.023	0.015	0	0	0	0	0
$T7$	0.020	0.024	0.021	0	0	0	0	0	0	0.016	0	0.019	0.155	0	0	0
$T8$	0.017	0.020	0.016	0	0.171	0	0	0	0	0.010	0	0.026	0.107	0.016	0	0
$T9$	0	0.021	0.021	0	0.101	0	0	0	0.018	0.017	0.047	0.032	0.011	0.202	0	0
$T10$	0	0.019	0.017	0.013	0	0.170	0	0	0.018	0.018	0.017	0.032	0.144	0.165	0	0
$T11$	0	0	0.024	0.016	0.140	0.158	0	0	0	0.053	0.043	0.048	0.051	0.074	0	0
$T12$	0	0	0	0.017	0	0.077	0	0	0.021	0.043	0.050	0.025	0.058	0.145	0	0
$T13$	0	0	0	0.013	0	0.171	0	0.034	0.043	0.052	0.046	0.105	0.078	0	0	0
$T14$	0	0	0	0.099	0.054	0	0.037	0.057	0.082	0.095	0	0.051	0.095	0	0.140	0
$T15$	0	0	0	0	0.089	0	0.149	0.064	0.082	0.060	0.162	0	0	0	0	0
$T16$	0	0	0.134	0	0.110	0	0.066	0.091	0	0	0.112	0	0	0	0	0
$T17$	0	0	0.133	0.058	0.018	0.106	0.170	0.170	0	0	0	0	0	0	0	0
$T18$	0	0.052	0	0.028	0.140	0.047	0.078	0	0	0	0	0	0	0	0.156	0.156
$T19$	0.068	0.091	0.049	0.030	0	0.208	0.012	0.055	0.117	0	0	0	0.107	0.091	0	0.091
$T20$	0.085	0.038	0.034	0.035	0	0.047	0.116	0.026	0.090	0	0.082	0	0.068	0.147	0.047	0.042
$T21$	0.042	0.039	0.036	0.030	0.046	0	0	0.018	0.039	0	0.081	0	0	0.098	0.138	0.064
$T22$	0.047	0.024	0.019	0.012	0	0	0	0.010	0.033	0.017	0.021	0.021	0.103	0.034	0.021	0.016
$T23$	0.112	0.039	0.098	0.022	0.019	0	0.178	0.163	0	0	0	0	0	0	0.081	0
$T24$	0.102	0.024	0.093	0.051	0	0	0.151	0.149	0	0	0	0	0	0	0.181	0.184
$T25$	0.045	0	0.048	0	0	0	0.151	0.133	0	0	0	0	0	0	0.150	0.139
$T26$	0.042	0.039	0.011	0	0	0.011	0.163	0	0	0	0	0	0	0	0.134	0.136
$T27$	0.012	0.013	0.011	0	0	0.054	0.033	0	0	0	0	0	0	0	0.181	0.031
$T28$	0.020	0.015	0	0	0.072	0.057	0.158	0.151	0	0	0	0	0	0	0	0.020
$T29$	0.010	0	0	0.086	0.086	0.047	0.149	0.148	0	0	0	0	0	0	0.148	0.149
$T30$	0	0	0.093	0.080	0.079	0.016	0.184	0	0	0	0	0	0	0	0.160	0.161
$T31$	0.072	0	0.103	0	0.128	0	0.170	0.145	0	0	0	0	0	0	0.188	0.012
$T32$	0.044	0.057	0.087	0.055	0.031	0	0.148	0	0	0	0	0	0	0	0.138	0.122
$T33$	0.060	0	0.064	0	0	0	0.154	0	0	0	0	0	0	0	0.149	0
$T34$	0.059	0.046	0	0.037	0.087	0	0.155	0.125	0	0	0	0	0	0	0.150	0.020
$T35$	0.038	0.031	0.037	0	0	0.077	0.052	0.154	0	0	0	0	0	0	0.149	0.127
$T36$	0.029	0.078	0	0	0.121	0	0.156	0.156	0	0	0	0	0	0	0.094	0.159
$T37$	0.033	0.032	0.133	0	0	0	0.161	0.161	0	0	0	0	0	0	0.175	0.163
$T38$	0.117	0.085	0	0	0	0	0	0	0	0	0	0	0	0	0.156	0.146
$T39$	0.117	0	0	0	0	0	0	0	0.085	0.103	0.145	0	0.107	0.088	0.025	0.107
$T40$	0.050	0	0.117	0	0	0	0	0.117	0.110	0.100	0	0	0.066	0	0.054	0.060
$T41$	0	0	0	0	0	0	0	0	0	0.040	0.127	0.049	0.023	0.050	0.101	0
$T42$	0	0	0	0	0	0	0.083	0	0.065	0.033	0.040	0.170	0.197	0.063	0	0
$T43$	0	0	0	0.173	0.166	0	0	0.059	0.048	0.052	0.058	0.052	0.143	0.038	0	0
$T44$	0	0	0	0	0.139	0.039	0.039	0.038	0.046	0	0.114	0	0.120	0.066	0.179	0.162
$T45$	0.016	0.014	0	0	0	0.067	0.187	0.187	0.041	0.086	0.131	0.113	0.056	0.060	0.187	0.021
$T46$	0.013	0.017	0	0	0	0.030	0.151	0.033	0.086	0	0.097	0.097	0.066	0.050	0.025	0.022

higher than or equal to 0.01 ($\Delta\overline{U} \geq 0.01$). The second condition was conceived using the same definition of the thickness of the boundary layer and was created because according to equation (2.2), the value of the deficit never reaches a value equal to 1. The total deficits were collected in a $3D$ array where the three dimensions were the number of the turbine, the wind direction and the wind speed bin. The speed bins in this case were considered having a size of $1m/s$. On the other hand, the deficits were classified based on the directions in bins of $22.5°$, starting from $0°$ and going until $337.5°$. In each bin the angle that gives the name to the interval is the middle value. Using the bin of $0°$ (which means that the wind is blowing fom North) as an example, the data collected in this interval had the wind direction ranging between $-11.25°$ and $11.25°$. The wind direction is important because depending on it, obviously the interceptions between wakes and rotors vary. In Table 3.1 there is an example of one of the matrices included in the $3D$ array. This particular case is for the speed bin of $5.5m/s$, which means that it is valid for speeds ranging from $5m/s$ to $6m/s$.

3.5 Research of the Inputs to the Model

Once that the deficits have been found for all the speeds and directions, the next step is to find the inputs to the model. The two inputs needed must describe the wind conditions in the 10 minutes of the time interval. Therefore, one input will define the wind speed and the other will characterise the wind direction.

3.5.1 1^{st} Input: Speed

In order to find the wind speed experienced by each turbine, a value for the undisturbed wind speed to use with the already-found deficits was needed. To find such an input an optimisation function included in MATLAB was used. The function that had to be minimised was the accumulated difference between the measured wind speed and the estimated wind speed at each turbine, as described in (3.7):

$$\Delta u_{acc} = \sum_{i=1}^{N_{turb}} |u_{measured,i} - u_{model,i}| \tag{3.7}$$

where N_{turb} is the number of turbines currently working. The value of N_{turb} is not always the same because sometimes it can happen that one or more turbines are not working for different reasons (e.g. shutdown for maintenance). In particular, this happened for a turbine for several months at the beginning of the year analysed. Therefore, considering N_{turb} constant would have led to wrong results.

The result of (3.7) was minimised by varying the speed input at the model. The value that minimised the result was saved and will from now on be called u_{opt}. In the meantime, the maximum wind speed experienced by any of the reliable turbines and the average wind speed throughout the wind farm were computed. The average wind speed throughout the wind farm was estimated by finding the mean value of the wind speeds experienced by all the reliable turbines. Afterwards, a relation between any two of the three wind speeds that have been found (u_{opt}, u_{max} and u_{avg}) was seeked. While no significant relation was found between the maximum wind speed and the optimal wind speed and also between the average wind speed and the maximum one, the comparison between u_{avg} and u_{opt} produced interesting results. These results are exposed in Figure 3.6, where:

- sse is the sum of squared error
- $rsquare$ is R^2
- dfe represents the degrees of freedom for error, which is equal to the number of observations minus the number of estimated coefficients, stored as a positive integer value [34]
- $adjrsquare$ is the adjusted R^2
- $rmse$ is the root mean square error.

In the bottom left corner of Figure 3.6, the equation of the line that best fits the scattered points is reported. It can be easily seen that it is extremely near to $y = x$ and therefore, u_{opt} can be approximated with the average wind speed.

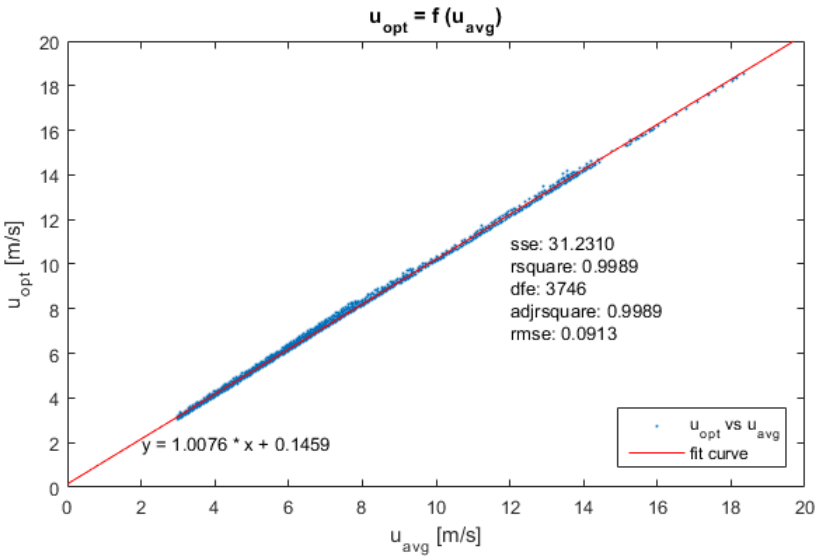

Figure 3.6: Optimal wind speed as a function of the average wind speed

Since the calculation of the average wind speed requires data from all the turbines, an attempt to find a different relation was made. Given the presence of two met masts within the wind farm, it seemed reasonable to look for a relationship between their measurements and the optimal wind speed. As a simplification, u_{opt} was considered equal to the average wind speed. This way, the calculations resulted easier and faster, without compromising the results in a significant way. As an initial analysis, the measurements of met masts and turbines for a random time slot were compared to see if they could be used. The results are shown in Figure 3.7, where the legend is missing because of its excessive size. However, the two met masts are represented by the two bigget X's in the graph. The graph represented in Figure 3.7 is a polar graph where the angle from the upper half of the vertical axis indicates the direction and the distance from the origin serves as the wind speed. Figure 3.7 therefore represents both the mean wind speed and direction according to each turbine and to both the met masts in a random time slot of 10 minutes.

Figure 3.7 allows also to verify the unreliability of one of the turbines labelled as such in Section 3.3. It can be easily seen that the met masts are not able to represent the undisturbed conditions of the wind. However, being those two measurements in the middle of the others, they might have a close relationship with the average wind speed and therefore with the optimal wind speed. In order to see if such a relationship exists, two graphs for each of the 16 angular sectors considered were plotted, one per met mast. This method allowed to see if at least in a specific case the measurements of the met masts were able to resemble the average wind speed. Four examples of the graphs obtained are reported in Figure 3.8.

In the captions in Figure 3.8, 81 and 82 are the ID's given to the two met masts by the management of the wind farm. Figures 3.8(a) and 3.8(c) are two examples that show how there is no direct relation between the average wind speed and the speed at either of the two met masts. Even though Figures 3.8(b) and 3.8(d) are two of the cases in which the data from the turbines seems to be related with the one from either of the met masts, it can be noted how the relation is not strong enough in order for

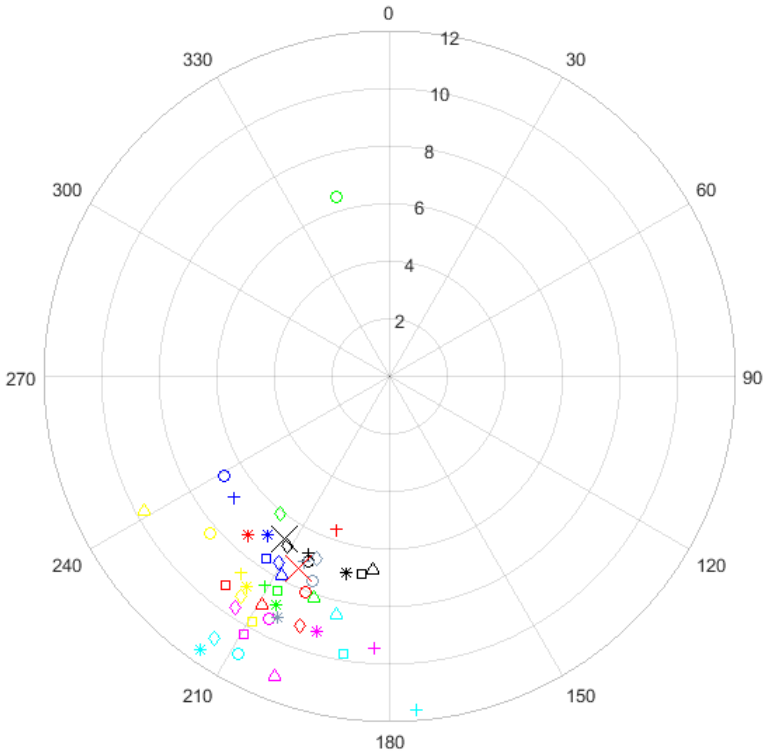

Figure 3.7: Comparison among the met masts and the turbines measurements

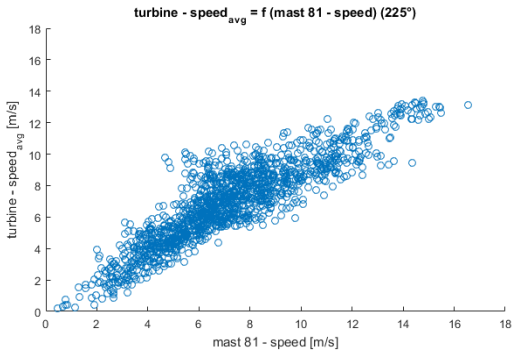

(a) Met mast 81 in angular sector $225°$

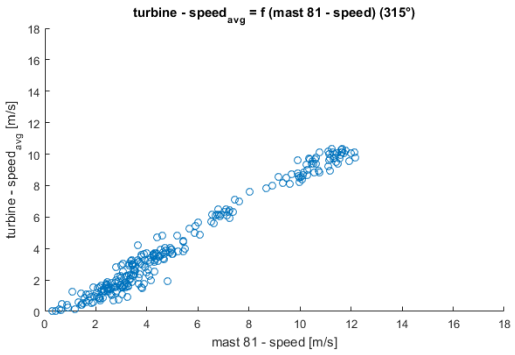

(b) Met mast 81 in angular sector $315°$

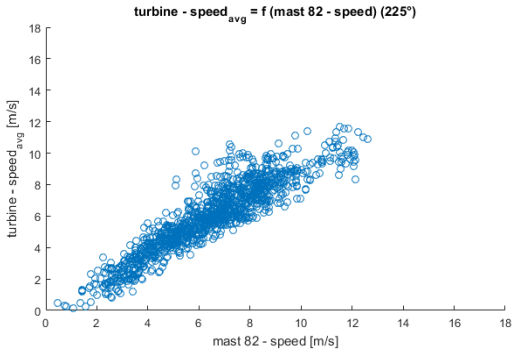

(c) Met mast 82 in angular sector $225°$

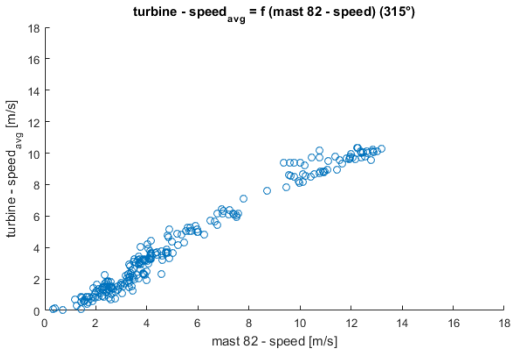

(d) Met mast 82 in angular sector $315°$

Figure 3.8: Comparisons between met masts data and turbines average data

the met masts data to be used in the model. As a last attempt, the average of the measurements of the two met masts was briefly used. However, no significant improvement was noticed. Consequently, the input to the model describing the wind speed was chosen to be the average of the wind speeds collected by the turbines, so that its value could be easily estimated from the measurements without further calculations.

3.5.2 2^{nd} Input: Direction

While the calculations to find the input describing the wind speed were carried out, also the ones relative to the other input were performed. This second input is needed, like the previous one, to find which column of the $3D$ array containing the deficits consider. In this case the choice was easier than in the case of the first input. In fact, the input chosen was simply the average of the directions of all the reliable turbines. However, such a calculation was not as simple as it may seem. Problems rose because in some cases it happened to make the calculations with values close to $0°$. This meant that there were values on both sides ($> 0°$ and $< 360°$). In order to solve this problem an external function of MATLAB was used.

3.6 Conclusions to the Chapter

To sum up this chapter, the structure of the physical model was defined and justified.

- The Jensen model was chosen as the wake model to be used
- The set of power curves that was considered the most reliable one is the one obtained from the medians and boxplots, with speed bins of $0.5m/s$ and no outliers
- The wake decay coefficient was set equal to 0.075
- The average speed and the average direction among the turbines were chosen as the inputs to the model

Moreover, the evolution of the wind field within the wind farm was explained and 6 turbines were found to be unreliable because they failed to measure either the wind speed or the wind direction.

Chapter 4

Results of the Physical Model

The results of the model elaborated and explained in Chapter 3 are exposed in this chapter. Several methods have been used in order to verify the validity of the physical model. Some of them will be explained in the following sections together with the explanations of the results and their consequences.

4.1 Degradation of the Wind

The degradation of the wind could be studied thanks to the deficits found previously using the method explained in Section 3.4 based on the Jensen model [1]. Thanks to the deficits, it was possible to see the evolution in space of the wind speed in the area of the wind farm. In order to properly represent in a graphical way this degradation, contour plots were used as they perfectly suit the situation. Contour plots are able to show how the wind speed behaves by collecting the results from the model and interpolating them to find the wind speed profile in the space among the turbines. The area of the plot (and ideally, also of the wind farm) is then divided in different areas depending on the wind speed estimated. An example of the results obtained using contour plots is shown in Figure 4.1.

The vector present in the graph stands for the input that has been used for the model while the contours in the graph characterise the circumscribed area based on the estimated wind speed in that portion of the wind farm. The sense of the vector indicates the direction the wind is blowing and the magnitude and the number nearby the mean wind speed estimated from the reliable turbines, as explained in Section 3.5. On the other hand, the black dots indicate the location of the turbines. The same type of plot was used to represent graphically the degradation of the wind as described by the measurements of the anemometers located on the nacelles of the turbines. These new results are shown in the other contour plot, in Figure 4.2.

In the case of Figure 4.2, the magnitude of the vector symbolises the maximum wind speed experienced by any of the turbines, which can also be seen as the undisturbed one. Consequently, the values shown in Figures 4.1 and 4.2 must not be compared, as they represent two different things. Since the speeds at the turbines are given by the model and the empirical data respectively, if the model works, the final result will be similar to the one obtained from the data, which means that the contour plots should

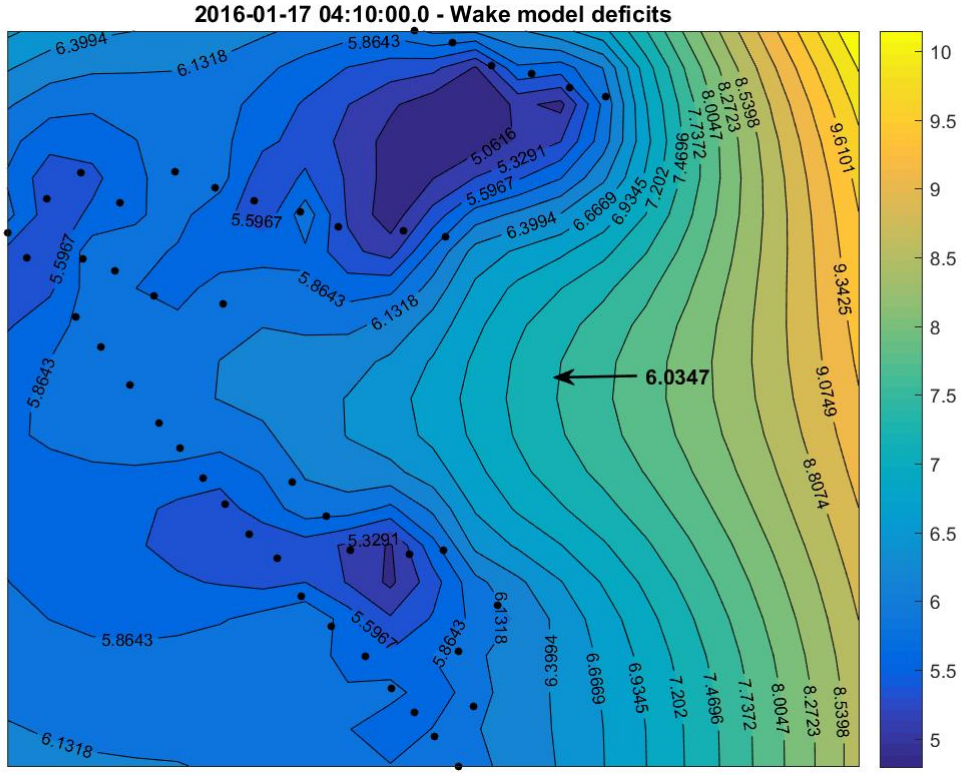

Figure 4.1: Contour plot representing the spatial degradation of the wind on $17/01/2016$ at $04 : 10$ according to the physical model

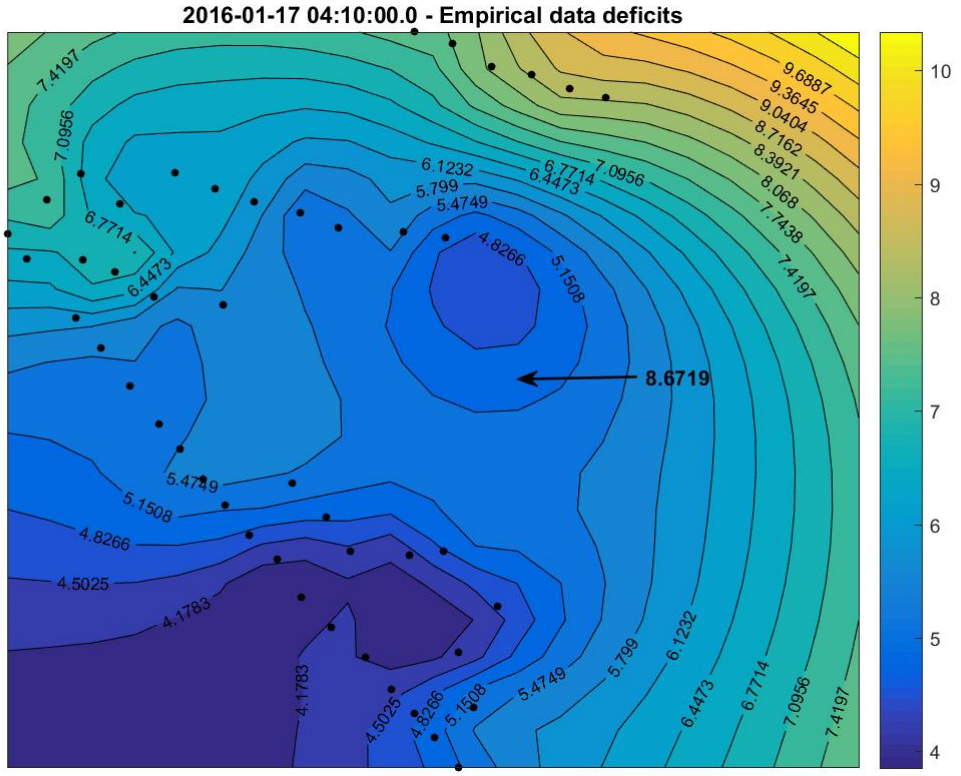

Figure 4.2: Contour plot representing the spatial degradation of the wind on $17/01/2016$ at $04 : 10$ according to the wind data

be similar. Unfortunately, this does not happen and the two contour plots differ one from the other. It can be noted how in both Figure 4.1 and Figure 4.2 the wind speed outside of the wind farm reaches much higer values than any turbine, even the ones that experience undisturbed wind. This happens because the only measurements available are the ones of the turbines and therefore, beyond them there are no bonds to limit the evolution of the wind speed and keep the interpolated value realistic. These shortcomings represent a first clue that the physical model formulated in Chapter 3 might not work and obtain the desired results.

4.2 Evolution of the Accumulated Difference

One possible problem that may happen when working with optimisation algorithms and minimisations in particular is that the stationary point located during the calculations might be a local one, while the one needed is the global minimum or maximum. To avoid this issue, the algorithm written with the objective to find the optimal wind speed u_{opt} (as explained in Section 3.5.1) was tested to verify that the minimum it identified previously was a global minimum and not a local one. To do so, the real conditions measured during the 10-minute time slot were compared with the results of the model obtained by always varying the wind speed U_∞ in equation (2.2), which is different from varying the input to the model. It is different because in this part of the study, the deficits have been assumed constant as in reality the wind conditions do not change. During these calculations, it happened only once that the wind speed U_∞ was equal to the average wind speed. The accumulated difference Δu_{acc} in this case has therefore been estimated as exposed by equation (4.1).

$$\Delta u_{acc} = \sum_{i=1}^{N_{turb}} |u_{measured,i} - u_{model,i}| \tag{4.1}$$

With $u_{model,i}$ that has been calculated in the following way:

$$u_{model,i} = U_\infty \cdot (1 - \Delta\overline{U}_i) \tag{4.2}$$

The evolution of the accumulated difference when varying U_∞ is shown in Figure 4.3.

It can be clearly seen how there is only one minimum, which therefore is both local and global. Consequently, the minimum found with the optimisation during the creation of the model is certainly a global one. Such a behaviour could have been easily predicted from equation (4.1), since without considering the absolute value, Δu_{acc} varies linearly with the speed resulted from the model. The demeanour also suggests that the model cannot be further improved under this aspect.

4.3 Comparison of the Wind Speed at the Turbines

Since the model has been created to predict the power output of the wind farm summing the power production of each single wind turbine, a suitable method to check the validity of the model is to compare

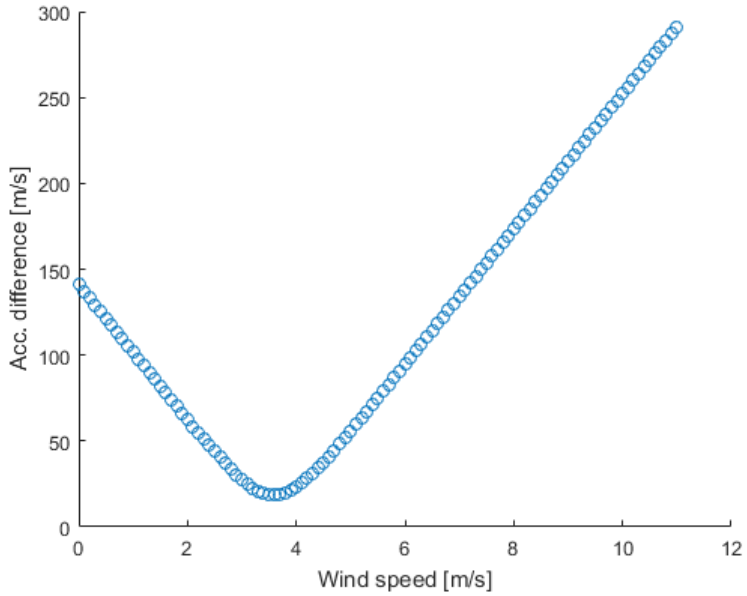

Figure 4.3: Behaviour of the accumulated difference when the undisturbed wind speed is varied

the measured wind speed at each turbine with the one estimated by the model itself. This comparison was made for a random time slot and was represented graphically in a normal cartesian graph. Such a graph is shown in Figure 4.4.

In Figure 4.4 there are two graphs because each of them is a better example of a particular issue that has been noted with the results of the model. In these graphs, on the x-axis there is ideally the number of the turbine, while on the y-axis the wind speed is represented. On the x-axis there are no labels because they would have created confusion without adding important information since this graph was plotted to check the validity throughout the wind farm and not to detect problems at the location of particular turbines.

Figure 4.4(a) better represents the tendency of underestimating the deficits by the model. Even though in Figure 4.4(b) this does not happen, the underestimation of the deficit is a problem that occurred very often when running the model. This issue was detected mostly along some particular directions. These directions were the most unfavourable ones because the wind was blowing parallel to the main line of turbines, thus creating numerous wakes that added one another.

Figure 4.4(b) shows, at least for the first turbines, how it was not possible for the model to create differences in wind speeds when no interception happened. In fact, according to the model most of the first turbines experience the same wind speed because the wind direction does not create interceptions between wakes and rotors in that area. As it can be seen from the measurements, this is not the case and actually, those same turbines in reality undergo some of the lowest wind speeds in the whole wind farm. Generally speaking, it is extremely unlikely that turbines encounter the same wind speed, not even if they are adjacent ones. This problem is less evident in Figure 4.4(a), as the measured speeds are much closer to the average wind speed used as input to the model.

In an attempt to improve the model, time was spent thinking about an additional feature to the model

that could make the results of the model closer to the measurements. This feature would make the curve created by joining all the points representing the results of the model more similar to the curve found doing the same with the points indicating the measurements. Unfortunately, since the model was purely based on the deficits created by the wakes, no additional method could be thought of in order to make the two curves more similar.

4.4 Turbine Experiencing the Highest Wind Speed

A useful feature of the model created is the ability to let the user know which turbine experiences the highest wind speed according to the measurement data and which should be the deficit that it expe-

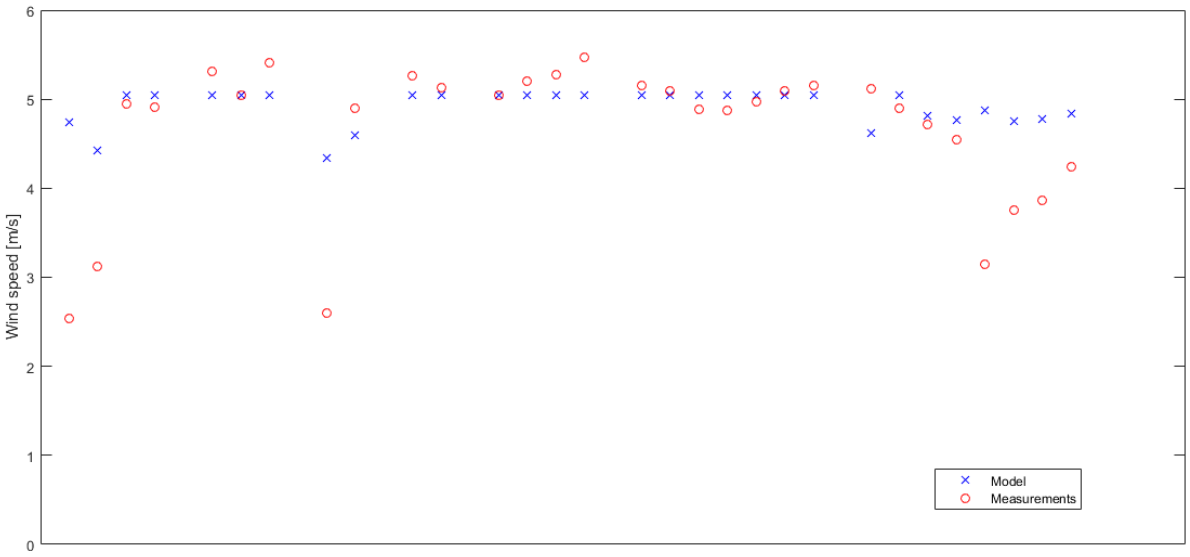

(a) First comparison

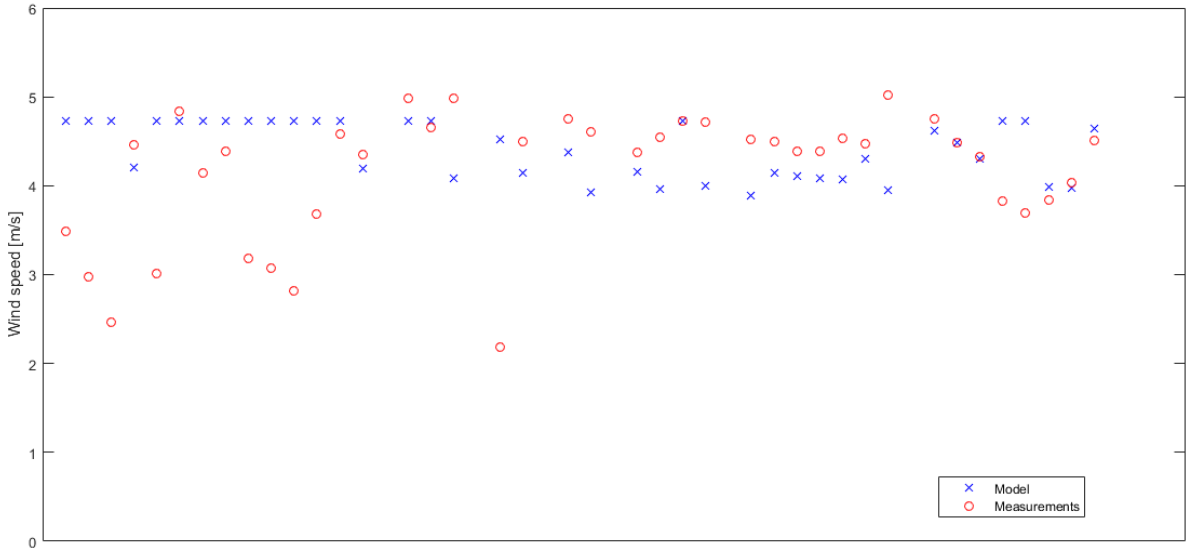

(b) Second comparison

Figure 4.4: Two comparisons of the wind speed at the location of each turbine according to the physical model

riences according to the model. It comes without saying that given the structure given to the model, this turbine should experience a deficit equal to zero. When long periods of time were analysed and simulated, the value of this deficit was always shown as soon as the calculations for a specific time slot were over. It sometimes happened that the value of this deficit was different from zero, which means that according to the model not only that turbine was not the one experiencing the highest wind speed, but it was also in the wake of another turbine. This aspect also highlights the presence of problems within the formulation and use of the model, most probably related to the lack of consideration of additional aspects that affect the performance of a wind turbine and a wind farm in general.

4.5 Shortcomings of the Wake Models in Literature

Given the results exposed in the previous sections of this chapter, it can be stated that the physical model created for the wind farm did not work. The aspects considered by the model were not enough to reproduce a realistic behaviour of the wind inside the area of the wind farm. In fact, even though analytical wake models are still the most widely used means of calculation in predicting the wake effect they cannot yet be applied to all the possible situations and layouts. Two aspects that were not given enough attention when the first analytical models were created are the roughness and the atmospheric stability [35]. These aspects were sequently considered and new versions of the Jensen model were created. An example is the new formulation of the wake decay coefficient k for the infinite wind farm case, which however is not the case of the farm considered in this study [36]:

$$k = \frac{u_{*free}}{u_{hfree}} = \frac{\kappa}{\ln\left(\frac{h}{z_0}\right) - \varphi_m\left(\frac{h}{L}\right)} \tag{4.3}$$

where:

- u_{*free} is the undisturbed friction velocity
- u_{hfree} is the wind speed at the height of the hub
- κ is the von Kármán constant and it's equal to 0.4
- h is the hub height
- z_0 is the roughness length
- $\varphi_m(h/L)$ is the correction relative to the stability (L) at hub height

Other research relative to the wake decay coefficient was carried out. An interesting formulation of the wake decay coefficient relates it to the roughness length z_0, which is connected to the ambient turbulence [37]:

$$k = \frac{0.5}{\ln\left(\frac{h}{z_0}\right)} \tag{4.4}$$

Further analysis led to the suggestion that its value is not constant and that it varies also along the downstream direction. In fact, the wake decay coefficient has been found to be dependent also on additional aspects, which are the shear-generated turbulence and the one originated by the turbine [38] [39] [40]. The second aspect limiting the validity of the Jensen model is the assumption of the top-hat behaviour of the deficit within the wake, which does not describe the phenomenon in a realistic way. Consequently, the distribution of the speed is far from being truthful. In fact, the velocity within the wake varies according to a Gaussian or a trigonometric distribution. This means that, contrarily to what has been mentioned about the Jensen model in Section 2.1.1, the speed does not actually varies depending on a single dimension, but changes along two dimensions [41]. A deeper explanation of a new model taking these aspects into account is presented in Appendix B.

Comparing results obtained from the application of the Jensen model to CFD simulation, it has also been found that using the values of coefficients suggested originally by Jensen [1] and in numerous other publications the wind speed predicted at the centreline is overestimated [35]. This statement is in accordance with what has been experienced with the results of the model here formulated. The same comparisons with CFD simulations highlighted that even in the most basic case like the one of a single wind turbine, the predicted expansion did not reproduce the results of the simulation. In order for the Jensen model to produce results closer to the simulations the values of the parametres had to be optimised. Still, the optimised results were in agreement with the CFD simulations only after many diameters (usually around 20 or more).

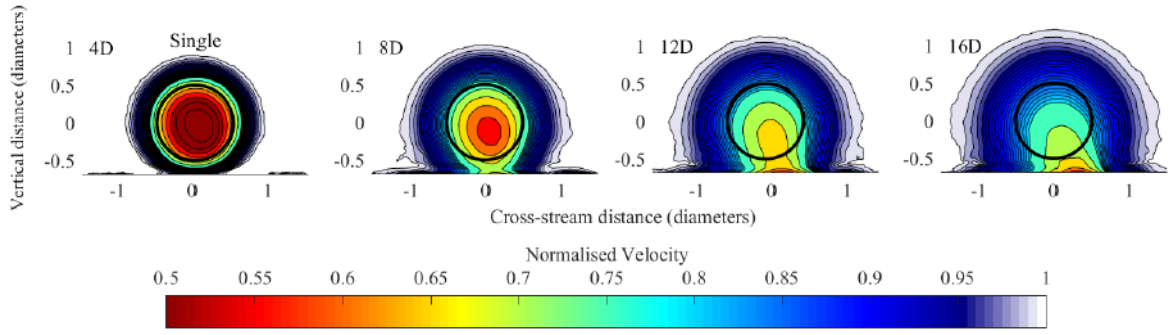

Figure 4.5: Shifting of the point with highest deficit within the wake (modified from [18])

Another problem that was detected within the model was relative to the superposition of the wakes. The models listed in Section 2.2 are reliable when isolated single turbines are analysed. However, they are not as reliable when several turbines come into play. In fact, there are numerous physical phenomena that are not accounted for when wakes are combined using those models. These phenomena appear in all the possible combinations between a wake and a rotor: when the two rotors are aligned, when the wake partially hits the rotor downstream and even when there is no interception between rotor and wake. One of the phenomena not considered is the shifting of the point with the highest deficit within the wake even when the turbine considered is isolated. In fact, this point moves towards two directions: rightwards because of the rotation given by the rotor and downwards. The movement happens towards the ground because the wake recovers energy faster in the upper side than in the lower side. This shifting is not

considered in the softwares used to predict the deficits and has only be treated with Dynamic Wake Meandering (DWM) [20] in the academic field. The movement of the wake here described is graphically represented in Figure 4.5.

Another physical phenomenon not accounted for in analytical models is the faster recovery of the wake behind two rotors. This happens when the two turbines are in line, therefore it is not a very common situation, but still the most studied one. When such a phenomenon happens, if there is a third turbine in line with the two previous ones and the same distance between turbines was used, the third turbine will end up producing more power than the second one [42]. This phenomenon is clear in Figure 4.6(b), where it is possible to note that the third turbine in row C with the layout and wind direction represented in Figure 4.6(a) produces a higher output than the second one.

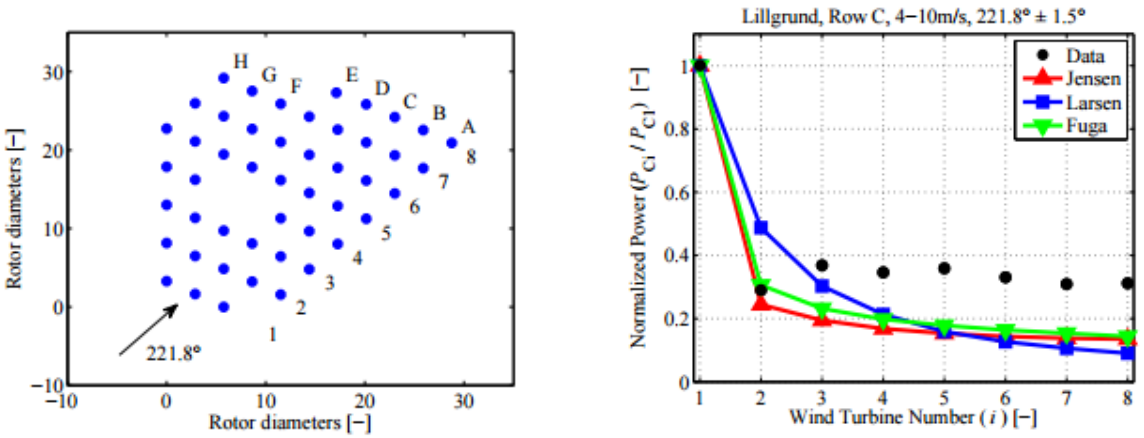

(a) Lillgrund wind farm layout

(b) Normalised output in row C of Lillgrund wind farm

Figure 4.6: Graphical explanation of the faster recovery after two turbines (modified from [42])

Also, it can be seen how this phenomenon has aftermaths on the following rotors as well. Fuga (which is mentioned in Figure 4.6(b)) is a linearised CFD model. This phenomenon is represented also in CFD simulations. In fact, comparing the deficits at $4D$ and $8D$ in Figure 4.5 with the ones at the same distance from the second wind turbine in case of inline rotors, i.e. $12D$ and $16D$ in Figure 4.7, respectively, it can be noted that the deficit created by the wake is just slightly greater.

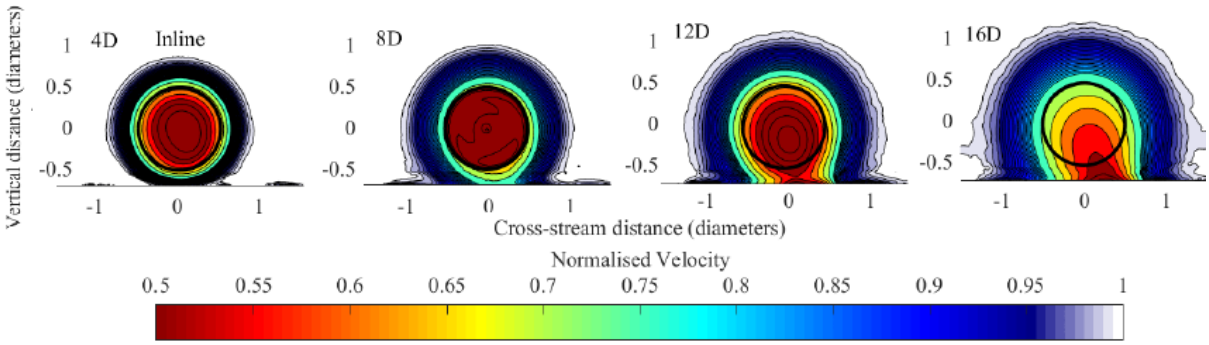

Figure 4.7: CFD simulation of the wake in case of two inline wakes (modified from [18])

The reason why the recovery happens faster after two turbines is the increased turbulence after the

stream meets the second turbine. The lack of consideration of this aspect has certainly created great discrepancies with reality in case of wind blowing parallel to the main line of turbines.

Even though a simple approach was used in case of partly offset rotors, they play an important role in the lack of consistency of results of analytical wake models. The deficit that is created by the two wakes only partly overlapping can be significantly higher than the one predicted using the superposition methods listed in Section 2.2. Obviously, this underestimation translates into a discrepancy in the power output. It is thought that the reason why the deficit is greater is the lower amount energy available between the two wakes. This leads to longer times and distances needed for the wakes to recover and reach again the undisturbed conditions. Because of the less energy available, the wakes recover energy from the undisturbed flow above and on the other side. The difference in behaviour of the deficit can be observed in Figure 4.8, where the CFD simulation in the case of two partly offset wakes is depicted.

Another difference between this case and the previous ones is in the spatial distribution of the Turbulent Kinetic Energy (TKE). In fact, in the previous cases it was almost symmetrical with respect to the vertical diameter of the rotor, while with two partly offset wakes the symmetry does not happen anymore.

Finally, one last phenomenon concerning the interaction between wakes happens even when they do not intercept each other. When two wakes are fully offset, the velocity field is affected mainly by the fact that the wake created by the upstream turbine is forced to the opposite side of the downstream wake. This happens because the downstream wake creates a different pressure field, which is able to force the upstream wake to move to the opposite side. This aspect can be observed comparing Figure 4.9 with Figure 4.5, especially at the downstream distance of 16 diameters from the first rotor. It is even better shown in Figure 4.10, where the interaction between the two wakes is represented from above.

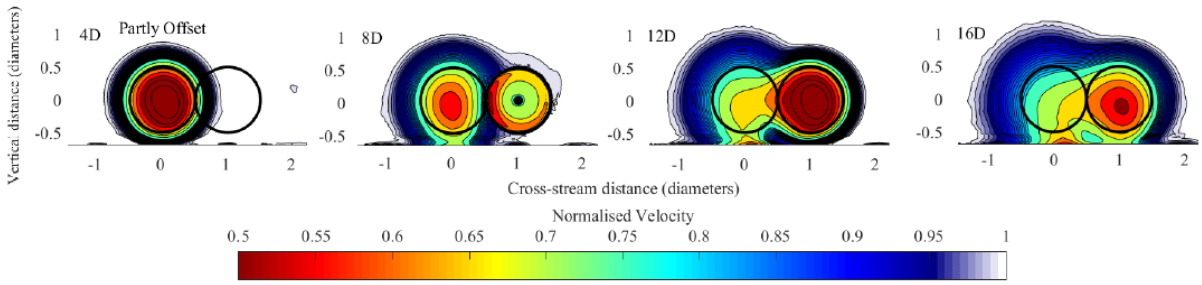

Figure 4.8: CFD simulation of the wake in case of two partly offset wakes (modified from [18])

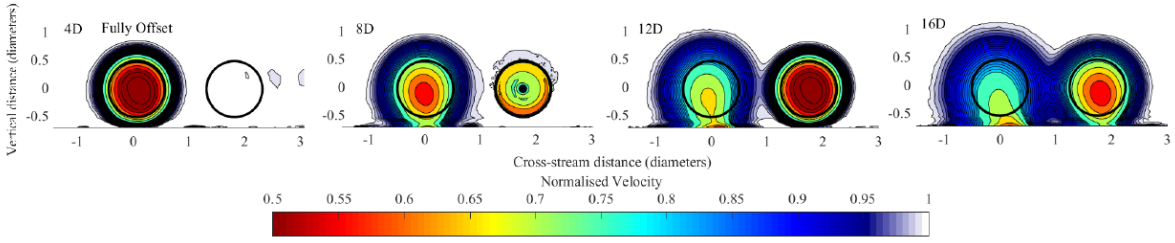

Figure 4.9: CFD simulation of the wake in case of two fully offset wakes (modified from [18])

It is interesting to note how the downstream wake does not suffer significant modification. In fact, comparing the velocity profile on the right at the distances of $12D$ and $16D$ of Figure 4.9 with the one

calculated for the dowstream distance of $4D$ and $8D$ in Figure 4.5 respectively it can be observed that no considerable difference is present. A similar phenomenon happens with the TKE field, which again is slightly pushed to the opposite side by the pressure field of the downstream rotor.

This aspect is not considered at all in the analytical model but it could be able to create noteworthy differences between a model and reality. This factor could have played an important role in a model like the one explained in Chapter 3, where the top-hat behaviour suggested by the Jensen model is maintained. In fact, not including this shifting of the upstream wake might have led to neglecting some interactions that actually happened.

To sum up this section, the three main aspects that are not considered by the currently available models are the following:

1. if the two wakes are aligned, the resulting one will recover faster than the one produced by a single turbine

2. if they intercept each other only partly, both of them will recover along a more extended distance

3. a certain wake can be forced to move by the pressure field created by another wake

The model that was found to be the one to best represent the actual behaviour of the single wake and its interaction with other ones is the Ainslie model [18]. Unfortunately, as stated before, this model was not developed to be easily implemented into a model, but to properly describe the wake itself [9].

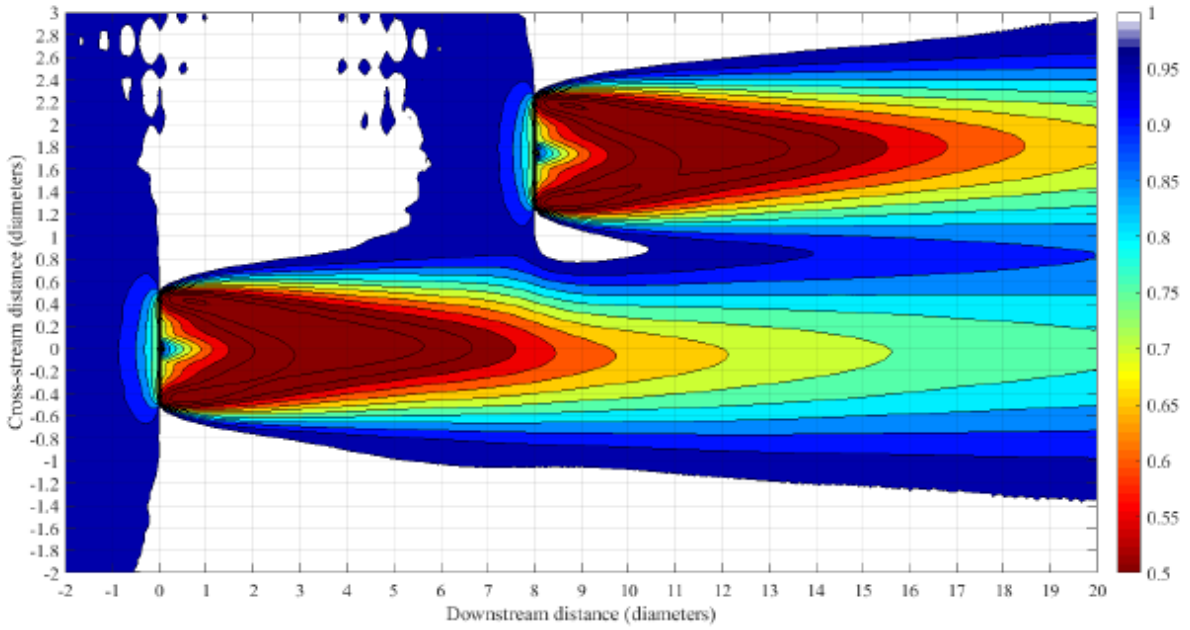

Figure 4.10: View from above of the interaction of two fully offset wakes [18]

4.6 Additional Shortcomings of the Model

To conclude this chapter, some additional reasons why the model did not manage to predict the power output of the wind farm will be reported. An important aspect not considered by the model but that could have played an important role in the success of the model is the inclusion of the wakes reflected by the ground. If the distance is big enough, a wake can reach the ground, be reflected and eventually be intercepted by a rotor both in its "direct" component and in its reflected one. A possible solution to this problem was to consider a second wind turbine symmetrical with respect to the ground and check if its wake was intercepted downstream. Therefore, using this method there would have been the real turbine which hub would have had coordinates (x, y, z) and the immaginary one with the hub at coordinates $(x, y, -z)$. This approach is the same used when the propagation of the plumes from the chimneys of the power plants is studied.

Another element that could have been considered is the variability of the ground within the wind farm. In the model, the only way the ground was taken into account was by selecting the wake decay coefficient, which value however was set according to values found in literature. Consequently, not only the model considered the effect of the ground on the wind profile constant but it also assumed the influence of the ground equal to a certain value which is not necessarily the real one.

The lack of consideration of some potential and verified obstacles is another one of the possible reasons why the model failed to reach its goals. Among the verified obstacles, the two met masts present in the wind farm can certainly be listed. However, there were other potential obstacles that were either not considered or not possible to consider. The main example can be the possible presence of the hill mentioned in Section 3.3 and detected using multiple consecutive quivers. The roads created to facilitate the installation of the wind turbines and their maintenance are other possible obstacles that could perhaps affect the wind field within the wind farm.

However, all these reasons are probably of secondary importance compared to the lack of a real wind field study of the area without the presence of the turbines. In fact, the physical model as it was explained in Chapter 3 was able to predict velocity deficits only if the rotor of a certain turbine was intercepted by the wake of an upstream one. Consequently, according to the model several turbines experienced the same wind speed even though they were far away from one another just because they were not in the wake of another one. This is obviously not realistic as the wind is extremely variable in space even in limited distances, not only along the same direction it blows but also in the other. This aspect created significant discrepancies in different directions of the wind. For example, when it was blowing perpendicular to the main line of turbines they were all experiencing undisturbed wind speed, but certainly not the same wind speed. The fact that the two most external turbines are around $8km$ away one from the other makes this statement stronger, because it is not realistic for the wind to be constant on such a wide area. However, this element created problems also in other cases where turbines in completely different conditions were assumed to encounter the same wind speed just because none of them intercepted any wake. This reason weighed more in the failure of the model because the main problem was not the wrong estimation of the velocity deficits (which however played an important role),

but the lack of defict values due to other effects that could have characterised the wind farm in a more thorough way.

A final possible reason of the lack of success in predicting the output of the farm is of a different nature compared to the one previously listed. The fact that the data provided were organised in 10-minute bins did not allow to properly consider the fluctuations to which the wind speed is subject to. Even though to a lesser extent, the same can be said for the wind direction as well. Within the 10 minutes the speed could peak, increasing significantly the energy produced during that interval but only slightly affecting the mean wind speed. As it has already been said, this happens because the power produced by the turbine is proportional to u^3.

4.7 Conclusions to the Chapter

In this chapter, the results obtained from the application of the physical model are exposed, highlighting its areas of failure and the relative reasons. The physical model failed to reproduce the wind field within the wind farm and therefore the wind speed experienced by any wind turbine. Also, no real possibility to improve the model as it is was found because only one aspect is considered. Even in this aspect, the phenomena considered are very limited compared to the ones actually happening in reality. To conclude the chapter, some other reasons why the model did not work are listed. Among them, the main ones seemed to be the lack of a study about the wind field before the installation of the turbines and the use of 10-minute time gaps, which are too long to properly describe a stochastic resource like wind.

Chapter 5

Empirical Model

After realising that the physical model exposed in Chapter 3 failed to predict the output, a new approach to the problem was needed. Given the numerous shortcomings of the previous model, improving it would have been far too complicated and time-consuming. Therefore, it was thought that the best way to reproduce what actually happens in the wind farm was to use the measurements from the farm itself. This way, all the elements would have been included even though it would have been impossible to discern the contribution of each aspect. Because of this element, this model can be defined as a ”black box”. To sum up, with this new approach, the deficits were not found from a wake model anymore, but using the data from the turbines. The measurements would have been then used to perform a statistical analysis of the conditions of the wind speed at the location of each turbine. Because of the nature of the calculations, the model will be addressed as both empirical and statistical model.

5.1 Elements Maintained from the Physical Model

Even though the approach to the problem is completely different, some aspects of the physical model could have been maintained. In fact, these elements were not strictly related to the wake models, but nonetheless were extremely important in the formulation of the previous model. The elements that remained unvaried are mainly two: the power curves and the list of unreliable turbines.

1. The power curves used previously were not changed as they did not have part in the failure of the physical model. The power curves were found dividing the velocity in bins of the size of $0.5m/s$ and calculating the median for the power of each bin after having eliminated the outliers. Their role in the calculation of the deficits was marginal as they were used to know the power output from which it was then possible to find C_p and consequently C_T, which is required according to equation (2.2). Afterwards, the power curves were used in order to find the output of each turbine after the wind speed at that location was estimated.

2. Having found a list of unrealiable turbines previously to this second approach to the creation of the model turned out to be an extremely useful aspect. In fact, since this second model is based

on the data of the turbines themselves using data which cannot be trusted would have certainly led to unreliable results. The turbines that were labelled as not reliable were overall 6, with 2 encountering problems mainly with the wind velocity and the remaining 4 having issues with the wind direction

5.2 Inputs to the Model

As explained for the physical model in Section 3.5, also in this second approach to the prediction of the power production the definition of two inputs is necessary. Again, one of the deficits will describe one quality relative to the wind direction, while the other will allow to characterise the wind speed throughout the whole wind farm.

5.2.1 1^{st} Input: Speed

In this second model, the choice of the input relative to the wind speed was not as difficult as the one made in Section 3.5.1. Because of the organisation of the data (exposed in Section 5.3) and the calculations necessary to estimate the wind speed experienced by a particular turbine (explained by the simple equation (5.1)) something able to describe the undisturbed wind speed was needed. The best data able to describe such a property of the wind is the maximum speed measured by any of the turbines within the wind farm. Obviously, the unreliable turbines were not considered when the maximum speed u_{max} was computed.

$$u = U_\infty \cdot (1 - \Delta\overline{U}) \tag{5.1}$$

The maximum speed u_{max} was chosen as the input relative to the wind speed because there was no other possible data able to substitute the undisturbed conditions of the wind because of the lack of a meteorological station (or met mast) external to the area limited by the turbines but still near enough to be reliable also in the wind farm. The maximum wind speed was calculated by collecting all the data for that particular time slot, eliminating the ones relative to the unreliable wind turbines and then identify the maximum value among the ones left.

5.2.2 2^{nd} Input: Direction

The other quality of the wind that was necessary to characterise was the direction the wind blows from. Two possibilities were considered as possible inputs to the model: the average wind direction among the turbines and the direction measured by the turbine experiencing the maximum wind speed, which again would be considered the undisturbed wind. Some pros and cons were listed for both possibilities before deciding on how to continue. For the average direction the following ideas were used to decide whether this trait was a good choice:

- It certainly suffers the influence of some factors that characterise the wind field within the wind farm. These factors could be attributes of the whole area or just local ones that affect the wind only in the surrounding area

- Since this value is obtained from several ones it is probably less influenced by these aspects as some of them might delete one another. Consequently, an average value should be less affected by these factors compared to a measured one

- If the model is kept as it is here formulated without the implementation of external data it should be easier to estimate the average wind direction compared to the undisturbed one

On the other hand, the qualities relative to the direction of the undisturbed wind that were identified were the following:

- If the one found is really the direction of the undisturbed wind, then it should not be affected by any other turbine and it should consequently be more reliable than any other data available

- There might be problems when finding which one of the turbines experiences the highest wind speed and therefore should be consulted in order to know the value of the direction of the undisturbed wind

- In order to solve this problem a table listing which turbine undergoes the highest wind speed according to the wind direction could be created

The final choice was eventually the average wind direction. The main reason for this decision is related to the last bullet point relative to the direction of the undisturbed wind. In fact, it would not be possible to know which direction to consider in order to find the turbine experiencing the highest wind speed if that same wind speed would be needed to find the direction itself. Using that solution would create a circle that would not allow a proper solution.

In order to properly calculate the average wind direction, the data for the 10 minutes of time slot were collected, then the data relative to the unreliable turbines eliminated and finally the requested data computed.

5.3 Organisation of the Data

In this second model, the data from the measurements are divided according to the input relative to the wind direction (average wind direction as explained in Section 5.2.2) and to the input related to the wind speed entering the wind farm (maximum wind speed as disclosed in Section 5.2.1). The data relative to the wind direction were organised in 36 bins representing angular sectors of 10° each. On the other hand, the velocity data were collected in bins of the size of $0.5m/s$, with the exception of the one representing the lowest speed and the one representing the highest one. The speeds were divided into these bins according to the following criteria:

- if the wind speed was lower than $3m/s$ the data was part of the first bin
- if $u \geq 14m/s$ the data was collected in the last bin
- for values in between, data were gathered in a certain bin labelled by the median wind speed. To better clarify, one piece of data was part of bin X if its value was within $X - 0.25$ and $X + 0.25$, where X could have been a value like $3.25m/s$, $3.75m/s$, $4.25m/s$ up to $13.75m/s$

Overall, the data was therefore collected depending on both the average wind direction and the maximum wind speed. Consequently, having 36 bins for the wind direction and 24 for the wind velocity, the global number of bins was $36 \cdot 24 = 864$. Unfortunately, some specific conditions never happened and consequently it was not possible to collect data in certain bins. The data from each turbine in a certain time slot were thus collected depending on the average wind direction and the maximum wind speed experienced by any of the turbines during those 10 minutes. After separating and collecting all the data in the specific bin it was possible to average them. The turbine that was found to undergo the highest average wind speed when those particular conditions happened was considered to be the one experiencing the undisturbed wind. Consequently, the wind velocity at the location of that specific turbine could be indicated as U_∞. After obtaining the averages for each turbine in each bin in which data were available it was possible to find a deficit describing the behaviour of that particular turbine when those specific conditions (wind speed and direction) occurred. To do so, the reverse of equation (5.1) was used:

$$\Delta\overline{U} = 1 - \frac{u}{U_\infty} \tag{5.2}$$

According to equation (5.2) and what has just been stated about the turbine experiencing the highest wind velocity, such a turbine has deficit $\Delta\overline{U} = 0$. Using equation (5.1) and having all the deficits is then possible to estimate the wind speed at the location of each turbine.

5.4 Solution for the Unreliable Turbines

The way the data were organised left the unreliable turbines without a deficit that would later be used to estimate the wind velocity at their location, according to (5.1). Consequently, a method able to find the value of the wind speed at those locations was needed. Given the unreliability of the deficits estimated with the Jensen model, this option was discarded. Initially, the choice was to extrapolate the value of the wind speed from the contour plots. When checking the results obtained from the extrapolation, it was noted that the velocities were overestimated by a great deal and therefore this model was not considered the most suitable. In the following attempt, the wind speed was found making a simple average among the turbines that were nearer than $1km$ from the one analysed. The value of $1km$ can be considered a good choice as the the highest minimum distance between any two turbines within the wind farm is equal to $707m$. Consequently, it could not happen that any of the unreliable turbines would remain without an

estimated wind speed at its location. Even though the results produced by this method made sense, it was thought that it could have still been improved.

Considering the simple average among the near turbines did not acknowledge in any way the distance from the measurements. Therefore, it was decided to give more importance to the data collected by the anemometers nearest to the analysed turbine. The best way to do so was deemed to be a weighed average using the reciprocal of the distances from the analysed turbine (indicated as T in Figure 5.1) as weights.

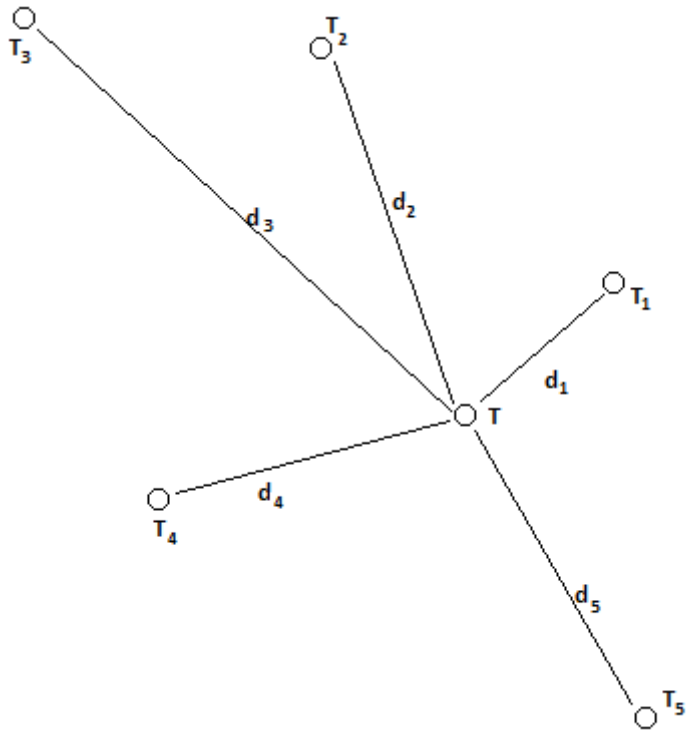

Figure 5.1: Example of layout used for equations (5.3) and (5.4)

Figure 5.1 is used as support to explain the calculations carried out to find the wind speed at the locations of the unreliable turbines, indicated with T. Assuming that each turbine is experiencing a wind speed u_x where x stands for the number of turbine and therefore varies between 1 and 5, the wind speed at the location of T is calculated according to equation (5.3).

$$u = \frac{\frac{1}{d_1} \cdot u_1 + \frac{1}{d_2} \cdot u_2 + \frac{1}{d_3} \cdot u_3 + \frac{1}{d_4} \cdot u_4 + \frac{1}{d_5} \cdot u_5}{\frac{1}{d_1} + \frac{1}{d_2} + \frac{1}{d_3} + \frac{1}{d_4} + \frac{1}{d_5}} \tag{5.3}$$

In order to avoid making this calculation every time the program was launched and given that the wind speed at a certain turbine is linearly proportional to the speed deficit ($u \propto \Delta\overline{U}$ according to (5.1)) the same formula was used to compute the deficits for the unreliable turbines. This way, the calculations could be done just once and the final result was not modified in any way.

$$\Delta\overline{U} = \frac{\frac{1}{d_1} \cdot \Delta\overline{U_1} + \frac{1}{d_2} \cdot \Delta\overline{U_2} + \frac{1}{d_3} \cdot \Delta\overline{U_3} + \frac{1}{d_4} \cdot \Delta\overline{U_4} + \frac{1}{d_5} \cdot \Delta\overline{U_5}}{\frac{1}{d_1} + \frac{1}{d_2} + \frac{1}{d_3} + \frac{1}{d_4} + \frac{1}{d_5}} \tag{5.4}$$

5.5 New Deficits

Giving a look to the deficits obtained is a good way to highlight the differences in results between the two models. Since both the velocity and the direction gaps have different sizes in the two models, the tables represent slightly different things. In fact, Table 3.1 shows the speed deficits valid for speeds ranging between $5m/s$ and $6m/s$ while Table 5.1 is used when the velocity is between $5m/s$ and $5.5m/s$ and Table 5.2 for values varying between $5.5m/s$ and $6m/s$. In this section, two tables are reported so that the same speed interval is covered. The differences in the results can be noted anyway because of the significant discrepancies in the values of the deficits.

In Table 5.1, the boxes with deficit equal to 0 indicate the wind turbines that in those angular and speed sectors experience the highest wind speed within the wind farm. By comparing Table 5.1 and Table 3.1 it can be noted how the deficits found from the empirical model are significantly higher. This most probably happens because all the aspects listed in Section 4.5 and Section 4.6 and possibly even more are taken into account, even though it is not known to what extent. Also, it is easy to see how for each angular sector there is only one deficit equal to 0 and that the amount of deficits close to that same value is extremely limited. These aspects highlight once more how not enough disturbances were considered in the physical model.

By comparing Table 5.1 and Table 5.2 it can be noted how the deficits are different even for the same angular sector. This probably happens mainly for two reasons:

1. The different value for the thrust coefficient C_T
2. The variability of the wind; in fact, even though the average conditions are extremely similar, the conditions within the 10 minutes of the slot could be significantly different

The main reason is probably the second one, as C_T should not vary significantly with a speed difference of $0.5m/s$ and also because according to the Jensen model the deficit $\Delta\overline{U}$ varies with $C_T^{0.5}$.

Table 5.1: Matrix containing the deficits for an average wind speed equal to $5.25m/s$ in a 10-minute slot for the empirical model

	0°	10°	20°	30°	40°	50°	60°	70°	80°	90°	100°	110°	120°	130°	140°	150°	160°	170°	180°	190°	200°	210°	220°	230°	240°	250°	260°	270°	280°	290°	300°	310°	320°	330°	340°	350°
$T1$	0.075	0.120	0.081	0.268	0.206	0.240	0.150	0.137	0.235	0.268	0.215	0.090	0.013	0.117	0.136	0.228	0.119	0.204	0.288	0.264	0.186	0.233	0.153	0.175	0.090	0.120	0.165	0.164	0.152	0.103	0.278	0.357	0.233	0.061	0.033	0.010
$T2$	0.116	0.128	0.104	0.270	0.290	0.320	0.238	0.204	0.242	0.297	0.259	0.225	0.397	0.425	0.323	0.317	0.205	0.248	0.315	0.323	0.235	0.270	0.206	0.206	0.121	0.150	0.197	0.179	0.158	0.068	0.194	0.311	0.306	0.169	0.094	0.075
$T3$	0.104	0.143	0.142	0.235	0.384	0.335	0.241	0.255	0.248	0.295	0.254	0.155	0.262	0.440	0.386	0.357	0.199	0.254	0.312	0.329	0.254	0.266	0.213	0.199	0.113	0.141	0.194	0.166	0.150	0.126	0.327	0.388	0.255	0.084	0.088	0.080
$T4$	0.134	0.149	0.138	0.211	0.408	0.328	0.296	0.239	0.257	0.297	0.282	0.260	0.431	0.389	0.274	0.267	0.175	0.247	0.311	0.333	0.263	0.269	0.195	0.190	0.113	0.142	0.183	0.169	0.109	0.024	0.109	0.214	0.365	0.386	0.191	0.082
$T5$	0.128	0.173	0.159	0.229	0.391	0.311	0.283	0.294	0.289	0.322	0.297	0.169	0.219	0.399	0.411	0.496	0.270	0.265	0.330	0.357	0.310	0.280	0.206	0.190	0.126	0.155	0.189	0.173	0.114	0.061	0.238	0.348	0.290	0.125	0.112	0.080
$T6$	0.085	0.102	0.070	0.258	0.371	0.232	0.304	0.238	0.270	0.313	0.255	0.164	0.307	0.401	0.364	0.317	0.169	0.182	0.265	0.323	0.252	0.199	0.161	0.167	0.107	0.143	0.171	0.121	0.067	0.010	0.085	0.088	0.033	0.035	0.091	0.041
$T7$	0.117	0.157	0.228	0.320	0.338	0.356	0.382	0.256	0.256	0.209	0.197	0.140	0.155	0.121	0.156	0.291	0.182	0.261	0.311	0.382	0.301	0.224	0.134	0.157	0.061	0.094	0.096	0.105	0.175	0.265	0.404	0.351	0.074	0.031	0.039	0.060
$T8$	0.059	0.060	0.097	0.312	0.329	0.255	0.302	0.243	0.245	0.213	0.231	0.246	0.410	0.275	0.186	0.266	0.149	0.215	0.254	0.377	0.254	0.172	0.121	0.150	0.048	0.070	0.100	0.127	0.160	0.228	0.313	0.255	0.043	0	0	0.007
$T9$	0.142	0.092	0.147	0.246	0.512	0.358	0.325	0.363	0.357	0.253	0.305	0.341	0.343	0.175	0.192	0.316	0.194	0.221	0.340	0.443	0.276	0.244	0.205	0.218	0.106	0.170	0.220	0.211	0.220	0.176	0.264	0.406	0.391	0.201	0.080	0.073
$T10$	0.122	0.092	0.158	0.228	0.489	0.313	0.323	0.359	0.400	0.281	0.255	0.237	0.430	0.478	0.460	0.409	0.252	0.213	0.357	0.447	0.281	0.201	0.168	0.224	0.127	0.121	0.232	0.218	0.242	0.249	0.377	0.374	0.191	0.103	0.069	0.057
$T11$	0.111	0.032	0.162	0.166	0.471	0.269	0.272	0.415	0.389	0.328	0.262	0.207	0.439	0.402	0.270	0.322	0.180	0.235	0.363	0.412	0.227	0.247	0.203	0.168	0.096	0.150	0.214	0.250	0.240	0.214	0.303	0.397	0.303	0.128	0.053	0.030
$T12$	0.057	0.003	0.157	0.103	0.382	0.198	0.237	0.346	0.390	0.362	0.257	0.195	0.404	0.439	0.356	0.309	0.176	0.234	0.354	0.410	0.240	0.206	0.150	0.208	0.093	0.182	0.211	0.254	0.300	0.212	0.227	0.386	0.332	0.162	0.062	0.031
$T13$	0.077	0	0.075	0.071	0.128	0.161	0.202	0.346	0.274	0.276	0.179	0.133	0.209	0.316	0.261	0.218	0.070	0.143	0.286	0.318	0.127	0.180	0.099	0.186	0.086	0.158	0.291	0.249	0.175	0.134	0.078	0.035	0.016	0.032	0.050	0.038
$T14$	0.057	0.002	0.160	0.116	0.170	0.139	0.166	0.335	0.453	0.375	0.373	0.258	0.208	0.072	0.067	0.175	0.160	0.245	0.327	0.347	0.224	0.289	0.161	0.232	0.114	0.070	0.150	0.157	0.167	0.187	0.226	0.129	0.113	0.162	0.147	0.023
$T15$	0	0.015	0.078	0	0.148	0.143	0.210	0.309	0.269	0.314	0.259	0.235	0.167	0.095	0.133	0.366	0.242	0.256	0.292	0.343	0.238	0.153	0.021	0.081	0.147	0.283	0.345	0.165	0.061	0.012	0.054	0	0	0.033	0.050	0.073
$T16$	0.076	0.034	0.102	0.019	0.046	0.031	0.180	0.172	0.395	0.311	0.292	0.265	0.168	0.022	0.047	0.132	0.234	0.338	0.305	0.257	0.058	0.043	0.180	0.119	0.073	0.208	0.178	0.089	0.054	0.038	0.029	0.089	0.045	0.094	0.120	0.002
$T17$	0.129	0.077	0.054	0.042	0.041	0	0.159	0.201	0.338	0.267	0.274	0.167	0.064	0.126	0.160	0.225	0.406	0.471	0.314	0.163	0.022	0.012	0.019	0.020	0.025	0.027	0.063	0.068	0.076	0.070	0.036	0.158	0.092	0.140	0.176	0.055
$T18$	0.362	0.103	0.011	0.000	0.067	0.240	0.179	0.136	0.262	0.193	0.228	0.341	0.337	0.133	0.070	0.169	0.138	0.192	0	0	0	0	0	0	0	0	0.032	0.032	0.023	0.013	0.006	0.083	0.028	0.138	0.420	0.402
$T19$	0.170	0.065	0.081	0.077	0.133	0.121	0.181	0.200	0.318	0.273	0.263	0.185	0.146	0.075	0.117	0.227	0.218	0.277	0.208	0.193	0.084	0.087	0.065	0.067	0.060	0.057	0.065	0.063	0.057	0.057	0.096	0.190	0.174	0.187	0.220	0.110
$T20$	0.107	0.024	0.042	0.044	0.123	0.055	0.117	0.164	0.261	0.239	0.214	0.072	0.004	0.043	0.194	0.297	0.116	0.164	0.169	0.193	0.064	0.082	0.009	0.031	0.078	0.016	0	0	0	0.043	0.219	0.397	0.354	0.200	0.150	0
$T21$	0.221	0.108	0.135	0.114	0.287	0.182	0.234	0.246	0.330	0.293	0.249	0.150	0.272	0.160	0.140	0.236	0.235	0.293	0.268	0.346	0.191	0.152	0.104	0.072	0.082	0.115	0.066	0.134	0.142	0.060	0.039	0.200	0.403	0.491	0.285	0.143
$T22$	0.221	0.108	0.135	0.114	0.287	0.182	0.234	0.246	0.330	0.293	0.249	0.150	0.272	0.160	0.140	0.236	0.235	0.293	0.268	0.346	0.191	0.152	0.104	0.072	0.082	0.115	0.066	0.134	0.142	0.060	0.039	0.200	0.403	0.491	0.285	0.143
$T23$	0.237	0.136	0.133	0.245	0.224	0.217	0.293	0.205	0.279	0.299	0.277	0.131	0.082	0	0.077	0.285	0.381	0.401	0.212	0.128	0.086	0.067	0.077	0.062	0.049	0.039	0.061	0.053	0.028	0.025	0.002	0.076	0.041	0.112	0.252	0.158
$T24$	0.391	0.441	0.323	0.236	0.293	0.215	0.254	0.298	0.305	0.252	0.219	0.134	0.141	0.073	0.162	0.348	0.370	0.447	0.255	0.188	0.151	0.137	0.109	0.111	0.073	0.066	0.082	0.062	0.047	0.058	0.029	0.086	0.085	0.180	0.460	0.441
$T25$	0.377	0.321	0.220	0.222	0.276	0.222	0.238	0.235	0.241	0.176	0.194	0.132	0.134	0.097	0.205	0.373	0.418	0.469	0.277	0.203	0.157	0.129	0.118	0.126	0.073	0.063	0.082	0.065	0.055	0.044	0.029	0.084	0.070	0.148	0.398	0.409
$T26$	0.412	0.334	0.234	0.197	0.308	0.274	0.210	0.194	0.201	0.083	0.154	0.136	0.139	0.118	0.272	0.449	0.497	0.528	0.339	0.266	0.196	0.168	0.152	0.178	0.090	0.075	0.094	0.079	0.075	0.049	0.045	0.094	0.076	0.138	0.391	0.458
$T27$	0.424	0.269	0.107	0.218	0.244	0.154	0.205	0.224	0.164	0.090	0.140	0.121	0.161	0.194	0.281	0.370	0.400	0.470	0.273	0.193	0.165	0.107	0.114	0.126	0.065	0.059	0.082	0.057	0.059	0.032	0.028	0.072	0.062	0.146	0.444	0.507
$T28$	0.355	0.188	0.022	0.146	0.237	0.128	0.216	0.137	0.150	0.070	0.152	0.168	0.227	0.209	0.262	0.344	0.386	0.453	0.260	0.153	0.107	0.081	0.095	0.090	0.033	0.030	0.060	0.034	0.039	0.010	0.013	0.038	0.038	0.100	0.392	0.453
$T29$	0.357	0.126	0	0.057	0.178	0.104	0.086	0.104	0.195	0.273	0.176	0.081	0.218	0.234	0.205	0.289	0.345	0.428	0.218	0.096	0.062	0.054	0.059	0.067	0.001	0.000	0.043	0.032	0.037	0	0	0.047	0.023	0.126	0.418	0.474
$T30$	0.338	0.215	0.087	0.225	0.214	0.157	0.151	0.142	0.186	0.156	0.166	0.154	0.198	0.175	0.236	0.350	0.369	0.468	0.295	0.198	0.139	0.139	0.123	0.146	0.078	0.064	0.092	0.098	0.101	0.055	0.064	0.114	0.142	0.267	0.450	0.464
$T31$	0.339	0.273	0.140	0.256	0.286	0.186	0.224	0.193	0.207	0.173	0.236	0.311	0.239	0.131	0.215	0.352	0.341	0.518	0.351	0.211	0.147	0.155	0.151	0.172	0.089	0.068	0.097	0.090	0.101	0.042	0.042	0.116	0.206	0.468	0.567	0.492
$T32$	0.420	0.262	0.081	0.312	0.175	0.187	0.095	0.109	0.163	0.109	0.122	0.065	0.154	0.130	0.241	0.352	0.362	0.411	0.171	0.170	0.162	0.177	0.165	0.187	0.079	0.059	0.083	0.065	0.077	0.021	0.023	0.075	0.065	0.169	0.438	0.547
$T33$	0.376	0.380	0.181	0.270	0.184	0.165	0.076	0.102	0.114	0.030	0.103	0.168	0.202	0.172	0.248	0.390	0.405	0.416	0.189	0.225	0.204	0.210	0.182	0.247	0.098	0.087	0.113	0.080	0.092	0.058	0.061	0.092	0.169	0.341	0.517	0.528
$T34$	0.420	0.333	0.177	0.221	0.135	0.116	0.053	0.091	0.083	0.032	0.118	0.180	0.246	0.130	0.188	0.305	0.322	0.447	0.271	0.254	0.208	0.204	0.175	0.284	0.109	0.080	0.126	0.079	0.106	0.048	0.054	0.096	0.205	0.407	0.536	0.504
$T35$	0.414	0.251	0.188	0.177	0.126	0.073	0.114	0.172	0.181	0.061	0.039	0.057	0.146	0.189	0.161	0.248	0.332	0.425	0.197	0.121	0.144	0.141	0.130	0.248	0.102	0.063	0.112	0.069	0.112	0.061	0.049	0.104	0.176	0.249	0.498	0.536
$T36$	0.348	0.195	0.155	0.093	0.031	0.099	0	0.219	0	0	0.127	0.214	0.174	0.063	0.032	0.114	0.266	0.400	0.176	0.087	0.085	0.080	0.060	0.181	0.067	0.018	0.075	0.030	0.059	0.018	0.016	0.061	0.132	0.271	0.505	0.489
$T37$	0.387	0.203	0.136	0.152	0.060	0.076	0.069	0.147	0.135	0.038	0	0.066	0.062	0.055	0.052	0.085	0.245	0.366	0.161	0.062	0.036	0.048	0.061	0.159	0.088	0.026	0.088	0.035	0.037	0.020	0.044	0.090	0.118	0.184	0.460	0.502
$T38$	0.346	0.239	0.131	0.125	0.036	0.067	0.040	0.124	0.068	0.023	0.035	0.086	0.073	0.048	0.032	0.069	0.182	0.273	0.123	0.058	0.053	0.080	0.089	0.158	0.101	0.078	0.112	0.039	0.070	0.067	0.061	0.105	0.151	0.218	0.419	0.432
$T39$	0.274	0.340	0.103	0.110	0	0.023	0.031	0	0.020	0.019	0.008	0	0	0.024	0	0	0	0	0.011	0.025	0.053	0.135	0.164	0.134	0.153	0.219	0.187	0.056	0.136	0.189	0.130	0.170	0.224	0.225	0.270	0.264
$T40$	0.321	0.279	0.163	0.162	0.088	0.210	0.187	0.144	0.088	0.047	0.053	0.057	0.061	0.075	0.054	0.137	0.096	0.135	0.274	0.400	0.265	0.231	0.174	0.304	0.180	0.108	0.227	0.076	0.095	0.175	0.158	0.202	0.270	0.328	0.403	0.413
$T41$	0.240	0.214	0.114	0.122	0.170	0.167	0.143	0.138	0.118	0.048	0.091	0.057	0.099	0.088	0.101	0.192	0.109	0.165	0.225	0.202	0.173	0.195	0.187	0.323	0.227	0.126	0.123	0.055	0.067	0.089	0.143	0.231	0.342	0.350	0.388	0.362
$T42$	0.227	0.197	0.130	0.138	0.143	0.102	0.083	0.132	0.088	0.057	0.099	0.058	0.103	0.073	0.117	0.201	0.250	0.299	0.264	0.359	0.229	0.159	0.119	0.192	0.044	0.023	0.082	0.181	0.347	0.416	0.334	0.279	0.278	0.251	0.186	0.241
$T43$	0.218	0.212	0.103	0.249	0.108	0.094	0.143	0.110	0.131	0.350	0.445	0.456	0.308	0.119	0.183	0.309	0.196	0.222	0.325	0.351	0.222	0.167	0.138	0.207	0.087	0.066	0.106	0.099	0.116	0.259	0.339	0.294	0.387	0.383	0.250	0.290
$T44$	0.402	0.271	0.124	0.239	0.143	0.105	0.084	0.162	0.124	0.070	0.175	0.232	0.399	0.265	0.267	0.295	0.279	0.314	0.328	0.381	0.211	0.250	0.158	0.224	0.172	0.161	0.105	0.100	0.209	0.226	0.216	0.290	0.285	0.364	0.499	0.547
$T45$	0.326	0.236	0.265	0.431	0.178	0.134	0.103	0.157	0.195	0.105	0.136	0.114	0.192	0.269	0.344	0.405	0.393	0.550	0.453	0.350	0.203	0.199	0.194	0.193	0.146	0.195	0.163	0.185	0.233	0.153	0.208	0.270	0.289	0.388	0.536	0.504
$T46$	0.227	0.227	0.040	0.263	0.186	0.221	0.154	0.131	0.175	0.087	0.093	0.086	0.102	0.074	0.202	0.407	0.435	0.427	0.308	0.274	0.207	0.227	0.108	0.208	0.167	0.084	0.141	0.230	0.165	0.152	0.163	0.183	0.255	0.258	0.266	0.293

Table 5.2: Matrix containing the deficits for an average wind speed equal to $5.75m/s$ in a 10-minute slot for the empirical model

	0°	10°	20°	30°	40°	50°	60°	70°	80°	90°	100°	110°	120°	130°	140°	150°	160°	170°	180°	190°	200°	210°	220°	230°	240°	250°	260°	270°	280°	290°	300°	310°	320°	330°	340°	350°
$T1$	0.024	0.152	0.019	0.271	0.012	0.141	0.111	0.250	0.342	0.245	0.249	0.122	0.004	0.030	0.143	0.192	0.227	0.155	0.265	0.295	0.296	0.283	0.185	0.175	0.168	0.112	0.159	0.130	0.183	0.098	0.279	0.368	0.212	0.040	0.011	0
$T2$	0.072	0.199	0.079	0.309	0.062	0.211	0.085	0.264	0.410	0.303	0.333	0.293	0.315	0.431	0.302	0.306	0.317	0.253	0.283	0.310	0.340	0.325	0.199	0.203	0.220	0.143	0.183	0.153	0.187	0.083	0.193	0.359	0.314	0.137	0.047	0.044
$T3$	0.040	0.177	0.115	0.337	0.094	0.222	0.078	0.279	0.456	0.273	0.292	0.166	0.169	0.360	0.367	0.352	0.305	0.264	0.269	0.304	0.378	0.320	0.203	0.215	0.179	0.141	0.183	0.150	0.183	0.113	0.328	0.409	0.235	0.116	0.060	0.056
$T4$	0.064	0.204	0.145	0.288	0.102	0.232	0.096	0.299	0.439	0.291	0.324	0.354	0.416	0.363	0.242	0.288	0.277	0.276	0.261	0.297	0.404	0.329	0.213	0.179	0.172	0.155	0.194	0.158	0.140	0.054	0.130	0.252	0.389	0.375	0.192	0.085
$T5$	0.055	0.215	0.149	0.362	0.143	0.217	0.187	0.360	0.463	0.335	0.328	0.194	0.150	0.296	0.481	0.533	0.403	0.274	0.251	0.341	0.434	0.322	0.215	0.197	0.180	0.165	0.181	0.152	0.162	0.078	0.224	0.404	0.264	0.113	0.056	0.069
$T6$	0.018	0.170	0.073	0.252	0.155	0.172	0.169	0.329	0.432	0.304	0.319	0.198	0.217	0.401	0.391	0.345	0.270	0.225	0.202	0.343	0.378	0.257	0.170	0.175	0.149	0.148	0.161	0.117	0.122	0.028	0.106	0.097	0.041	0.011	0.024	0.022
$T7$	0.031	0.224	0.268	0.500	0.229	0.271	0.189	0.335	0.353	0.368	0.246	0.154	0.148	0.086	0.177	0.263	0.327	0.265	0.249	0.350	0.386	0.256	0.159	0.196	0.120	0.089	0.112	0.134	0.200	0.243	0.422	0.317	0.089	0.030	0.024	0.083
$T8$	0	0.153	0.131	0.400	0.229	0.225	0.139	0.308	0.324	0.336	0.263	0.359	0.345	0.270	0.169	0.225	0.274	0.206	0.214	0.354	0.339	0.219	0.133	0.151	0.100	0.079	0.115	0.140	0.163	0.204	0.327	0.229	0.050	0.005	0	0.020
$T9$	0.058	0.186	0.183	0.359	0.378	0.355	0.178	0.359	0.420	0.406	0.309	0.398	0.281	0.146	0.196	0.297	0.312	0.255	0.314	0.422	0.334	0.276	0.185	0.196	0.155	0.179	0.232	0.220	0.223	0.170	0.287	0.428	0.407	0.163	0.067	0.095
$T10$	0.062	0.186	0.256	0.249	0.376	0.353	0.198	0.432	0.427	0.404	0.289	0.261	0.358	0.518	0.500	0.450	0.328	0.263	0.356	0.394	0.296	0.251	0.169	0.206	0.184	0.141	0.230	0.206	0.259	0.198	0.370	0.356	0.188	0.083	0.061	0.102
$T11$	0.047	0.152	0.221	0.197	0.345	0.297	0.117	0.356	0.442	0.412	0.292	0.259	0.368	0.420	0.298	0.325	0.266	0.249	0.352	0.369	0.269	0.283	0.185	0.151	0.148	0.143	0.204	0.225	0.236	0.195	0.310	0.385	0.318	0.099	0.055	0.066
$T12$	0.033	0.124	0.184	0.202	0.239	0.211	0.127	0.358	0.438	0.416	0.288	0.212	0.309	0.469	0.399	0.342	0.243	0.247	0.316	0.363	0.282	0.231	0.139	0.211	0.149	0.156	0.218	0.221	0.278	0.204	0.242	0.366	0.361	0.101	0.044	0.034
$T13$	0.091	0.137	0.035	0.066	0.132	0.185	0.256	0.310	0.340	0.376	0.231	0.104	0.161	0.313	0.316	0.252	0.154	0.159	0.239	0.251	0.205	0.210	0.097	0.171	0.151	0.162	0.293	0.218	0.167	0.135	0.079	0.040	0.043	0.009	0.014	0.025
$T14$	0.029	0.060	0.044	0.154	0.200	0.102	0.159	0.343	0.470	0.458	0.415	0.311	0.152	0.046	0.112	0.193	0.220	0.238	0.285	0.319	0.238	0.306	0.153	0.221	0.158	0.088	0.176	0.143	0.169	0.204	0.243	0.102	0.098	0.140	0.111	0.036
$T15$	0.024	0	0.033	0.221	0.022	0.072	0.083	0.245	0.315	0.393	0.365	0.295	0.148	0.040	0.190	0.397	0.338	0.258	0.259	0.276	0.238	0.169	0.029	0.133	0.140	0.304	0.286	0.120	0.041	0.007	0.090	0.057	0.032	0.029	0.036	0.075
$T16$	0.005	0.037	0.019	0.157	0.015	0.034	0.141	0.286	0.356	0.358	0.319	0.306	0.148	0.010	0.073	0.179	0.284	0.316	0.323	0.230	0.068	0.030	0.198	0.119	0.100	0.207	0.141	0.070	0.092	0.049	0.078	0.051	0.059	0	0.026	0.016
$T17$	0.028	0.052	0.036	0	0	0	0.112	0.221	0.283	0.339	0.287	0.172	0.064	0.116	0.196	0.239	0.441	0.468	0.329	0.115	0.013	0.010	0.035	0.014	0.030	0.048	0.080	0.079	0.099	0.057	0.093	0.099	0.105	0.073	0.075	0.070
$T18$	0.249	0.108	0.003	0.027	0.045	0.163	0.025	0.131	0.199	0.277	0.291	0.369	0.292	0.152	0.080	0.120	0.175	0.154	0	0.002	0	0	0.017	0	0.006	0.022	0.054	0.045	0.046	0.014	0.043	0.030	0.047	0.076	0.376	0.460
$T19$	0.091	0.084	0.041	0.134	0.143	0.096	0.091	0.233	0.317	0.348	0.286	0.206	0.131	0.081	0.145	0.240	0.262	0.248	0.197	0.160	0.083	0.096	0.069	0.063	0.087	0.059	0.075	0.064	0.070	0.061	0.143	0.157	0.186	0.109	0.147	0.131
$T20$	0.034	0.054	0	0.154	0.160	0.034	0	0.210	0.309	0.306	0.219	0.065	0.018	0.068	0.240	0.353	0.182	0.120	0.155	0.148	0.060	0.113	0.003	0.029	0.117	0	0	0	0	0.058	0.287	0.388	0.379	0.088	0.078	0.020
$T21$	0.158	0.158	0.086	0.222	0.256	0.203	0.120	0.289	0.378	0.376	0.266	0.186	0.258	0.146	0.133	0.224	0.267	0.258	0.219	0.295	0.194	0.165	0.099	0.064	0.143	0.087	0.082	0.140	0.123	0.046	0.076	0.195	0.425	0.440	0.197	0.104
$T22$	0.158	0.158	0.086	0.222	0.256	0.203	0.120	0.289	0.378	0.376	0.266	0.186	0.258	0.146	0.133	0.224	0.267	0.258	0.219	0.295	0.194	0.165	0.099	0.064	0.143	0.087	0.082	0.140	0.123	0.046	0.076	0.195	0.425	0.440	0.197	0.104
$T23$	0.137	0.141	0.150	0.221	0.311	0.179	0.204	0.219	0.279	0.390	0.279	0.154	0.076	0.030	0.100	0.269	0.387	0.370	0.202	0.101	0.069	0.065	0.079	0.054	0.051	0.050	0.087	0.062	0.061	0.021	0.041	0.018	0.036	0.017	0.164	0.206
$T24$	0.339	0.319	0.284	0.293	0.291	0.158	0.217	0.287	0.319	0.339	0.218	0.148	0.137	0.096	0.209	0.339	0.411	0.396	0.243	0.174	0.125	0.122	0.107	0.095	0.077	0.071	0.108	0.087	0.066	0.041	0.054	0.046	0.068	0.101	0.413	0.456
$T25$	0.322	0.293	0.259	0.263	0.289	0.217	0.156	0.251	0.241	0.300	0.212	0.149	0.157	0.109	0.237	0.365	0.441	0.424	0.301	0.192	0.119	0.130	0.103	0.105	0.080	0.067	0.109	0.085	0.063	0.026	0.047	0.044	0.058	0.084	0.330	0.432
$T26$	0.350	0.329	0.315	0.265	0.286	0.295	0.099	0.261	0.197	0.268	0.184	0.153	0.198	0.127	0.309	0.446	0.508	0.474	0.380	0.251	0.147	0.176	0.123	0.147	0.105	0.079	0.125	0.099	0.066	0.021	0.055	0.057	0.064	0.080	0.301	0.466
$T27$	0.420	0.333	0.223	0.247	0.271	0.222	0.103	0.201	0.151	0.206	0.186	0.141	0.198	0.175	0.290	0.360	0.429	0.438	0.356	0.209	0.106	0.124	0.084	0.099	0.069	0.058	0.106	0.081	0.057	0.014	0.028	0.042	0.050	0.125	0.393	0.548
$T28$	0.392	0.244	0.209	0.268	0.245	0.194	0.053	0.113	0.118	0.194	0.156	0.192	0.247	0.195	0.273	0.311	0.417	0.393	0.279	0.158	0.064	0.097	0.046	0.073	0.044	0.040	0.076	0.061	0.038	0.009	0.016	0.020	0.017	0.060	0.314	0.476
$T29$	0.374	0.178	0.171	0.227	0.187	0.156	0.027	0.083	0.199	0.262	0.213	0.091	0.247	0.251	0.211	0.263	0.367	0.376	0.229	0.086	0.019	0.063	0	0.036	0	0.000	0.048	0.045	0.009	0	0	0	0	0.115	0.389	0.480
$T30$	0.326	0.242	0.246	0.232	0.215	0.186	0.095	0.153	0.147	0.230	0.204	0.174	0.234	0.194	0.253	0.316	0.401	0.396	0.305	0.177	0.105	0.156	0.070	0.105	0.083	0.068	0.092	0.107	0.079	0.044	0.070	0.085	0.111	0.239	0.417	0.450
$T31$	0.301	0.259	0.311	0.188	0.214	0.197	0.210	0.230	0.127	0.253	0.293	0.326	0.266	0.175	0.226	0.288	0.384	0.444	0.382	0.182	0.116	0.173	0.091	0.137	0.080	0.076	0.111	0.104	0.074	0.031	0.055	0.091	0.150	0.452	0.544	0.471
$T32$	0.398	0.286	0.320	0.244	0.216	0.201	0.142	0.149	0.151	0.221	0.143	0.111	0.263	0.162	0.244	0.348	0.417	0.280	0.163	0.148	0.124	0.187	0.110	0.148	0.057	0.068	0.089	0.091	0.059	0.007	0.029	0.069	0.049	0.109	0.392	0.537
$T33$	0.359	0.371	0.395	0.252	0.181	0.176	0.179	0.134	0.086	0.168	0.163	0.188	0.279	0.233	0.279	0.392	0.460	0.303	0.184	0.203	0.181	0.229	0.131	0.177	0.094	0.095	0.111	0.121	0.101	0.026	0.058	0.092	0.103	0.312	0.515	0.495
$T34$	0.408	0.359	0.273	0.189	0.192	0.132	0.047	0.088	0.096	0.130	0.153	0.207	0.291	0.147	0.230	0.285	0.382	0.413	0.277	0.218	0.193	0.228	0.131	0.174	0.098	0.097	0.103	0.116	0.100	0.028	0.044	0.090	0.163	0.346	0.527	0.445
$T35$	0.450	0.317	0.197	0.219	0.184	0.124	0.134	0.101	0.157	0.105	0.113	0.048	0.185	0.222	0.159	0.266	0.288	0.318	0.197	0.109	0.100	0.147	0.096	0.128	0.079	0.086	0.096	0.099	0.109	0.039	0.049	0.082	0.127	0.208	0.465	0.510
$T36$	0.362	0.240	0.125	0.145	0.190	0.160	0.093	0.019	0	0.047	0.164	0.231	0.145	0.057	0.045	0.184	0.242	0.301	0.212	0.055	0.033	0.091	0.044	0.083	0.058	0.062	0.084	0.067	0.087	0.005	0.014	0.031	0.087	0.241	0.470	0.462
$T37$	0.412	0.256	0.076	0.137	0.163	0.096	0.225	0.158	0.120	0.067	0.023	0.037	0.029	0.022	0.025	0.183	0.201	0.281	0.199	0.046	0.014	0.050	0.011	0.075	0.041	0.060	0.069	0.078	0.083	0.030	0.027	0.059	0.082	0.165	0.434	0.500
$T38$	0.367	0.298	0.102	0.152	0.157	0.103	0.140	0.078	0.067	0.043	0.053	0.076	0.051	0.025	0.023	0.132	0.155	0.208	0.161	0.035	0.030	0.103	0.053	0.070	0.074	0.115	0.104	0.072	0.116	0.066	0.051	0.067	0.123	0.192	0.393	0.416
$T39$	0.297	0.420	0.123	0.184	0.118	0.062	0.041	0	0.039	0	0	0	0	0	0	0	0	0	0.049	0	0.054	0.200	0.130	0.050	0.142	0.256	0.180	0.067	0.196	0.182	0.124	0.112	0.222	0.192	0.254	0.235
$T40$	0.332	0.316	0.202	0.266	0.197	0.223	0.163	0.097	0.085	0.074	0.089	0.044	0.094	0.073	0.069	0.107	0.155	0.125	0.266	0.328	0.246	0.225	0.166	0.194	0.174	0.116	0.222	0.103	0.142	0.135	0.133	0.177	0.291	0.293	0.371	0.342
$T41$	0.269	0.288	0.229	0.263	0.191	0.143	0.060	0.144	0.125	0.123	0.143	0.078	0.114	0.089	0.103	0.191	0.234	0.125	0.160	0.167	0.176	0.232	0.164	0.245	0.252	0.118	0.115	0.111	0.103	0.100	0.121	0.192	0.353	0.340	0.395	0.352
$T42$	0.207	0.240	0.190	0.241	0.237	0.159	0.035	0.138	0.097	0.124	0.128	0.087	0.143	0.109	0.121	0.232	0.349	0.214	0.170	0.305	0.262	0.192	0.094	0.120	0.071	0.018	0.093	0.169	0.384	0.410	0.323	0.252	0.290	0.207	0.228	0.186
$T43$	0.194	0.221	0.203	0.257	0.168	0.123	0.022	0.165	0.186	0.253	0.442	0.531	0.332	0.142	0.197	0.304	0.298	0.207	0.306	0.301	0.244	0.212	0.119	0.116	0.121	0.086	0.100	0.123	0.088	0.219	0.325	0.290	0.399	0.349	0.316	0.241
$T44$	0.391	0.278	0.278	0.288	0.222	0.152	0.054	0.155	0.133	0.200	0.173	0.292	0.394	0.276	0.267	0.275	0.332	0.241	0.333	0.352	0.189	0.265	0.122	0.152	0.199	0.158	0.102	0.096	0.202	0.220	0.225	0.246	0.279	0.307	0.455	0.549
$T45$	0.263	0.291	0.281	0.262	0.243	0.186	0.044	0.171	0.140	0.202	0.170	0.131	0.219	0.266	0.381	0.360	0.440	0.502	0.456	0.305	0.187	0.226	0.143	0.122	0.175	0.208	0.148	0.170	0.223	0.130	0.218	0.222	0.282	0.351	0.531	0.458
$T46$	0.225	0.239	0.197	0.251	0.208	0.197	0.044	0.152	0.122	0.198	0.148	0.104	0.131	0.090	0.247	0.400	0.426	0.341	0.298	0.245	0.180	0.248	0.074	0.144	0.208	0.063	0.100	0.220	0.129	0.132	0.165	0.170	0.213	0.223	0.235	0.257

5.6 Degradation of the Wind

Just like it has been done for the physical model in Section 4.1, here the spatial evolution of the wind velocity field is analysed. Once again, the degradation of the wind is studied starting from the deficits like the ones shown in Table 5.1. Also, just like in Section 4.1 the best way to study the wind speed throughout the wind farm is the use of the contour plots. These contour plots are organised like the ones in Figures 4.1 and 4.2, with the black dots indicating the locations of the wind turbines and the vector representing both the inputs. In both cases, the speed and the magnitude of the vector represent the undisturbed wind, i.e. the maximum wind speed experienced by any of the turbines. Again, the direction is given by the average of all the wind directions recorded by the turbines for both the contour plot obtained from the model and the one found using the measurements. In Figure 5.2, the contour plot describing the results of the model is shown. On the other hand, the plot obtained from the data is reported in Figure 5.3. As it happened for the physical model, the results of the model do not really resemble the measurements. However, although the contours are of significantly different shape, the values of the wind speeds are closer than in the case of the physical model exposed in Figures 4.1 and 4.2. These results highlight the variable nature of the wind, because not even using measurements of the wind turbines themselves it was possible to reproduce the actual wind velocity field within the wind farm. As it has been done for the physical model in Section 4.1, the time slot analysed has been chosen randomly in order not to affect the results of the whole research. Again, the results outside of the limit of the turbines are not reliable as there are no measurements outside of that area in order to limit the evolution of the function elaborated by the program in order to create the plots.

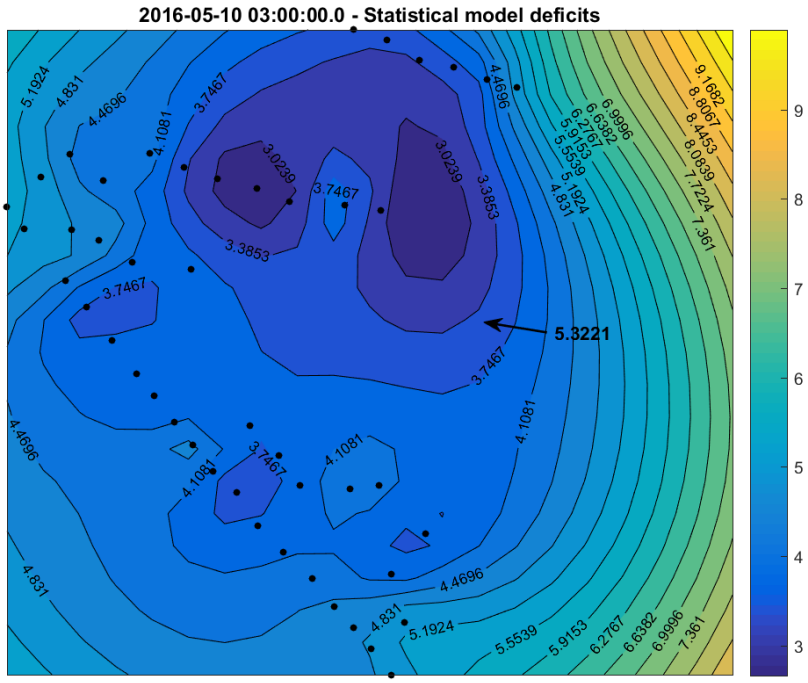

Figure 5.2: Contour plot representing the spatial degradation of the wind on $10/05/2016$ at $03:00$ according to the empirical model

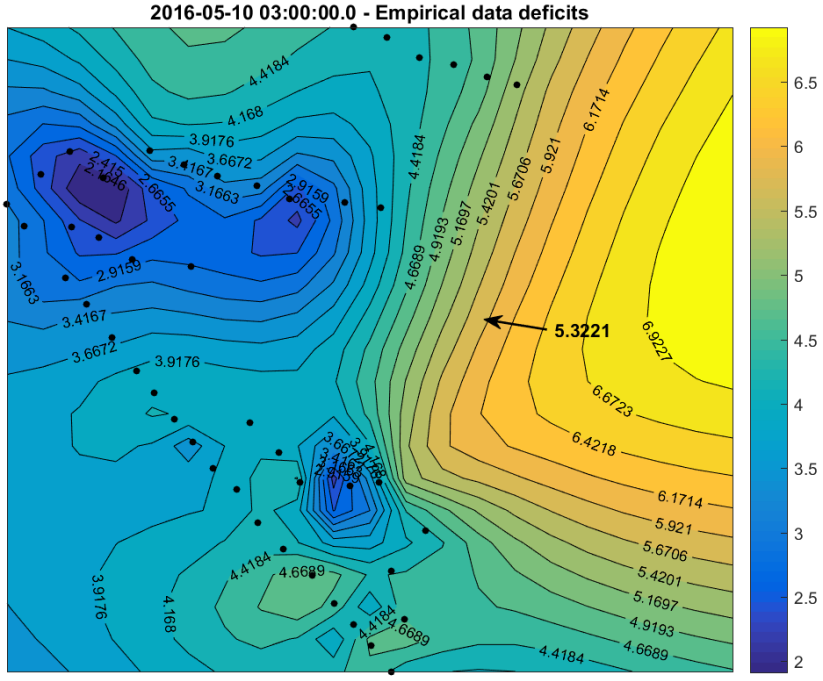

Figure 5.3: Contour plot representing the spatial degradation of the wind on $10/05/2016$ at $03 : 00$ according to the wind data

5.7 Comparison of the Wind Speed at the Turbines

As it has been done in Section 4.3, the speeds estimated at the location of the turbines and the one measured by the anemometers were compared in order to further check the validity of the results and of the model itself. On the x-axis, the identification number of the turbine is ideally reported, while on the y-axis there is the wind speed that has been either computed or measured. As the legends in Figure 5.4 show, the estimations of the model and the measurements are reported with a blue X and a red circle, respectively. As in the previous examples reported throughout the whole essay, the time slots used in these graphs has been selected randomly.

Figure 5.4(a) reports a good set of results, at least as far as the points on the right hand side of the graph are considered. It can be noted how the behaviour predicted by the model reproduces the measured behaviour in a satisfying way, at least on the right side. However, the comparison is not as good on the left hand side, where the model seems to be able to ”understand” which turbines are the fastest among that group but fails to calculate the right value of the wind speed. Another discrepancy that can be seen in Figure 5.4(a) is the turbine experiencing the highest velocity within the wind farm. According to the measurements such a turbine is among the ones here represented in the left side of the graph, while according to the results of the model it is on the other side. This means that the two turbines are far away one from the other. This fact emphasises once more the variability typical of the wind because even though averagely the wind speed is fastest at the location of a certain turbine, it can happen that in other cases it is another one (far away from it, in addition) undergoing the greatest speed. This happens even though the wind conditions are extremely similar as the wind speed and direction are contained in the same bins.

In Figure 5.4(b), a not-as-good example is reported. In this case the results of the model do not resemble the measurement in any significant way. However, there is one characteristic in common with Figure 5.4(a), as the results reported on the right hand side of the graph have values closer to the measurements compared to the ones shown on the left hand side. This might mean that the model better predicts and reproduces the behaviour of those turbines. Again, like in Figure 5.4(a) the wind turbine that measures the highest value for the wind velocity is different from the one averagely doing it.

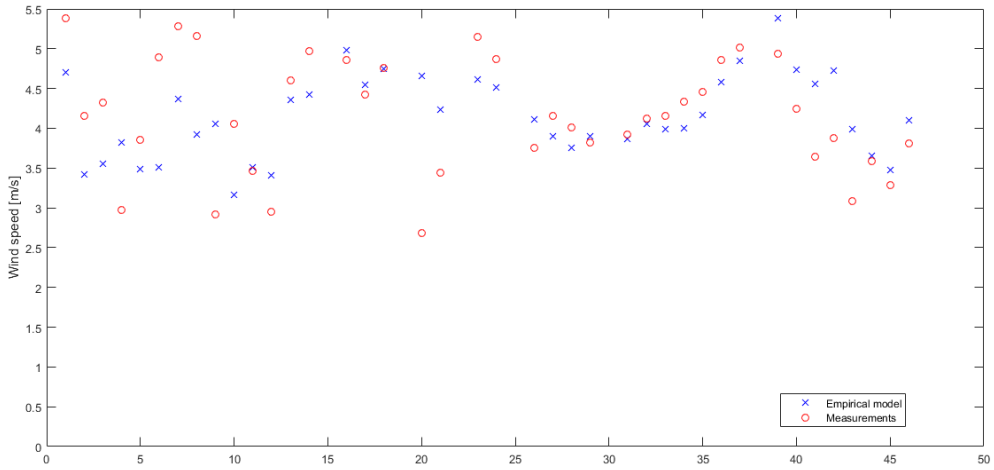

(a) First comparison

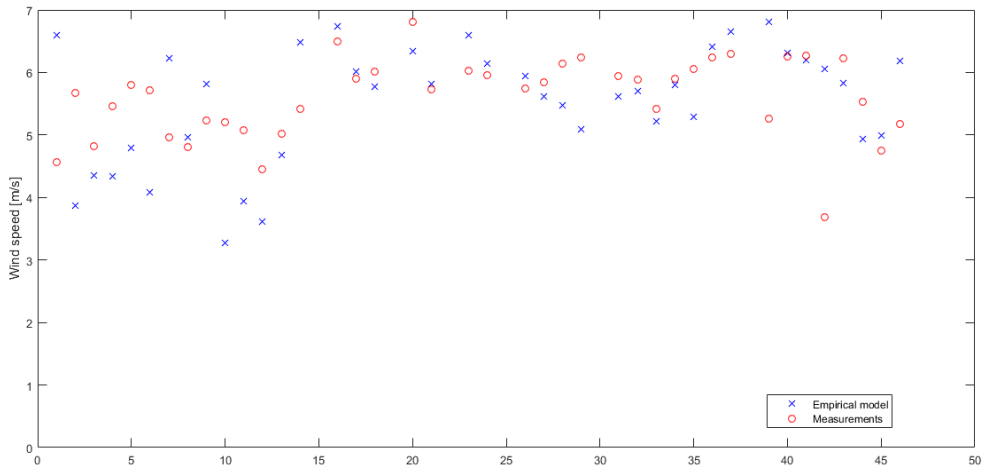

(b) Second comparison

Figure 5.4: Two comparisons of the wind speed at the location of each turbine according to the empirical model

5.8 Prediction of the Wind Farm Production

Despite in some cases the results of the model failed to reproduce the behaviour of the wind speed at each turbine, an attempt to predict the output of the whole wind farm was made. Since the predicted velocity values at the locations of some turbines were overestimated compared to the measurements

while in others they were underestimated it could be possible that these errors compensate each other, leading to an overall value for the power output that resembled the actual one. The full results of the 3 months that have been simulated are reported in Appendix C. In this section, some examples of the comparisons during short periods of time are reported. To verify the coherence of the results of the model with the measurements the Mean Error (ME) has been initially calculated and reported in the various graphs. The ME is calculated as reported in equation (5.5):

$$ME = \frac{\sum_{t=1}^{n} E_{measured,t} - E_{model,t}}{n} \tag{5.5}$$

where t indicates the time slot and n the number of time slots in the interval of time considered.

Given the possibility that the prediction might be either higher or lower than the measurements, it was thought that the ME was not the most suitable choice. In fact, the ME does consider the sign of the numerator and therefore can lead to wrong conclusions. This may happen because an error in which the model overestimates the production by a great deal can ”delete” several other errors in which the result of the model was an underestimation. To solve this issue, the Mean Absolute Error (MAE) was used instead of the ME. As it can be seen in the definition of the MAE in equation (5.6), the difference between the two is small but significant.

$$MAE = \frac{\sum_{t=1}^{n} |E_{measured,t} - E_{model,t}|}{n} \tag{5.6}$$

The absolute error has been preferred to the relative one because if the measured energy is low the latter error increases dramatically. The most extreme possible consequence possible of this aspect would have happened when predicting the whole month of December 2016 (which results are shown in Figure C.6 in Appendix C). In this case, having for a certain period of time a production of energy exactly equal to 0, the percentage error would have been infinite.

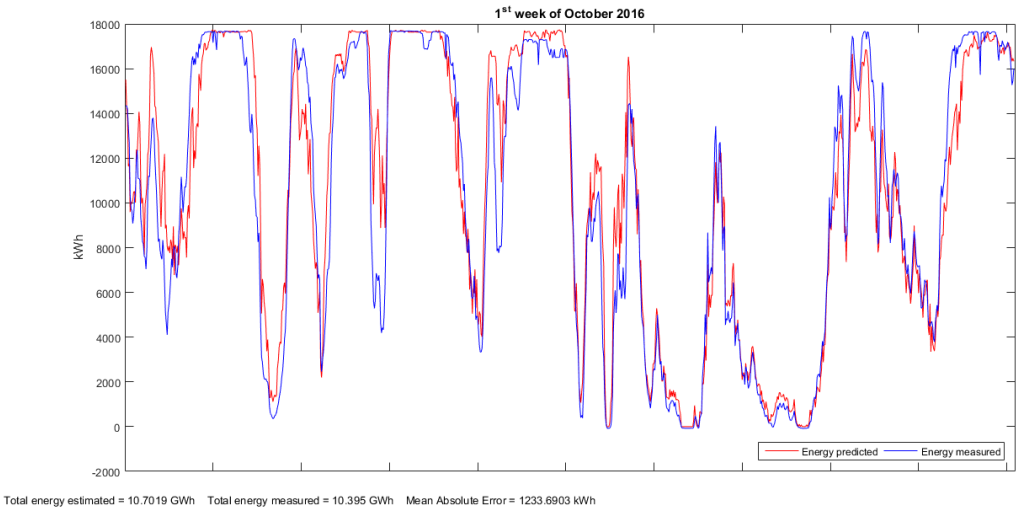

Figure 5.5: Comparison between measurements and results of the empirical model relative to the power output during the 1^{st} week of October 2016

In Figure 5.5 the prediction of the energy output of the entire wind farm is compared with the measurements collected during the same time span. On the y-axis the energy produced during each 10-minute time slot and expressed in kWh is measured, while on the x-axis the time is reported but not shown. Figure 5.5 shows how the model is able to reproduce the behaviour of the wind farm during a somewhat long period of time, replicating also part of the temporary fluctuations. However, the model at times fails to properly predict the output and either overpredicts or underpredicts the output by a significan amount. Even though in these cases the error is significant in terms of absolute value, the relative error does not reach high values. In fact, the MAE estimated during this period of time is equal to $1233.6903kWh$, which divided by the maximum energy reached during this interval is equal to 7%.

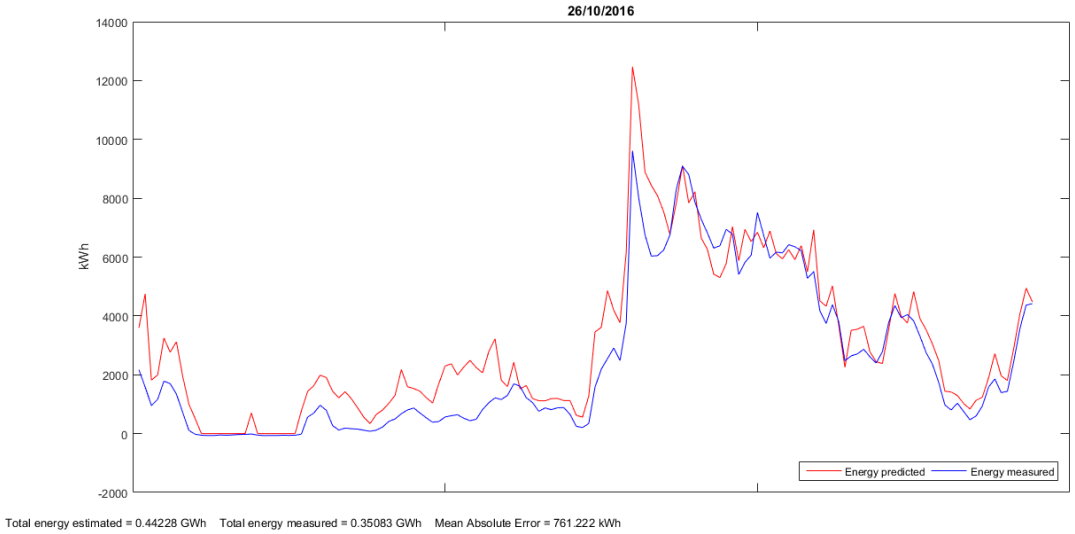

Figure 5.6: Comparison between measurements and results of the empirical model relative to the power output on $26/10/2016$

Figure 5.6 shows the prediction during a single day and compares it with the actual data. It can be easily seen how in this case the model was able to produce satisfactory results. The MAE reported in the notes below the x-axis is equal to $761.222kWh$, which is lower than the MAE of the month (reported in Figure C.1 in Appendix C). If this value is divided by the maximum energy measured, the percentage error is between 7% and 8%, which is not too high.

The same happens also in Figure 5.7, where the comparison is made for a single day in November. Differently from Figure 5.6, in Figure 5.7 there is also a spike in which the model overpredicts significantly the output. Certainly this spike affects the value of the MAE and increases it considerably. Given the somewhat long duration of the spike it is not realistic to say that the cause for the spike was a wind gust (or a series of). It is possible that a higher-speed air current went across a limited area of the wind farm affecting only a limited amount of turbines. Even though the turbines affected might have been just a few, the model suffered more severe consequences as it assumed that that one was the undisturbed wind speed entering the whole wind farm. In this case the Mean Absolute Error is equal to $1072.12kWh$, which is pretty high if we consider that for around half of the day the measured energy is below $2000kWh$. However, if we consider that it also peaks around $11000kWh$, the final result can be considered satisfactory.

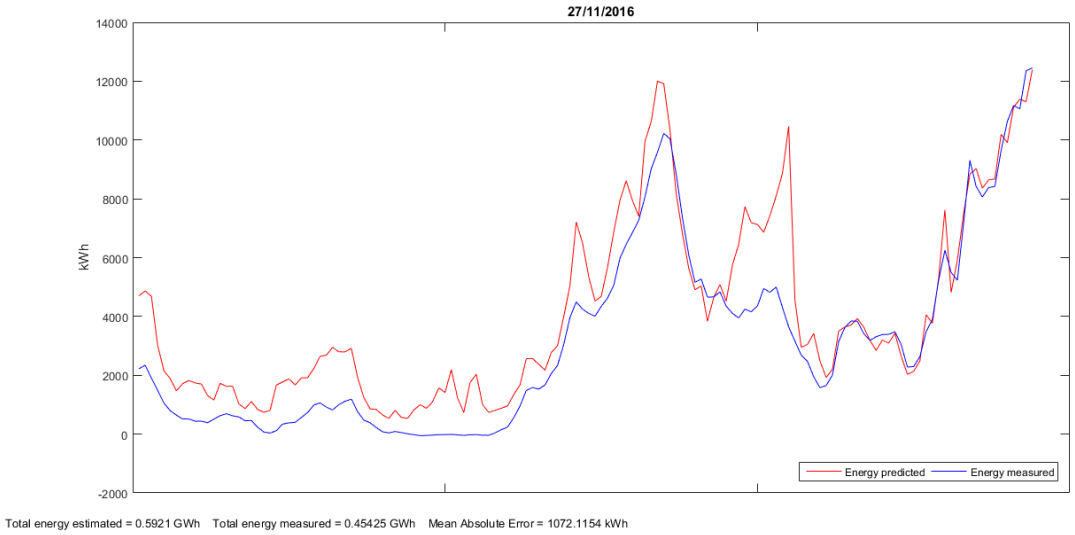

Figure 5.7: Comparison between measurements and results of the empirical model relative to the power output on $27/11/2016$

Given the nature of the previous graphs, analysing them further by looking at the evolution of the difference between the results of the model and the real measurements can help in making additional observations. It is important to mention that the difference in value is reported in absolute terms, therefore with this graph alone periods of overprediction and periods of underprediction cannot be distinguished. For example, Figure 5.8 shows the evolution of the difference in value during the day $27/11/2016$. It was chosen to analyse this particular date because it perfectly highlights some of the differences in results between this model and the one exposed in Chapter 7. The difference is rather limited in absolute terms, except for the spike already highlighted when Figure 5.7 was described. In fact, the difference between the measurements and the prediction is below $1000kWh$ for a good part of the day. However, it is important to state that the spike in difference reaches a value close to $7000kWh$.

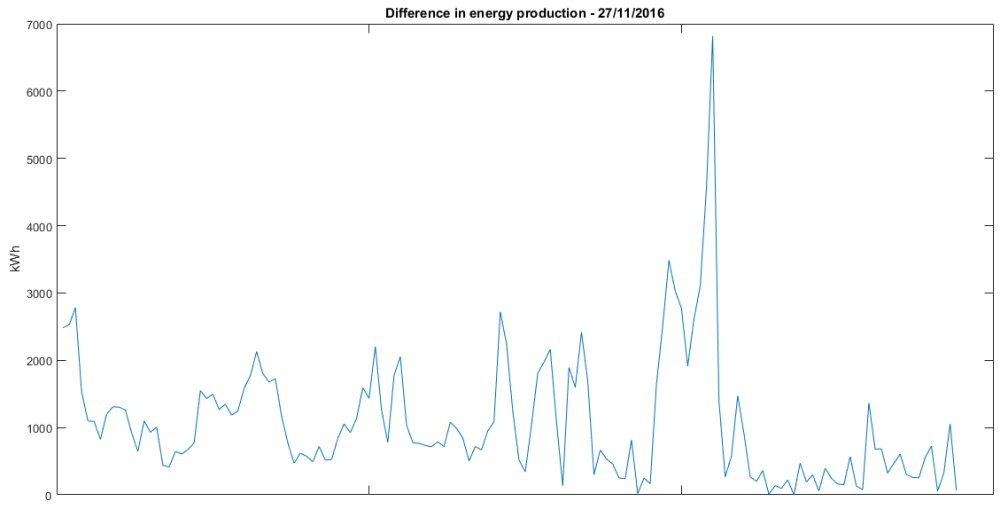

Figure 5.8: Difference between the prediction and the measurements on $27/11/2016$

5.9 Standard Deviation of the Speeds

As it has been noted and stated throughout the last few sections, this second model did not always produce results that resembled the measurements. One reason that has been already mentioned is the variability of the wind in both time and space. In order to highlight the variable nature of the wind, the standard deviations σ of the velocities at the locations of the turbines during the period of time used to create the deficits were estimated. Since the estimation of the deficits required to deal with discrete data and not with a continuous function, the standard deviation has been estimated as shown in equation (5.7):

$$\sigma = \sqrt{\frac{1}{N-1}\sum_{i=1}^{N}|u_i - \overline{u}|^2} \tag{5.7}$$

where $\overline{u}$ is the mean of the wind speed during the period of time analysed:

$$\overline{u} = \frac{1}{N}\sum_{i=1}^{N} u_i \tag{5.8}$$

with N indicatng the amount of data considered during the calculations of the standard deviation σ.

In Table 5.3 and Table 5.4, the values of the standard deviations for the same wind conditions as the ones relative to Table 5.1 and Table 5.2 are shown. The cases in which the standard deviation is equal to 0 indicate that the data relative to those turbines were not considered as the turbine was among the group of the unreliable ones. In Table 5.3, the standard deviation ranges between $0.348m/s$ and $1.845m/s$. On the other hand, in Table 5.4, the highest and lowest values are $1.933m/s$ and $0.200m/s$, respectively. In both cases, a lot of the values reported in the tables are close to $1m/s$. Considering that the tables are relative to the wind speeds between $5m/s$ and $5.5m/s$ for the former and between $5.5m/s$ and $6m/s$ for the latter, it can be said that the values of the standard deviations are rather high. This is because of the variable and stochastic nature of the wind. These values prove what has been mentioned before about the cause for the lack of coherent results. In fact, if the standard deviation of the measurements can go up to $1.933m/s$ when collecting data which highest possible value is $6m/s$, a coefficient obtained using that same data will not be able to thoroughly describe reality. For this reason, the model is not able to properly predict the behaviour of every single turbine. However, because the errors produced by the model partly compensate one another, this second model manages to predict the energy output of the wind farm with a better accuracy.

Table 5.3: Standard deviation of the data used to create the deficits for speeds between $5m/s$ and $5.5m/s$

	0°	10°	20°	30°	40°	50°	60°	70°	80°	90°	100°	110°	120°	130°	140°	150°	160°	170°	180°	190°	200°	210°	220°	230°	240°	250°	260°	270°	280°	290°	300°	310°	320°	330°	340°	350°
$T1$	0.704	1.017	1.164	1.435	0.998	1.122	1.411	1.185	1.130	1.314	1.143	1.340	1.043	0.848	0.856	1.038	0.878	1.094	1.278	1.189	1.030	1.297	0.997	0.999	0.853	0.912	0.816	0.871	0.988	0.970	0.999	1.136	1.100	0.842	0.759	0.868
$T2$	0.662	0.839	0.972	1.546	1.067	1.164	1.305	1.212	1.145	1.268	1.019	1.302	1.169	1.072	1.065	1.150	0.994	1.061	1.204	1.243	1.017	1.181	1.063	1.006	0.754	0.883	0.892	0.903	0.977	0.812	0.968	0.947	0.887	0.867	0.900	1.004
$T3$	0.717	0.850	1.104	1.581	0.909	1.440	1.235	1.351	1.066	1.238	1.047	1.270	1.156	0.814	0.921	1.034	0.944	1.108	1.237	1.232	0.978	1.147	1.073	0.961	0.814	0.887	0.862	0.919	1.034	0.946	0.970	1.058	0.957	0.793	0.884	1.025
$T4$	0.745	0.883	0.836	1.435	1.104	1.453	1.267	1.367	1.076	1.221	1.095	1.171	0.874	0.915	1.001	1.124	0.857	1.086	1.218	1.215	1.137	1.060	1.032	0.904	0.759	0.852	0.859	0.786	0.801	0.642	0.909	1.124	0.842	0.926	0.851	0.839
$T5$	0.759	0.928	1.070	1.248	0.778	1.513	1.214	1.186	1.076	1.208	1.080	1.203	1.179	0.881	1.071	0.782	0.991	1.124	1.161	1.279	1.030	1.047	1.021	0.916	0.776	0.833	0.868	0.824	0.844	0.737	1.050	1.065	0.889	0.904	0.850	0.918
$T6$	0.723	0.859	1.002	1.250	0.905	1.592	1.469	1.281	1.124	1.211	1.176	1.329	1.132	0.943	1.044	1.115	0.968	1.038	1.169	1.232	1.043	1.029	1.022	0.920	0.823	0.827	0.835	0.763	0.785	0.552	0.819	0.974	0.749	0.725	0.732	0.827
$T7$	0.736	1.052	0.941	1.030	0.622	0.898	0.794	0.813	1.181	0.983	0.880	0.860	0.956	0.875	1.007	0.935	0.826	1.164	1.125	1.135	0.863	0.949	0.924	0.821	0.630	0.716	0.581	0.645	0.812	0.744	0.686	1.072	0.824	0.648	0.751	0.978
$T8$	0.643	0.799	0.745	1.064	0.984	0.828	0.811	0.894	1.161	1.144	1.002	0.911	0.906	1.056	1.040	0.972	0.925	1.084	1.132	1.106	0.868	0.912	0.864	0.759	0.658	0.743	0.593	0.651	0.734	0.697	0.596	1.035	0.774	0.597	0.642	0.870
$T9$	0.765	0.655	0.646	1.136	0.724	0.990	0.763	0.794	1.037	1.016	1.011	0.792	0.867	0.814	0.924	0.890	0.834	1.050	1.014	0.990	0.852	0.842	0.939	0.839	0.670	0.746	0.689	0.766	0.732	0.590	0.758	0.818	0.778	0.913	0.647	0.904
$T10$	0.805	0.613	0.885	0.951	0.681	0.862	0.911	0.780	1.043	0.991	1.008	0.906	0.848	0.788	0.920	0.885	0.849	1.025	1.039	1.060	0.903	0.894	0.897	0.805	0.737	0.768	0.808	0.780	0.830	0.752	0.740	0.827	0.961	0.751	0.616	0.868
$T11$	0.986	0.640	0.721	1.050	0.968	1.016	0.916	0.740	1.063	0.995	1.059	0.971	0.776	0.857	1.009	1.058	1.066	1.050	0.951	1.061	0.954	0.956	0.891	0.803	0.792	0.802	0.663	0.772	0.853	0.590	0.796	0.817	0.876	0.849	0.521	0.808
$T12$	0.584	0.469	0.218	0.933	0.812	0.923	0.893	0.794	1.117	0.960	1.039	0.986	0.799	0.865	1.049	1.039	0.971	1.026	0.944	1.041	0.908	0.887	0.930	0.712	0.746	0.907	0.622	0.920	0.891	0.538	0.789	0.800	0.789	0.854	0.505	0.724
$T13$	1.130	1.095	0.944	1.265	0.846	1.252	1.124	0.662	1.050	1.035	1.192	1.376	0.855	0.739	0.938	1.103	0.912	1.057	1.089	1.053	0.817	0.808	0.843	0.848	0.805	0.868	0.758	0.801	0.822	0.713	0.611	0.799	0.667	0.675	0.821	1.030
$T14$	0.469	0.411	0.669	0.837	0.746	0.848	0.837	0.695	0.620	1.002	0.875	0.867	0.910	0.755	0.782	0.866	0.653	0.854	0.889	0.817	0.790	0.730	0.914	0.645	0.775	0.749	0.685	0.841	0.690	0.655	0.719	0.764	0.804	0.818	0.857	0.702
$T15$	0.267	0.621	0.683	0.801	0.808	0.983	1.002	0.776	1.253	0.984	0.891	0.944	0.949	0.790	0.941	0.920	0.972	0.833	0.855	0.806	0.789	0.842	0.913	0.697	0.821	0.692	0.866	0.927	0.573	0.518	0.714	0.540	0.504	0.567	0.506	0.838
$T16$	0.566	0.583	1.079	0.513	1.071	0.672	1.046	0.942	0.945	1.210	1.064	1.173	1.083	0.870	0.817	0.769	0.820	0.866	0.925	0.874	0.902	0.829	0.913	0.734	0.660	0.909	0.774	0.753	0.668	0.643	0.570	0.839	0.804	0.883	0.682	0.428
$T17$	1.028	1.213	1.030	0.558	1.131	0.727	1.258	1.196	1.240	1.255	1.156	1.261	1.071	0.873	0.833	1.010	0.815	0.842	1.041	1.070	0.836	0.725	0.726	0.606	0.588	0.679	0.471	0.557	0.598	0.625	0.530	0.967	0.881	0.972	0.907	0.564
$T18$	1.192	1.219	0.953	0.703	1.094	0.867	1.108	1.053	0.973	1.359	1.192	1.105	1.042	0.887	1.018	1.083	0.822	0.909	0.869	0.735	0.824	0.729	0.747	0.543	0.615	0.624	0.425	0.532	0.535	0.586	0.614	0.987	0.873	1.054	0.911	0.940
$T19$	0	0	0	0	0	0	0	0	0	0	0	0	0	0	0	0	0	0	0	0	0	0	0	0	0	0	0	0	0	0	0	0	0	0	0	0
$T20$	0.763	0.803	1.021	0.770	0.571	0.955	0.982	1.084	0.878	1.175	1.162	1.224	0.957	0.787	0.864	0.885	0.752	0.824	0.991	0.804	0.728	0.711	0.790	0.612	0.635	0.859	0.542	0.858	0.994	1.102	1.102	0.832	0.871	1.033	0.712	0.603
$T21$	0.784	0.782	1.039	1.039	0.622	0.970	0.985	0.683	0.822	0.817	0.965	0.940	0.820	0.889	0.863	0.946	0.805	0.891	0.846	0.849	0.723	0.840	0.803	0.599	0.571	0.756	0.442	0.713	0.769	0.816	0.669	0.911	0.819	0.725	0.965	0.906
$T22$	0	0	0	0	0	0	0	0	0	0	0	0	0	0	0	0	0	0	0	0	0	0	0	0	0	0	0	0	0	0	0	0	0	0	0	0
$T23$	0.831	1.096	0.860	0.839	0.633	0.713	0.706	0.949	1.101	0.909	0.886	1.147	1.022	0.641	0.834	0.872	0.740	0.856	0.936	0.917	0.862	0.697	0.736	0.587	0.654	0.653	0.427	0.515	0.603	0.549	0.574	1.010	0.841	1.081	0.937	0.635
$T24$	0.747	0.775	1.050	0.578	0.491	0.861	0.914	0.681	0.762	0.845	0.897	0.877	0.818	0.627	0.786	0.738	0.797	0.934	0.931	0.801	0.723	0.755	0.685	0.598	0.610	0.679	0.425	0.482	0.522	0.631	0.630	0.987	0.956	0.974	0.894	0.721
$T25$	0	0	0	0	0	0	0	0	0	0	0	0	0	0	0	0	0	0	0	0	0	0	0	0	0	0	0	0	0	0	0	0	0	0	0	0
$T26$	0.940	0.882	0.912	0.742	0.590	0.692	1.090	0.860	0.985	0.804	0.879	0.946	1.099	0.838	1.077	0.838	0.825	0.930	1.186	1.085	0.977	0.810	0.791	0.737	0.716	0.659	0.542	0.644	0.764	0.636	0.619	0.932	0.793	0.858	0.976	0.688
$T27$	0.970	0.652	1.045	1.047	0.589	0.586	1.024	0.913	0.985	1.005	0.767	0.851	0.943	0.632	0.984	0.872	0.871	0.995	0.977	0.905	0.905	0.730	0.732	0.712	0.679	0.685	0.485	0.605	0.711	0.562	0.588	0.886	0.821	0.875	0.826	0.664
$T28$	0.954	0.780	0.891	0.721	0.781	0.521	1.181	0.953	0.954	0.982	0.922	0.944	0.882	0.783	1.016	0.845	0.939	1.102	1.210	0.958	0.908	0.759	0.830	0.657	0.669	0.736	0.545	0.572	0.680	0.594	0.643	0.799	0.814	0.821	0.898	0.725
$T29$	1.126	0.841	0.997	0.887	0.585	0.625	0.850	0.866	0.933	1.089	0.994	0.862	0.949	0.838	0.813	0.899	1.008	1.100	1.217	0.880	0.848	0.802	0.762	0.691	0.696	0.729	0.541	0.504	0.653	0.565	0.649	0.890	0.776	0.949	0.828	0.808
$T30$	0	0	0	0	0	0	0	0	0	0	0	0	0	0	0	0	0	0	0	0	0	0	0	0	0	0	0	0	0	0	0	0	0	0	0	0
$T31$	1.069	1.072	1.205	0.833	0.787	0.801	0.912	0.959	1.163	1.145	0.917	0.915	0.865	0.847	0.824	0.909	0.918	1.005	1.054	1.051	1.011	0.889	0.856	0.702	0.706	0.748	0.531	0.552	0.762	0.616	0.684	0.982	1.047	0.929	0.673	0.921
$T32$	1.007	1.027	1.092	0.726	0.348	0.839	1.007	0.956	0.899	1.141	1.054	1.040	1.072	0.789	0.920	0.864	0.984	1.232	1.109	1.065	1.130	0.980	1.000	0.727	0.726	0.742	0.686	0.774	0.823	0.588	0.669	0.952	1.000	1.151	0.869	0.941
$T33$	0.996	1.002	1.056	0.738	0.562	0.758	0.960	1.080	0.981	0.993	0.906	1.235	1.126	0.909	0.937	0.931	0.973	1.191	1.160	1.090	1.193	0.972	1.019	0.823	0.749	0.749	0.752	0.778	0.755	0.656	0.789	0.937	1.110	1.065	0.773	0.865
$T34$	0.886	1.092	1.246	1.032	0.638	0.931	1.065	1.084	0.884	0.896	0.870	1.174	1.103	0.956	0.825	1.024	1.029	1.012	1.249	1.037	1.134	1.019	1.036	1.017	0.904	0.840	0.930	0.764	0.857	0.671	0.839	1.055	1.131	0.949	0.799	0.793
$T35$	0.909	1.103	1.026	1.179	0.689	0.676	1.383	0.876	0.867	0.882	0.722	0.810	0.990	0.923	0.935	0.907	0.945	0.994	1.190	0.786	1.030	0.901	0.930	0.928	0.750	0.688	0.754	0.613	0.866	0.663	0.702	1.007	1.170	0.996	0.679	0.585
$T36$	0.867	1.196	1.153	1.012	0.495	0.607	1.050	1.490	0.664	1.113	0.759	0.945	1.149	0.929	0.801	0.865	0.982	1.111	1.195	1.092	1.094	0.854	0.770	0.908	0.779	0.678	0.694	0.527	0.790	0.679	0.794	0.959	1.188	1.098	0.759	0.785
$T37$	1.013	1.212	1.108	0.789	0.833	0.701	1.011	0.886	1.071	1.281	1.098	1.085	1.141	1.043	0.918	0.988	1.085	1.240	1.381	1.020	1.134	0.846	0.848	0.957	0.923	0.683	0.756	0.688	0.723	0.709	0.839	1.017	1.172	1.098	0.865	0.752
$T38$	0	0	0	0	0	0	0	0	0	0	0	0	0	0	0	0	0	0	0	0	0	0	0	0	0	0	0	0	0	0	0	0	0	0	0	0
$T39$	0.829	0.884	1.250	0.982	0.743	0.672	1.167	0.670	0.586	1.322	0.974	0.793	0.960	0.911	0.811	0.712	0.767	1.085	1.143	0.968	1.131	0.915	0.949	0.914	0.908	0.811	0.871	0.838	0.960	0.842	0.948	0.894	1.011	0.818	0.813	0.850
$T40$	0.518	0.939	0.944	1.201	0.792	0.878	1.215	0.708	0.528	1.100	0.570	0.691	0.907	0.721	0.642	0.810	0.762	0.816	0.992	0.692	0.926	0.855	0.764	0.713	0.784	0.736	0.770	0.667	0.943	0.799	0.767	0.839	0.919	0.724	0.725	0.789
$T41$	0.577	0.990	0.715	1.370	0.789	1.049	1.212	0.815	0.722	1.012	0.730	0.669	0.937	0.641	0.786	1.044	0.738	0.939	1.084	0.919	0.946	0.784	0.855	0.732	0.724	0.729	0.715	0.621	0.849	0.609	0.851	0.900	0.850	0.640	0.713	0.951
$T42$	0.590	0.942	0.730	1.148	0.817	0.923	1.016	1.070	0.814	1.094	0.713	0.675	0.937	0.627	0.798	0.793	0.846	0.918	1.016	0.796	0.895	0.890	0.905	0.774	0.801	0.743	0.665	0.954	0.793	0.671	0.800	0.727	0.770	0.827	0.548	0.944
$T43$	0.543	0.960	0.857	1.278	0.601	0.939	1.090	0.946	0.880	1.343	0.957	0.820	1.093	0.824	0.848	0.827	0.875	0.920	0.943	0.854	0.894	0.790	0.882	0.898	0.752	0.733	0.538	0.642	0.878	0.801	0.670	0.711	0.735	0.725	0.734	0.963
$T44$	0.980	0.949	1.053	1.084	0.569	0.852	0.859	1.088	0.828	1.007	0.917	0.856	0.964	0.868	0.826	0.850	0.805	0.720	0.856	0.876	0.933	0.873	0.884	0.892	0.708	0.794	0.550	0.698	0.942	0.649	0.672	0.952	0.789	0.948	0.730	0.717
$T45$	0.985	0.921	1.832	1.845	0.512	0.716	0.764	1.033	0.971	1.159	0.757	0.752	0.942	0.705	0.664	0.816	0.840	0.729	0.804	0.858	0.798	0.862	0.884	0.847	0.731	0.780	0.631	0.639	0.742	0.628	0.618	0.843	0.745	0.754	0.719	0.786
$T46$	0.806	0.623	0.634	0.731	0.514	1.158	0.833	0.913	0.983	1.089	0.710	0.742	0.895	0.706	0.686	0.788	0.883	0.907	0.797	0.735	0.872	0.837	0.757	0.716	0.701	0.758	0.627	0.744	0.717	0.554	0.641	0.766	0.779	0.817	0.764	0.856

Table 5.4: Standard deviation of the data used to create the deficits for speeds between $5.5m/s$ and $6m/s$

	0°	10°	20°	30°	40°	50°	60°	70°	80°	90°	100°	110°	120°	130°	140°	150°	160°	170°	180°	190°	200°	210°	220°	230°	240°	250°	260°	270°	280°	290°	300°	310°	320°	330°	340°	350°
$T1$	0.504	1.053	1.086	1.418	0.724	0.563	1.227	1.445	1.289	1.596	1.624	1.178	1.161	0.931	0.897	1.011	1.066	0.877	1.321	1.306	1.291	1.233	1.019	1.093	0.983	0.779	0.793	0.852	0.826	0.924	0.930	1.123	1.255	0.769	0.851	0.721
$T2$	0.915	0.999	0.929	1.125	0.886	0.977	1.048	1.262	1.294	1.405	1.641	1.333	1.333	1.146	1.218	1.106	1.135	0.962	1.230	1.342	1.236	1.187	1.029	1.046	1.034	0.774	0.781	0.917	0.770	0.909	0.886	1.051	1.057	0.920	0.716	0.794
$T3$	0.528	1.035	1.026	1.380	1.306	1.261	1.025	1.380	1.200	1.199	1.352	1.094	1.212	1.028	1.142	1.192	1.187	0.938	1.085	1.330	1.219	1.144	1.091	1.077	0.940	0.858	0.838	0.967	0.914	0.936	0.939	1.057	1.056	0.948	0.795	0.980
$T4$	0.649	1.067	0.990	1.491	1.286	1.117	0.969	1.346	0.982	1.182	1.294	1.136	1.144	0.978	1.093	1.082	1.108	0.985	0.983	1.251	1.182	1.097	0.955	0.964	0.967	0.818	0.877	0.933	0.776	0.833	0.740	1.243	0.830	0.880	0.987	0.825
$T5$	0.421	1.148	1.014	1.363	1.483	1.339	1.179	1.426	1.091	1.092	1.279	1.028	1.263	0.954	1.228	1.015	1.274	1.001	0.964	1.238	1.184	1.142	0.972	1.008	0.924	0.842	0.815	0.857	0.819	0.910	0.922	1.111	1.067	0.918	0.630	0.847
$T6$	0.432	1.268	0.954	0.885	1.586	1.358	1.368	1.390	1.119	1.293	1.371	1.160	1.361	0.922	1.066	1.237	1.130	0.946	1.020	1.149	1.139	1.050	0.926	1.013	0.945	0.823	0.719	0.809	0.755	0.820	0.700	1.025	0.889	0.710	0.647	0.783
$T7$	0.591	1.048	0.726	1.287	0.849	0.843	0.939	1.154	0.875	0.939	1.126	0.872	1.019	0.858	0.886	1.160	0.988	0.980	0.952	1.234	1.100	1.097	0.872	1.055	0.765	0.790	0.635	0.690	0.718	0.963	0.808	1.144	0.941	0.659	0.669	0.968
$T8$	0.578	0.698	0.779	1.310	1.163	0.762	0.998	1.173	0.813	0.904	1.149	1.017	0.986	1.026	0.946	1.111	0.931	0.846	1.029	1.065	1.134	1.123	0.722	0.936	0.739	0.789	0.628	0.652	0.696	0.830	0.598	1.138	0.905	0.678	0.652	0.832
$T9$	0.649	0.844	0.807	1.151	1.592	1.006	0.936	0.986	0.888	0.909	1.030	0.909	0.931	0.874	0.844	1.121	0.924	0.875	0.954	1.033	0.993	0.975	0.749	0.982	0.803	0.799	0.644	0.832	0.564	0.596	0.688	0.968	0.785	0.760	0.643	0.755
$T10$	0.669	0.977	1.165	1.383	1.563	1.150	0.965	1.163	0.884	0.933	1.212	1.040	1.186	0.904	1.086	1.027	1.039	0.801	0.897	1.160	1.016	1.000	0.887	0.963	0.817	0.837	0.701	0.846	0.788	0.794	0.673	0.765	1.063	0.740	0.675	0.826
$T11$	0.688	0.986	1.214	1.571	1.638	1.652	1.057	1.256	0.813	1.040	1.197	1.165	1.054	0.885	1.002	1.022	1.062	0.781	1.055	1.206	1.095	1.072	0.843	0.962	0.769	0.710	0.614	0.893	0.824	0.751	0.726	0.864	0.866	0.760	0.685	0.749
$T12$	0.642	0.848	1.113	1.310	1.138	1.139	0.795	1.135	0.640	1.021	1.130	1.013	1.111	0.778	1.134	1.027	0.951	0.939	0.907	1.172	0.959	0.996	0.743	0.894	0.712	0.635	0.688	0.940	0.639	0.710	0.700	0.894	0.758	0.671	0.619	0.481
$T13$	1.527	1.247	0.958	1.357	1.262	1.287	1.252	1.194	0.721	0.996	1.150	1.078	1.041	0.856	0.960	1.091	0.943	0.902	1.094	1.076	1.112	0.955	0.804	0.845	0.833	0.820	0.734	0.751	0.622	0.609	0.624	0.793	0.750	0.534	0.744	0.803
$T14$	0.448	0.559	0.757	0.692	1.276	0.541	0.848	0.963	0.598	1.039	1.152	0.871	1.041	0.843	0.781	0.833	0.854	0.702	0.955	1.058	0.947	0.767	0.804	0.811	0.739	0.737	0.633	0.702	0.597	0.778	0.649	0.776	0.979	1.043	0.807	0.663
$T15$	0.906	0.424	0.779	1.203	0.300	0.522	0.719	1.012	0.857	0.858	1.265	0.843	0.993	0.994	0.853	0.890	0.929	0.783	0.864	0.954	0.942	0.820	0.772	1.067	0.598	0.823	0.848	0.707	0.450	0.682	0.799	0.905	0.809	0.615	0.660	1.139
$T16$	0.404	0.549	0.741	1.776	1.097	0.615	1.077	0.953	0.875	1.125	1.447	1.061	1.135	1.032	0.734	0.865	0.790	0.884	1.124	1.014	0.994	0.768	0.926	0.962	0.685	0.783	0.641	0.582	0.701	0.695	0.645	0.873	0.978	0.662	0.656	0.549
$T17$	0.646	0.602	1.185	1.126	0.915	0.737	1.236	0.876	0.938	1.243	1.558	1.351	1.067	0.906	0.698	0.817	0.662	0.901	1.162	1.108	0.742	0.672	0.780	0.707	0.655	0.543	0.420	0.482	0.666	0.655	0.624	1.023	1.175	0.965	1.008	0.609
$T18$	1.062	0.837	1.078	1.195	1.083	0.741	0.729	0.894	0.973	1.288	1.494	1.113	1.048	0.702	0.786	0.646	0.562	0.854	0.918	0.917	0.692	0.688	0.772	0.678	0.657	0.543	0.450	0.460	0.570	0.658	0.685	0.905	1.121	0.842	1.050	0.756
$T19$	0	0	0	0	0	0	0	0	0	0	0	0	0	0	0	0	0	0	0	0	0	0	0	0	0	0	0	0	0	0	0	0	0	0	0	0
$T20$	0.690	0.772	0.743	0.899	1.130	0.570	0.679	1.105	0.849	1.256	1.307	0.906	0.984	1.006	0.896	0.946	0.921	0.659	0.928	0.876	0.804	0.580	0.740	0.763	0.648	0.699	0.589	0.718	1.072	1.064	0.941	0.834	0.932	0.879	0.732	0.652
$T21$	0.674	0.798	1.129	1.024	1.137	0.384	0.639	0.928	0.737	0.883	0.956	0.841	0.978	0.837	0.754	0.846	0.802	0.788	0.849	0.912	0.925	0.652	0.700	0.904	0.587	0.610	0.465	0.607	0.717	0.876	0.651	0.912	0.841	0.652	0.876	0.752
$T22$	0	0	0	0	0	0	0	0	0	0	0	0	0	0	0	0	0	0	0	0	0	0	0	0	0	0	0	0	0	0	0	0	0	0	0	0
$T23$	0.825	1.097	1.027	0.200	0.830	0.844	0.767	0.815	0.862	1.103	1.172	1.064	1.076	0.922	0.647	0.784	0.694	0.977	0.909	1.057	0.727	0.666	0.768	0.566	0.643	0.538	0.451	0.449	0.544	0.632	0.605	0.725	1.088	0.702	0.848	0.807
$T24$	0.833	0.929	0.895	0.632	0.925	0.662	0.664	0.657	0.848	0.916	1.031	0.912	1.033	0.904	0.672	0.694	0.639	0.989	1.032	0.995	0.828	0.645	0.587	0.590	0.649	0.539	0.494	0.519	0.487	0.595	0.563	0.782	1.083	0.674	1.050	0.806
$T25$	0	0	0	0	0	0	0	0	0	0	0	0	0	0	0	0	0	0	0	0	0	0	0	0	0	0	0	0	0	0	0	0	0	0	0	0
$T26$	0.788	0.756	0.990	0.660	0.839	1.102	0.925	1.130	0.669	1.141	1.004	1.025	1.278	1.126	0.973	0.870	0.819	1.160	1.339	1.206	1.031	0.837	0.642	0.839	0.657	0.540	0.565	0.626	0.538	0.524	0.644	0.820	0.937	0.681	1.079	0.750
$T27$	0.850	1.003	1.042	0.895	1.619	0.611	1.113	0.796	0.498	0.985	0.909	1.012	1.179	1.024	0.736	0.839	0.852	1.010	1.212	1.143	0.973	0.680	0.648	0.794	0.653	0.568	0.539	0.596	0.483	0.494	0.556	0.867	0.989	0.825	0.898	0.564
$T28$	0.834	1.009	0.974	0.987	1.933	0.638	1.216	0.735	0.505	0.960	0.911	0.956	1.116	1.125	0.815	0.901	0.893	1.232	1.247	1.160	1.001	0.685	0.623	0.764	0.651	0.601	0.525	0.545	0.483	0.531	0.568	0.781	0.908	0.686	0.952	0.721
$T29$	1.036	0.893	0.876	1.146	1.763	0.595	1.082	0.761	0.690	1.096	1.027	0.984	1.136	0.865	0.765	0.857	0.888	1.283	1.309	1.015	0.974	0.727	0.679	0.834	0.669	0.624	0.465	0.540	0.488	0.688	0.609	0.813	0.877	0.867	0.896	0.992
$T30$	0	0	0	0	0	0	0	0	0	0	0	0	0	0	0	0	0	0	0	0	0	0	0	0	0	0	0	0	0	0	0	0	0	0	0	0
$T31$	0.950	1.162	0.988	0.836	1.287	0.595	0.750	0.819	0.810	0.989	1.033	0.803	1.094	1.150	0.747	0.872	0.758	1.174	1.227	1.068	0.983	0.911	0.727	0.796	0.692	0.627	0.569	0.651	0.627	0.570	0.653	0.847	0.992	1.010	0.725	1.012
$T32$	1.024	0.929	1.047	0.825	1.204	0.574	1.029	0.837	0.683	1.097	1.250	1.229	1.415	1.225	0.871	0.815	0.849	1.299	1.164	1.021	1.045	1.050	0.756	0.899	0.697	0.678	0.635	0.731	0.711	0.534	0.721	0.944	0.955	0.880	1.067	0.821
$T33$	0.923	0.985	0.993	0.420	0.970	0.567	0.986	0.878	0.758	1.128	1.188	1.206	1.280	1.241	1.006	0.811	0.915	1.299	1.023	1.099	1.093	1.092	0.704	0.938	0.720	0.632	0.637	0.643	0.756	0.517	0.698	0.911	0.815	1.064	0.838	0.923
$T34$	0.935	1.073	1.320	1.025	1.215	0.614	1.385	0.968	0.712	1.005	1.133	1.120	1.234	1.282	0.953	1.059	0.895	1.139	1.146	1.152	1.137	1.151	0.734	1.045	0.787	0.753	0.696	0.768	0.682	0.606	0.715	0.889	0.993	1.020	0.787	0.975
$T35$	0.866	0.911	1.122	0.866	1.176	0.497	1.051	0.859	0.749	1.056	1.000	0.812	1.193	1.098	0.826	0.957	0.917	1.256	1.230	0.942	0.974	0.955	0.776	0.939	0.777	0.641	0.635	0.684	0.778	0.651	0.646	0.911	1.064	0.947	0.979	0.721
$T36$	1.005	0.832	0.613	0.874	1.046	0.481	1.691	1.272	0.465	0.823	1.120	0.974	1.207	1.066	0.671	1.035	1.053	1.124	1.188	1.169	0.985	1.088	0.827	0.961	0.769	0.689	0.892	0.643	0.674	0.531	0.604	0.903	1.134	1.095	0.849	0.795
$T37$	1.139	0.862	0.954	0.614	1.078	0.416	1.078	0.864	0.675	1.043	1.173	1.015	0.926	1.015	0.663	1.239	1.088	1.345	1.510	1.307	1.016	1.132	0.983	0.966	0.738	0.762	0.618	0.678	0.604	0.538	0.562	1.004	1.119	1.029	0.919	0.666
$T38$	0	0	0	0	0	0	0	0	0	0	0	0	0	0	0	0	0	0	0	0	0	0	0	0	0	0	0	0	0	0	0	0	0	0	0	0
$T39$	0.997	1.005	1.033	0.689	1.006	0.392	1.085	0.497	0.285	0.839	0.773	0.667	0.928	0.993	0.613	0.792	0.493	0.686	1.284	1.155	1.033	1.037	0.836	0.915	0.943	0.888	0.911	0.825	0.999	0.841	0.767	0.789	1.050	0.780	0.956	0.960
$T40$	0.850	0.978	1.053	0.853	1.161	0.741	0.922	0.734	0.271	0.752	0.636	0.548	1.025	1.018	0.641	0.817	0.836	0.902	1.061	0.937	0.768	0.972	0.782	0.850	0.818	0.910	0.795	0.728	1.020	0.715	0.593	0.752	0.898	0.903	0.894	0.876
$T41$	0.848	1.088	0.992	1.081	1.284	0.766	0.934	0.809	0.493	0.911	0.872	0.661	1.051	1.073	0.863	0.913	0.975	0.896	1.007	1.055	0.988	0.869	0.762	0.797	0.722	0.841	0.651	0.777	0.816	0.551	0.584	0.799	0.843	0.608	0.774	0.898
$T42$	0.672	1.069	1.036	1.036	1.486	0.826	1.000	0.887	0.485	0.892	0.944	0.775	1.078	1.126	0.853	1.045	0.933	0.952	0.919	0.829	0.926	0.961	0.678	0.876	0.883	0.826	0.609	1.048	0.973	0.780	0.726	0.765	0.775	0.680	0.834	0.826
$T43$	0.660	0.986	1.031	1.180	1.210	0.693	0.874	1.039	0.825	0.780	0.947	0.802	1.245	1.098	0.876	0.950	0.987	0.775	0.655	0.866	0.909	0.966	0.631	0.926	0.776	0.844	0.597	0.666	0.682	0.904	0.638	0.749	0.796	0.794	0.967	0.896
$T44$	0.836	1.033	1.257	1.349	1.458	0.624	1.029	0.822	0.651	0.936	1.065	1.018	0.984	1.016	0.853	1.001	0.952	0.685	0.756	1.026	0.972	0.933	0.690	1.076	0.702	0.731	0.561	0.692	0.697	0.823	0.617	0.877	0.780	0.842	0.860	0.843
$T45$	0.733	1.223	1.201	1.094	1.293	0.587	1.006	0.802	0.544	1.043	0.940	0.970	1.028	1.049	0.826	0.922	0.904	0.947	1.020	1.043	0.857	0.925	0.690	0.995	0.740	0.833	0.606	0.777	0.739	0.635	0.535	0.738	0.769	0.806	0.797	0.942
$T46$	0.733	0.902	1.076	1.251	1.319	0.463	0.902	0.852	0.574	1.053	0.867	0.876	1.134	1.090	0.908	0.881	0.836	0.881	0.891	0.764	0.908	0.847	0.740	0.909	0.710	0.643	0.613	0.775	0.727	0.646	0.653	0.767	0.742	0.724	0.895	0.867

5.10 Attempt to Improve the Model

Since in some cases the model was not able to reproduce the actual behaviour within the wind farm and of the wind farm itself, some attempts to improve the model were carried out. Initially, the difference in energy production was studied in terms of the wind direction. By doing so, it was hoped that some kind of pattern would be found. Mainly, the goal was to find one or more directions in which the difference between the results of the model and the measurements was constanly higher than in the others. If the goal was fulfilled some improvements in case the wind was blowing from that direction could be made. The results of this first attempt are reported in Figure 5.9, where the difference in energy production is plotted as a function of the wind direction.

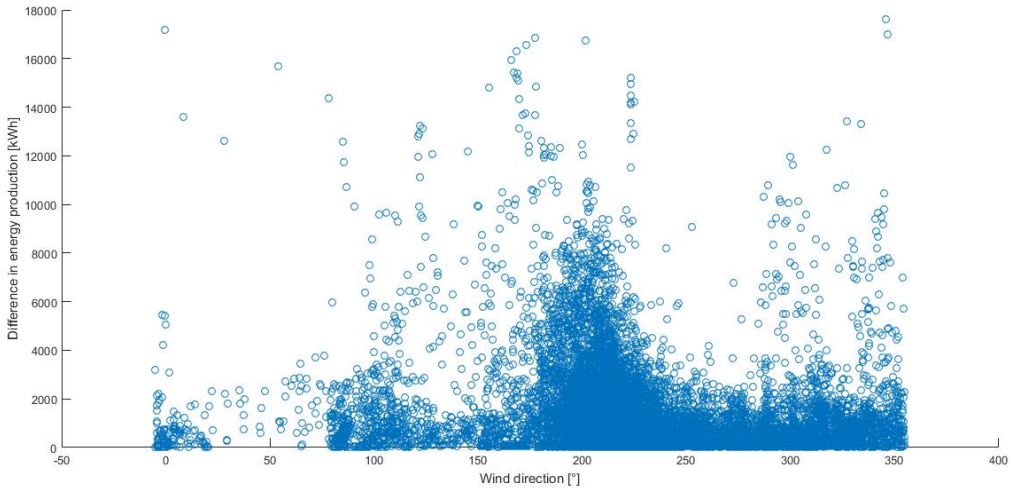

Figure 5.9: Difference in energy production as a function of the wind direction

It can be noted how the circles are scattered around the whole graph, with a peak a bit after $200°$. However, this peak does not highlight a useful pattern since it happens because that one is the direction the wind blows from most often from. In addition to this, in the same direction there are cases in which the difference is extremely low and even equal to 0. Also, some cases in which the difference is as high as or even higher than the levels reached in that direction can be found for other values on the x-axis. For these reasons, no useful input to improve the model were obtained from this analysis.

In another attempt to improve the model, the possible dependence of the difference in energy production on the temperature was studied. In order to carry out a correct analysis, the meteorological data collected by each turbine was studied to check their reliability. It was found that not all the turbines produced reliable data. In fact, a turbine was found to collect data that were significantly different from the ones nearby, which is not possible since the variable taken into account was the temperature. For this reason, this turbine was neglected when studying the metorological conditions. Once again, the difference in energy production was plotted in a cartesian coordinate system, where it was indicated on the y-axis while the temperature was on the x-axis. The temperature indicated on the x-axis is the average of the temperature data collected by the turbines. Such a plot is reported in Figure 5.10. Just like in the previous case, no pattern was recognised looking at the plot. Again, the majority of the data is

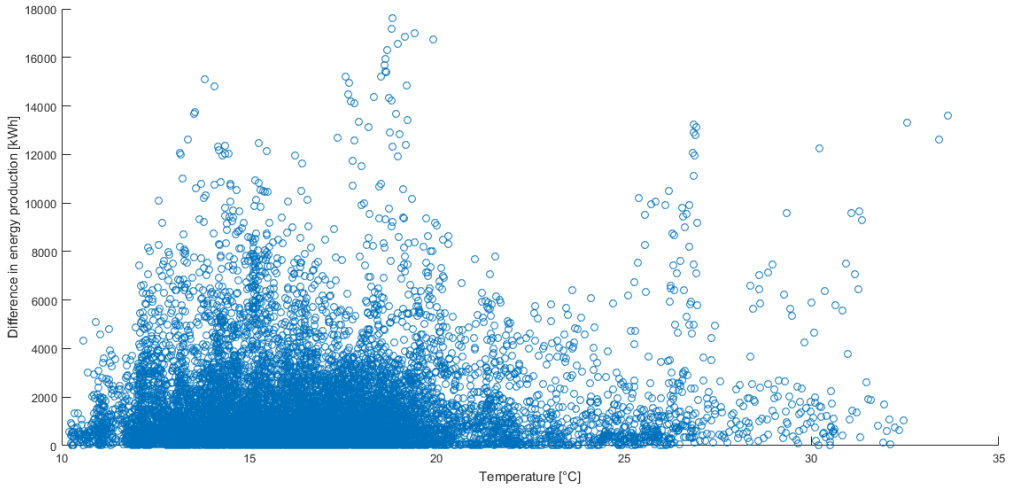

Figure 5.10: Difference in energy production as a function of the ambient temperature

located in an interval of the x-axis making impossible to find a possible relation between the two sets of data. Also, just like in Figure 5.9, the circles are scattered all around the graph highlighting even more the fact that no relation is present.

A further analysis on the difference in energy production was carried out when it was compared with either the average or maximum (and according to the model, undisturbed) wind speed. Once again, no clear relation could be identified, even after dividing the data also according to the direction the wind was blowing from.

In order to search for an improvement, the accumulated difference of the wind speed at the turbines was studied. The accumulated difference is calculated like in equation (3.7). The accumulated difference was then plotted as a function of the wind direction. It was hoped that this new analysis could produce different results as in the accumulated difference the errors do not erase one another like in the difference in energy production. However, as shown in Figure 5.11, also in this case no important pattern was

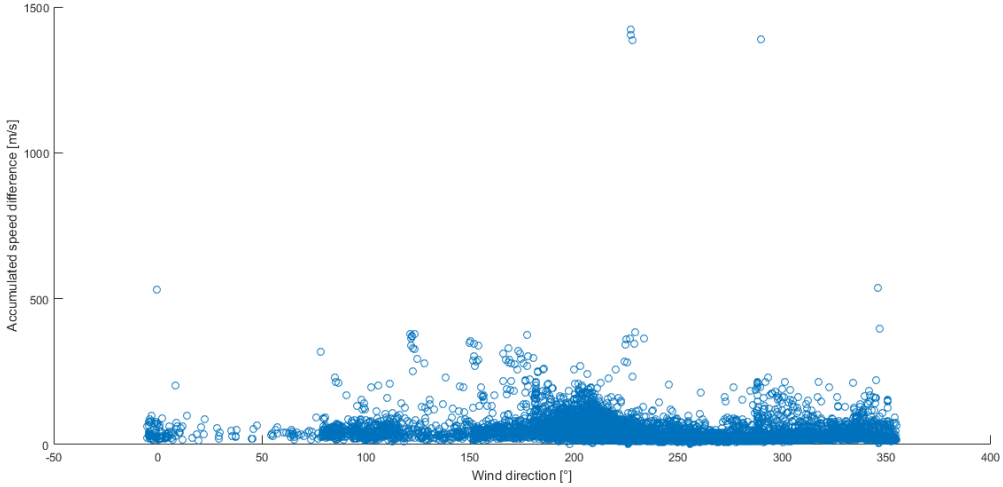

Figure 5.11: Accumulated wind speed difference as a function of the wind direction

found. The results are similar to the ones in Figure 5.9, but it can be easily noted in this case that there are a few points with an extremely high accumulated difference. These points can help in understanding to what extent the fact that the errors erase one another can affect the results of a model.

Sequently, a possible and easily-implementable correlation between the wind speed and the other meteorological variables was seeked. It was thought that one variable would not be enough to describe the wind speed and therefore in this new analysis $3D$ plots were used. This way, the wind speed was studied as a function of two meteorological variables and not only one. Since the variables that were thought to possibly affect the wind speed were 3, a series of $3D$ plots was created. The meteorological variables taken into account were pressure (p), temperature (T) and humidity (ϕ). In this series of graphs, the wind speed was always put on the z-axis, while the variables on the x-axis and y-axis varied. The plots obtained were three:

1. Temperature vs Pressure vs Wind speed
2. Temperature vs Humidity vs Wind speed
3. Pressure vs Humidity vs Wind speed

The graphs obtained are shown in Figure 5.12. They are reported in a smaller format as the images are not able to properly report the information contained in the plots. In this case, the data used came from the met masts within the wind farm since the instrumentation on the turbines was not able to measure the humidity and also because the measurement from the met masts should be more reliable. Also this analysis did not lead to results as the points were scattered all over the graph, with no identifiable behaviour. To conclude, all the analysis explained in the last section did not lead to any possible improvement to the model, which therefore remained unchanged.

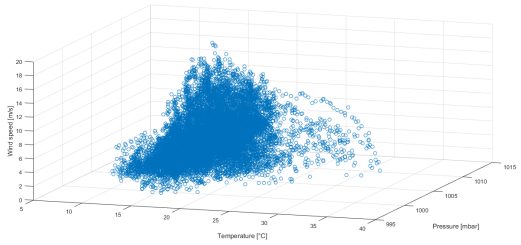

(a) T vs p vs u

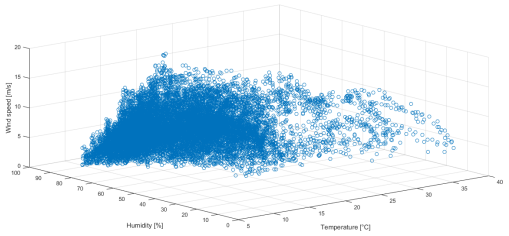

(b) T vs ϕ vs u

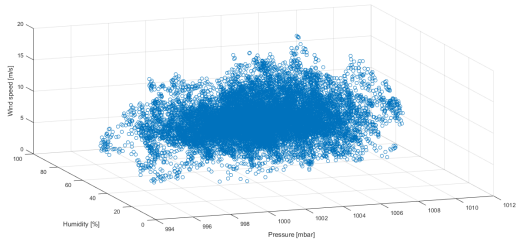

(c) p vs ϕ vs u

Figure 5.12: Series of $3D$ graphs involving the meteorological variables

5.11 Possible Ameliorations

In order to have the model to predict in a better way the output of the wind farm a few possible ameliorations should be done. However, some of these improvements are not directly related to the model itself. One of the problems encountered was the lack of data relative to some conditions of the wind. This happened because the data used for the training of the model was just relative to 9 months. When characterising a site based on its wind, data is collected for a long period of time, even several years. This way it is possible to find at least an average condition for every season of the year without it being affected by the variable conditions that may happen uniquely in a year. Having more data would have allowed to better characterise some of the conditions of the wind, which instead were strongly influenced by some data with a very high standard deviation. Also, it would have permitted to find data relative to some conditions that never occurred during those 9 months.

However, this improvement alone would have not been enough to significantly improve the model. In fact, the most important amelioration would probably be to include the variability of the wind within the model. With this additional feature, the model would probably be better at reproducing some of the fluctuations of the speed happening within the wind farm.

Alternatively, if the interval covered by each time slot were shorter, the variability of the wind would affect to a lesser way the results of the model. In case of shorter intervals, the fluctuations would still be present but their effect would be diminished. In addition to this, since the power produced by a turbine is proportional to u^3, decreasing the influence of the fluctuations on the wind speed would translate in an even bigger reduction of their impact on the energy produced.

5.12 Conclusions to the Chapter

In this chapter, the structure of the empirical model has been exposed. Initially, the reasons why the power curves and the list of unreliable turbines were maintained from the physical model were explained. Then, it was explained how the maximum wind speed and the average wind direction were decided to be the inputs to the model. Subsequently, the organisation of the data and the solution for the unreliable turbines were uncovered.

In the next sections, the results obtained from the application of this second model were revealed, showing better results compared to the physical model. However, the results were not extremely precise and therefore the standard deviations of the wind speeds used to create the deficits were analysed. Finally, some possible improvements were studied or suggested. Among the ones that have been studied, no real applicable amelioration was found and consequently, the model was kept as it was.

Chapter 6

Creation of the Series of Equations

The last step towards the conclusion of the project was the creation of a series of equations representing the behaviour of the deficits collected using the empirical model. This last operation would allow the team of the wind farm to quickly know the output of each working turbine once the conditions of the wind entering the wind farm were known. This way, they would be able to quickly communicate the amount of power the wind farm is able to send to the grid. Also, this method would allow not to take into account the turbines that have been shut down because of different reasons.

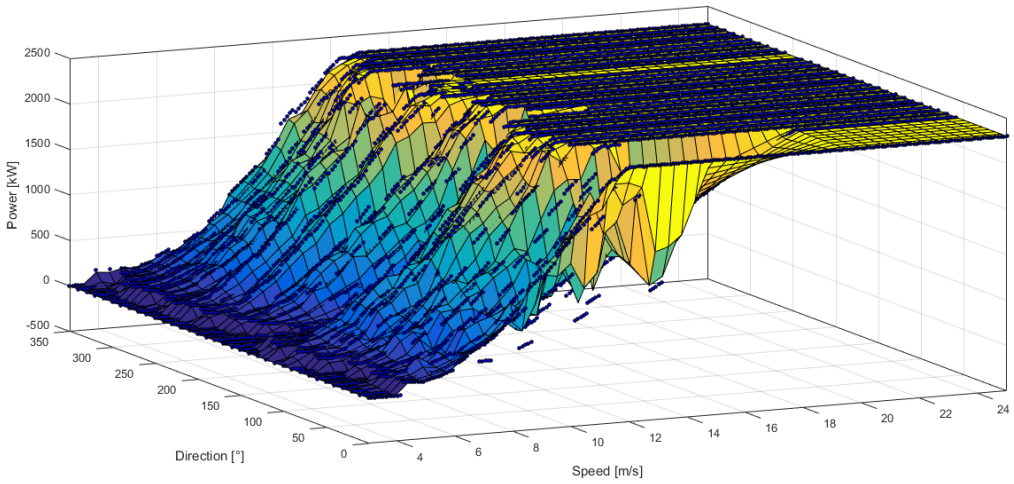

Figure 6.1: Example of set of data obtained from the deficits of the empirical model

In Figure 6.1, an example of the set of data that was attempted to reproduce in order to describe the behaviour of that particular turbine is shown. Even though it is a $3D$ graph, Figure 6.1 shows in a clear way how the the power output significantly varies according to the direction.

6.1 Software Used

Having the deficits for the vast majority of combinations of wind speed and direction, it was possible to estimate the power output of each turbine according to those particular conditions. After these calcula-

tions, the outputs and relative inputs were saved and organised based on the turbine they were referred to. Once the data was organised, all the inputs and outputs needed were available and easy to connect among them. In these cases, the most suitable approach to find an equation able to reproduce the behaviour represented by the inputs and outputs is the surface fitting.

Two methods have been selected as possible when applying the surface fitting. The first one is based on the calculation of the best possible set of parametres relative to a type of equation given by the user. In order for this procedure to work properly, the user needs to have an idea on the type of equation governing the analysed phenomenon. This approach was studied with the help of Prof. Pedro Sebastião using his online platform Fitteia [43]. The second method needs specific software, which is able to find the most suitable type of equation among the ones included in their sets and find a set of parametres describing that equations that is able to maximise R^2. In this case, the software used to try to create this set of equations were TableCurve 3D [44] and CurveExpert [45].

Since the second approach is easier for the user, it was initially chosen to find the equations describing the behaviour of the turbines. Also, the calculations were originally carried out only for one turbine, while the other calculations would have been done if satisfactory results were found with any of the software or approaches.

6.2 First Attempts

As it has just been stated, in the first attempts to find an equation emulating the production of power from the wind turbines the software using their own sets of equations were used. In this case, results with an extremely good value of R^2 were found. However, they were not able to properly reproduce the behaviour of the turbine because the obtained surface was almost constant with the direction and therefore not able to reproduce the oscillations of the data. This feature can be seen comparing Figure 6.2 and Figure 6.1.

The results reported in Figure 6.2 have been taken from the software TableCurve 3D and follow the equation reported in (6.1). Despite this problem with the direction, this curve has been indicated to reach a value for R^2 equal to 0.99999907. Similar results have been found also using CurveExpert, but they presented the same kind of problems, especially being almost constant with the wind direction.

$$z = a + 0.25 \cdot b \cdot \left(1 + erf\left(\frac{x-c}{\sqrt{2}\cdot d}\right)\right) \cdot \left(1 + erf\left(\frac{y-e}{\sqrt{2}\cdot d}\right)\right) \tag{6.1}$$

where:

- x is the wind speed in m/s
- y is the wind direction in $^\circ$
- z is the power output in kW
- $a = 2.1850562$

- $b = 2300.0094$
- $c = 8.7884548$
- $d = 2.1245277$
- $e = -2826.5238$
- erf indicates the error function

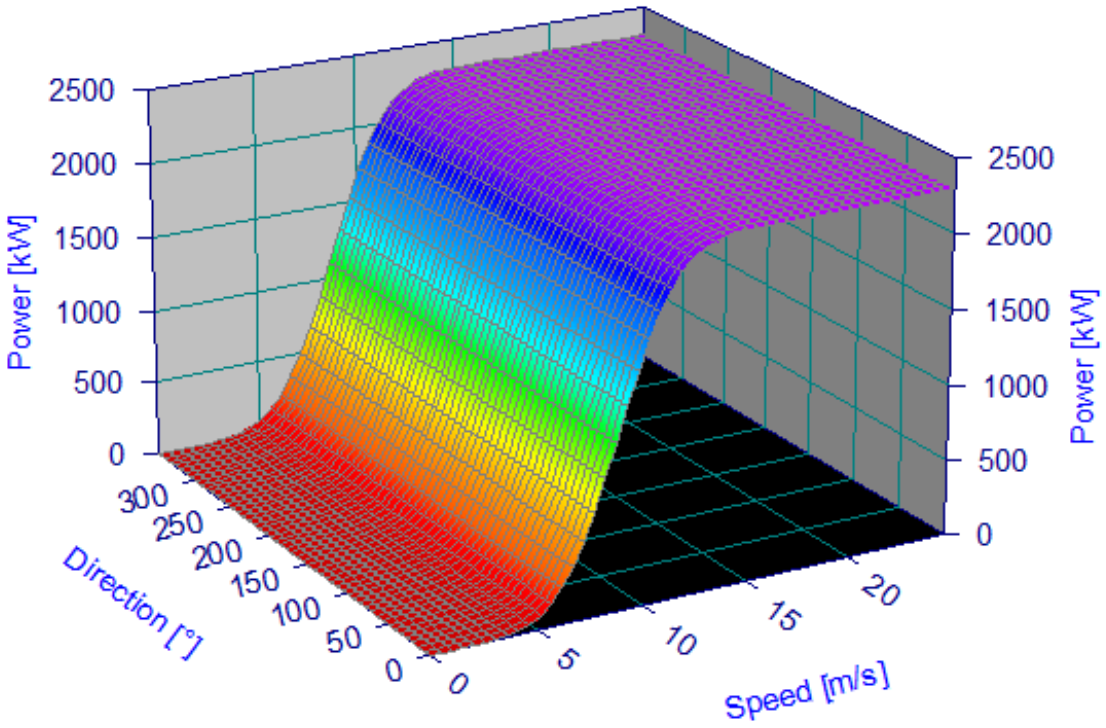

Figure 6.2: Best fit relative to the power production of a single turbine

Since the main issue with the curve indicated by equation (6.1) is relative to the lack of fluctuations, a series of equations involving trigonometric functions has been taken into account. In this case, the best result comes from an equation involving the cosine and having 66 parameters and therefore too long to report here. However, despite the complexity of the equations, it was not possible to obtain a proper reproduction of Figure 6.1. With this new equation $R^2 = 0.9747244$, which is even lower than the previous case.

In Figure 6.3, the behaviour of the curve is shown. However, in spite of the fluctuations along the axis of the direction, the function fails to reproduce the behaviour of the data as it can be seen in Figure 6.4, where the difference between the data and the function is reported. In Figure 6.4, the points highlighted in blue indicate when the data has a higher value than the function, while the red points mark the opposite.

The main reasons why these functions involving the cosine and this function in particular fail to reproduce the desired behaviour are probably two. The first one is relative to the period of the oscillations,

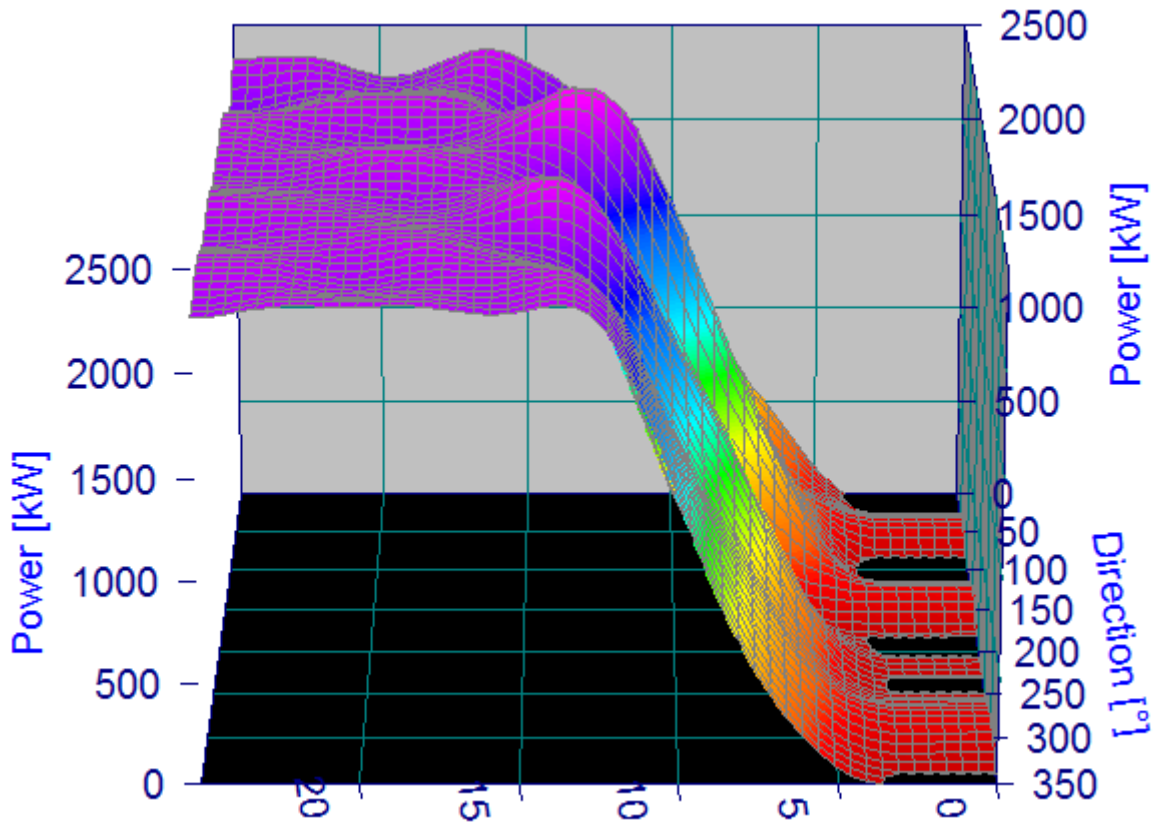

Figure 6.3: Curve fitting obtained considering trigonometric functions

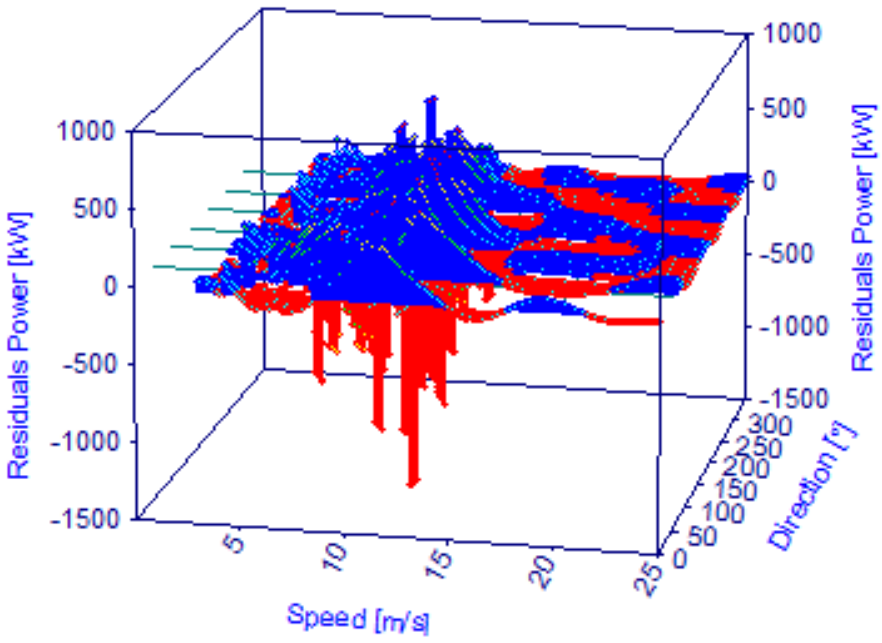

Figure 6.4: Residuals between the data and the equation involving the trigonometric functions

as the data has a highly irregular one, which is difficult to reproduce for an analytical function. The second one is about the amplitude of these fluctuations, as there are almost none with the same amplitude

among the data. This is a further issue which is extremely difficult to reproduce and therefore leads the analytical function to not reach its goal.

Since the functions obtained using the software products CurveExpert and TableCurve 3D did not reproduce the data, an additional attempt using the functions present in their sets was made. After running the software and obtaining the best results relative to R^2, two equations were selected. The equations were chosen based on their complexity and value of R^2. As a next step, these functions were optimised using MATLAB in order to minimise the accumulated difference first and then to maximise R^2. The first equation considered is shown in (6.2):

$$\begin{aligned} z = a + b \cdot \cos(x") + c \cdot \sin(x") + d \cdot \cos(y") + e \cdot \sin(y") + f \cdot \cos(2x") + g \cdot \sin(2x") + h \cdot \cos(2y") + \\ i \cdot \sin(2y") + j \cdot \cos(3x") + k \cdot \sin(3x") + l \cdot \cos(3y") + m \cdot \sin(3y") + n \cdot \cos(4x") + o \cdot \sin(4x") + \\ p \cdot \cos(4y") + q \cdot \sin(4y") + r \cdot \cos(5x") + s \cdot \sin(5x") + t \cdot \cos(5y") + u \cdot \sin(5y") + v \cdot \cos(6x") + \\ aa \cdot \sin(6x") + ab \cdot \cos(6y") + ac \cdot \sin(6y") + ad \cdot \cos(7x") + ae \cdot \sin(7x") + af \cdot \cos(7y") + \\ ag \cdot \sin(7y") + ah \cdot \cos(8x") + ai \cdot \sin(8x") + aj \cdot \cos(8y") + ak \cdot \sin(8y") \end{aligned} \tag{6.2}$$

where z is the power output in kW and x" and y" are two variables indicating the wind speed in m/s and the direction in $^\circ$, but varying between 0 and 2π. The function represented in (6.2) has been chosen because of a relatively good initial value of R^2 and limited amount of free parameters (33). In Figure 6.5, the results of the optimisation in terms of the accumulated difference are shown together with the data that the function should resemble.

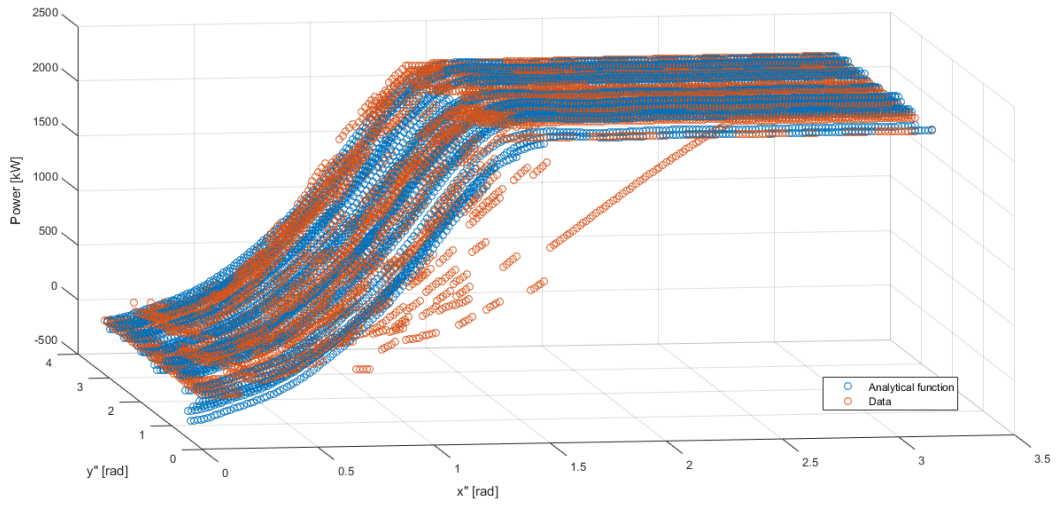

Figure 6.5: Results of the optimisation relative to the accumulated difference of (6.2)

As shown in Figure 6.5, not even by minimising the accumulated difference it was possible to obtain a satisfactory result. In fact, the analytical equation still fails to reproduce the data obtained from the empirical model. Therefore, a second optimisation was run. This time with the objective of maximising

the R^2, in case the results from the software were not the best possible. The outcome of this second optimisation is shown in Figure 6.6.

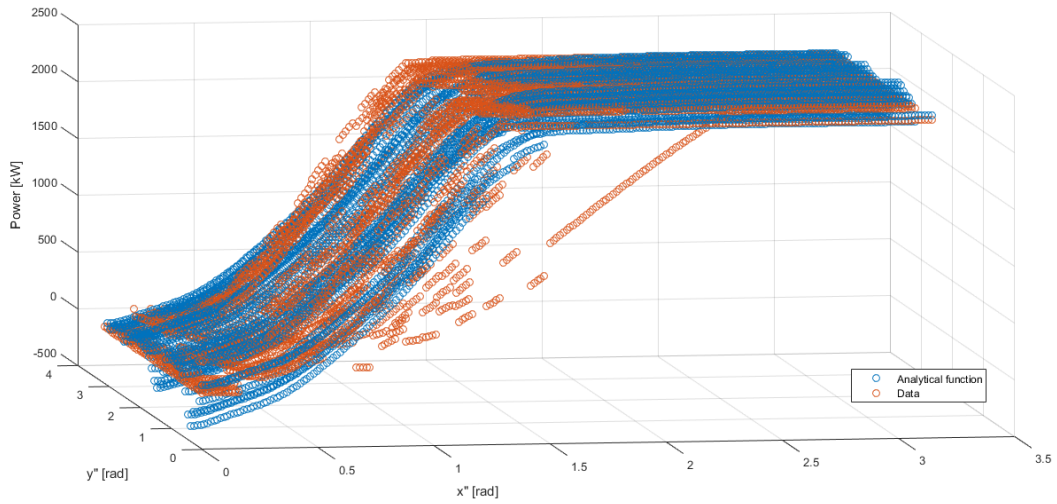

Figure 6.6: Results of the optimisation relative to the R^2 of (6.2)

The two equations found through the optimisations actually are pretty similar, with slight differences mainly in the amplitude of the fluctuations. Consequently, the results of the optimisation fail to reproduce the data and therefore any function of the family indicated in (6.2) cannot be used to calculate the power output of any of the turbines in the wind farm.

The second family of equations considered for the creation of the function reproducing the behaviour of the wind turbines within the wind farm is shown in (6.3). Like for (6.2), equation (6.3) was shown to have a good initial value as R^2 and a relatively low amount of free parametres, 21.

$$\begin{aligned} z = a + b\cdot\cos(x") + c\cdot\cos(y") + d\cdot\cos(2x") + e\cdot\cos(x")\cos(y") + f\cdot\cos(2y") + g\cdot\cos(3x")+ \\ h\cdot\cos(2x")\cos(y") + i\cdot\cos(x")\cos(2y") + j\cdot\cos(3y") + k\cdot\cos(4x") + l\cdot\cos(3x")\cos(y")+ \\ m\cdot\cos(2x")\cos(2y") + n\cdot\cos(x")\cos(3y") + o\cdot\cos(4y") + p\cdot\cos(5x")+ \\ q\cdot\cos(4x")\cos(y") + r\cdot\cos(3x")\cos(2y") + s\cdot\cos(2x")\cos(3y") + t\cdot\cos(x") \end{aligned} \tag{6.3}$$

where every symbol has the same meaning as in (6.2).

As for equation (6.2), two different optimisations were run using the analytical function portrayed in (6.3). Again, the first one attempts to minimise the accumulated difference, while the second one tries to maximise R^2. The results of the former are shown in Figure 6.7, where it can be seen that the optimised function does not behave as desired. In this case, there seem to be issues not only with the oscillations but also with the region in which the surface of the data flattens.

The outcome of the maximisation of R^2 relative to equation (6.3) is shown in Figure 6.8. Also this second optimisation fails to find a series of values for the parametres in order for the analytical equation to resemble the data. The behaviour of this new curve is extremely similar to the one portrayed in Figure 6.7, with small discrepancies in the amplitude of the oscillations and a significant one in the first power

curve, i.e. the one for the wind blowing from $0°$. That probably happens because for a wind direction of $0°$, y" is equal to $0rad$, which could lead to some strange behaviours in the function.

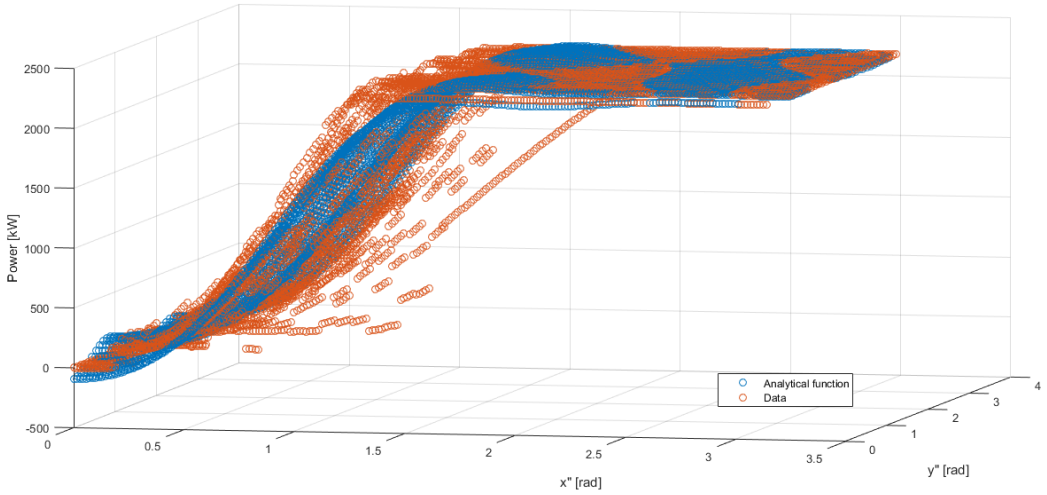

Figure 6.7: Results of the optimisation relative to the accumulated difference of (6.3)

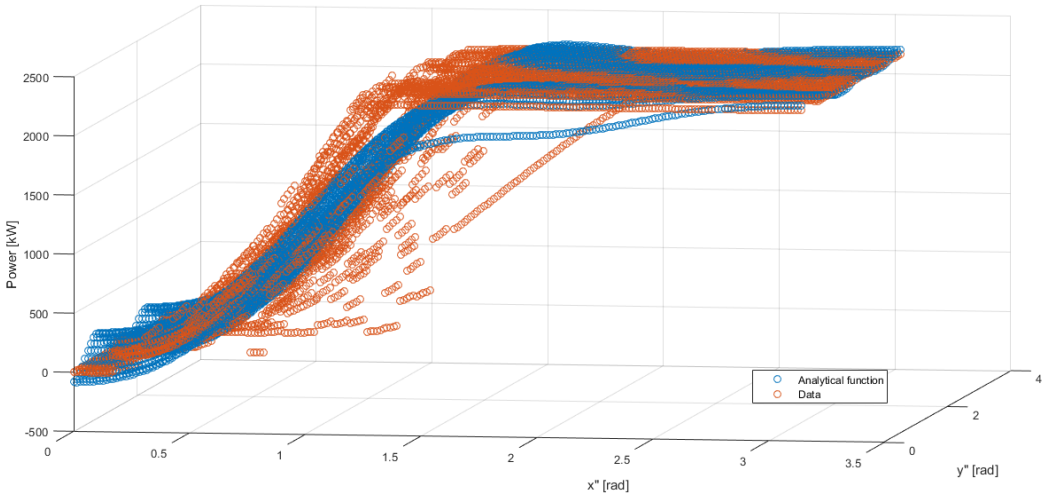

Figure 6.8: Results of the optimisation relative to the R^2 of (6.3)

6.3 Second Approach

Given the lack of consistency in the results obtained using the software with their own sets of equations, a new approach was used. In this second method, after finding a function resembling the power curve for each direction, a pattern between each single parametre characterising the function and the wind direction had to be found. In this second procedure, the online platform Fitteia [43] was used with the additional help of Prof. Pedro Sebastião.

As a first step, a function that could resemble the behaviour of a power curve had to be found. The best curve in this case seemed to be the Five Parameter Logistic (5PL) Fit. Two different versions of this

curve were found online. The first one used was the one shown in equation (6.4) because it is the one contained in the online platform.

$$f(x) = a + \left(\frac{d}{1 + \left(\frac{x}{c}\right)^b} \right)^e \tag{6.4}$$

As it can bee seen from (6.4) and realised from the name of the function, this equation is based on 5 free parametres. Equation (6.4) was fitted to resemble each single power curve, obtaining 5 different parametres for each one. Afterwards, each parametre was plotted based on the direction (which means all the parametres a in one plot, all the parametres b in another one and so on) to find a possible function that having only the direction as input could return the specific value of the parametre for the particular direction. If such a function could be found, it would be used to substitute the parametre in the 5PL equation. Unfortunately, no pattern between the wind direction and the relative values of the parametres was found. Consequently, some modifications were needed. The first path that was followed was to decrease the number of free parametres, blocking the other ones. Studying the values of the 5 parametres found from the fittings, the ones that seemed more constant with the direction and to less affect the curve when varied were identified and blocked. Eventually, a series of 36 curves (one for each angular sector) depending on a single parametre was found. The parametre that was left as the free one was c. However, it was not possible to find an equation able to reproduce the values of such a parametre depending on the wind direction.

Sequently, a second version of the 5PL equation usable in MATLAB was found. Again, the function was based on 5 parametres but in this case their ”meaning” was clearer and therefore it was possible and easier to decrease their number. This second version of the 5PL Fit is shown in equation (6.5) [46]:

$$f(x) = d + \frac{a - d}{\left(1 + \left(\frac{x}{c}\right)^b\right)^e}, \tag{6.5}$$

where:

- a is the minimum asymptote
- b is the Hill’s slope, i.e. the steepness of the curve
- c indicates the inflection point
- d stands for the maximum asymptote
- e is the asymmetry factor

In the case of $e = 1$, the curve becomes symmetrical and has 4 free parametres. As it was done for the first version of the 5PL equation, some of the parametres were blocked and the others kept free. In this case, the parametres that were blocked were only three: a, d and e. The parametre a was fixed at a value of 125 because it was a good approximation of the power output at a wind speed of $3m/s$ along the different directions. In case of a satisfactory final result, such a value could have been varied or optimised in order to have a better fitting. The parametre d was blocked at 2300 as this is the rated

power of the wind turbines in the wind farm. Finally, e was set equal to 1 in order to have a symmetrical curve. This operation can be suggetsed by the fact that the difference between the 5PL and the 4 Parameter Logistic Fit is the presence of the parametre e. Eventually, the equation to fit to the power curves was depending only on two parametres.

$$f(x) = 2300 + \frac{125 - 2300}{1 + \left(\frac{x}{c}\right)^b} \tag{6.6}$$

Afterwards, the equation (6.6) was fitted to some of the 36 power curves and the relative values of b and c were saved. The values of the parametre c were then plotted (direction vs parametre) and another fit was seeked. If such a fit could have been found, the fitting of the power curves would have been continued with the remaining angular sectors. Also, if this fit would have been found as well the same calculations would have been carried out for the parametre b. The fit "direction vs parametre" was attempted with three different software products: Fitteia, CurveExpert and MATLAB. Given the behaviour of 4 random values of the parametre c, in Fitteia it was attempted to reproduce its behaviour with the function $\frac{\sin(x)}{x}$. The results of this first attempt are shown in Figure 6.9.

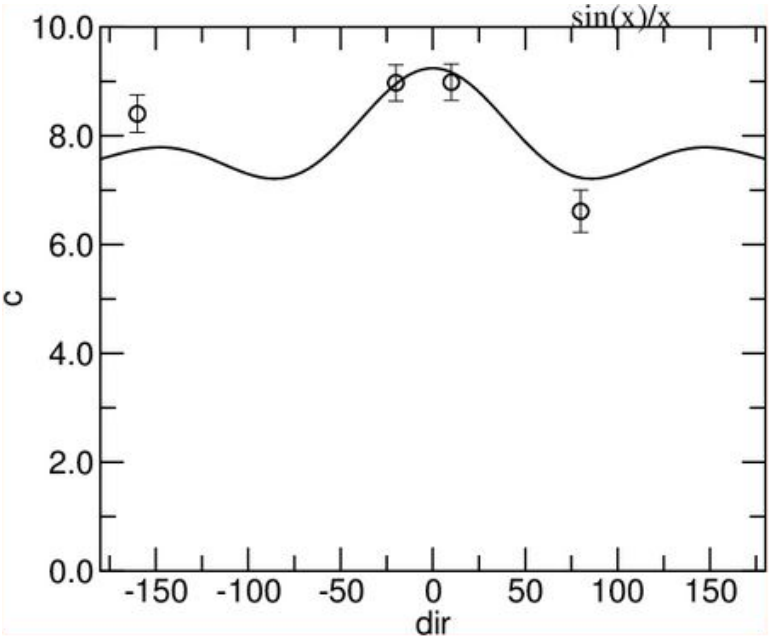

Figure 6.9: Fitting of the parametre c depending on the wind direction with Fitteia

Since $\frac{\sin(x)}{x}$ failed to reproduce the behaviour and that a further use of Fitteia would have required the user to decide which type of equation to use, the following attempts were made using first CurveExpert and then MATLAB. The results from the fitting with the former software are shown in Figure 6.10. It can be noted how in spite of the limited amount of points, the fit was not successful. Consequently, it was deemed as unnecessary to continue the fit with this software.

As a last attempt, MATLAB was used in order to find a good fit. Initially, some good results were obtained and therefore an increased number of points were used to find the fit. The results for fit obtained using MATLAB are shown in Figure 6.11.

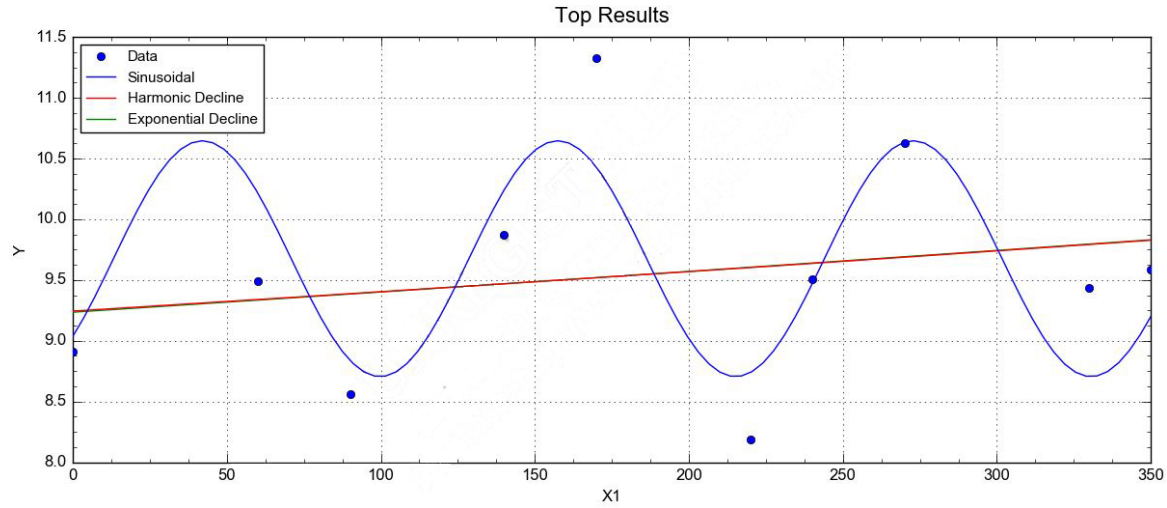

Figure 6.10: Fitting of the parametre c depending on the wind direction with CurveExpert

Just like in the previous cases, the fitting depicted in Figure 6.11 fails to reproduce the values of the parametre c having the wind direction as input. Therefore, after all these attempts using several different approaches to the problem, it was thought that the objective of finding an analytical function giving the power output of the turbine as a result using only undisturbed wind speed and direction as inputs cannot be reached, at least using the tools available.

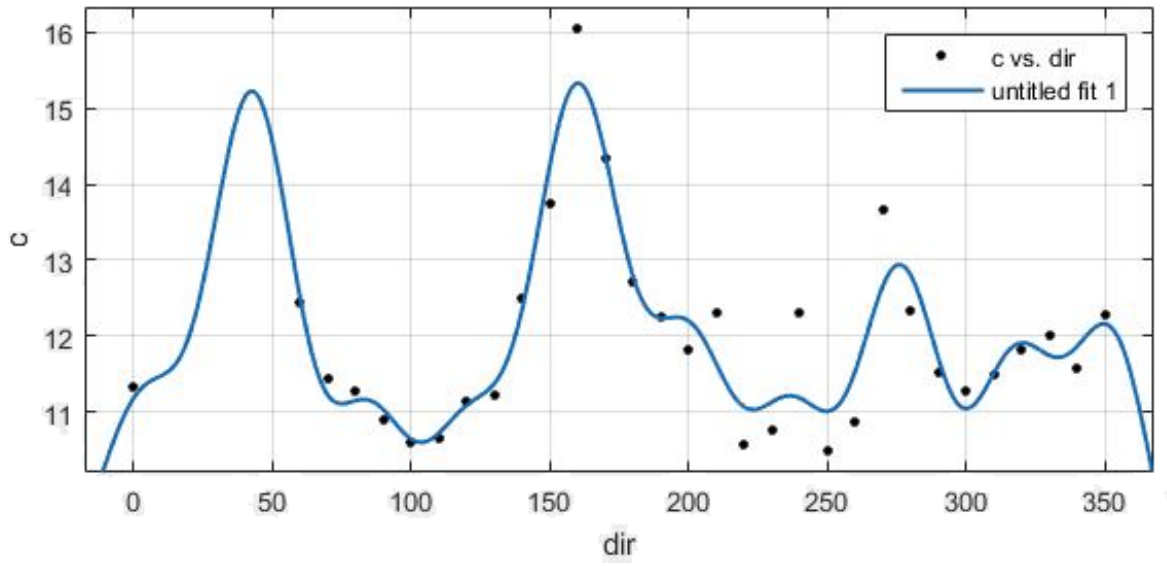

Figure 6.11: Fitting of the parametre c depending on the wind direction with MATLAB

6.4 Conclusions to the Chapter

In this chapter, it was attempted to create a set of equations that could reproduce the results of the empirical model. If such a set had been created, it would have been possible to calculate the power output of each turbine and of the wind farm using only the forecasted wind speed and direction. To

try to create these equations, the technique of the surface fitting was used. Initially, specific software was used, unsuccessfully though. Therefore, a second approach was used. In this case, a curve for each direction was created and the realitve parametres characterising it saved. Subsequently, a pattern between each parametre and the wind direction was seeked. In case this pattern had been found, it would have substituted the parametre itself in the general equation. As in the previous case, satisfactory results were not found even after decreasing the amount of parametres and therefore it was thought that this task could not be fulfilled.

Chapter 7

Empirical Power Model

Since in every step of a model usually the margin of error increases, it was thought that a new model with the minimum amount of steps possible could be created. In this case, a similar approach to the one used in the empirical model was adopted. In order to have the least amount of steps possible in the creation of the model, the power output of the whole wind farm was studied and organised depending on the conditions of the incoming wind. For these reasons, this model will be called empirical power model from now on.

7.1 Organisation of the Data

The variables chosen to characterise the wind are the same as the ones used in the empirical model: maximum wind speed and average wind direction. The reasons behind these choices are identical to the ones exposed in Section 5.2. Also the criteria used to create the speed and direction bins were the same as in the empirical model (velocity bins of $0.5m/s$ and direction bins of 10°). The time slots considered for the creation of this third model were only the ones in which all of the turbines were working. This decision was taken in order to maintain the possible error as low as possible, even though the absence of a single turbine would have averagely created an error of $\approx 2\%$. Unfortunately, this choice decreased even more the amount of data to use for the creation, going from 9 to 6 months. For the creation of this last model, the measurements from all the turbines have been considered reliable, as there was no possible way to check their accuracy. Among the remaining data relative to the power output, only the ones reporting a positive value were considered. All the ones relative to the same time slots were then summed in order to find the power output of the whole wind farm during those 10 minutes. Afterwards, the wind velocity and direction for that time gap were studied in order to know where to collect that particular piece of data. After analysing all the possible time slots, the average power output was found and saved within a matrix having the speed bins in different rows and the direction ones in the columns. Obviously, since in the empirical model not all the possible wind conditions occurred, the same happened in this case where the amount of time slots available was even lower. The matrix obtained through this organisation of the data is shown in Table 7.1.

Table 7.1: Matrix containing the average power output of the wind farm depending on the wind conditions

	0°	10°	20°	30°	40°	50°	60°	70°	80°	90°	100°	110°	120°	130°	140°	150°	160°	170°	180°	190°	200°	210°	220°	230°	240°	250°	260°	270°	280°	290°	300°	310°	320°	330°	340°	350°
$3.25m/s$	0.3	0.6	0.2	0.1	0.2	0.4	0.3	0.1	0.3	0.2	0.2	0.3	0.7	0.4	0.3	0.4	0.4	0.3	0.3	0.2	0.3	0.3	0.2	0.3	0.3	0.3	0.2	0.4	0.4	0.3	0.3	0.3	0.4	0.3	0.4	0.2
$3.75m/s$	0.9	0.8	0.6	0.6	0.7	1.1	0.4	0.5	0.9	0.6	1.0	1.0	1.6	1.0	0.9	0.5	1.0	0.9	0.6	0.7	1.3	0.9	1.2	0.9	1.3	1.0	1.2	1.8	1.3	1.1	1.0	1.0	0.8	0.8	1.0	0.7
$4.25m/s$	1.4	1.4	1.7	1.2	1.1	1.4	1.8	0.8	1.5	1.5	2.3	3.3	1.8	2.3	2.0	1.8	2.0	1.8	1.5	1.5	2.1	2.2	2.5	2.8	3.0	2.7	2.6	4.5	3.3	3.3	2.9	2.6	2.2	2.3	1.7	1.7
$4.75m/s$	3.4	4.1	3.4	2.9	1.9	2.2	3.4	4.0	3.5	4.1	3.3	5.0	4.3	4.6	4.8	3.9	3.8	3.2	2.7	3.4	3.5	3.9	4.7	5.6	6.1	6.0	6.2	6.1	6.1	5.9	5.4	4.3	3.8	3.8	3.6	2.9
$5.25m/s$	5.9	5.3	4.1	5.1	4.3	5.6	5.3	5.9	5.2	6.3	6.5	6.8	6.1	7.1	6.9	6.0	6.0	5.5	4.8	5.1	6.1	6.8	8.0	8.5	9.0	8.9	7.8	8.1	7.7	8.3	7.9	6.9	7.8	7.1	5.6	5.3
$5.75m/s$	8.6	9.0	6.5	7.4	9.6	8.5	8.0	9.6	8.4	8.4	8.9	9.3	9.3	9.1	9.9	8.1	7.9	8.2	7.1	7.4	8.0	9.9	10.3	11.4	11.4	12.3	11.9	11.6	13.3	12.5	11.7	9.3	10.1	9.5	8.0	8.0
$6.25m/s$	11.3	10.9	12.0	11.3	9.6	13.5	13.1	11.1	11.4	11.1	14.0	10.6	12.0	10.4	12.6	12.3	10.2	10.3	8.3	10.5	12.2	12.5	14.5	17.3	16.4	15.5	14.9	15.4	14.5	17.1	14.6	13.7	13.3	14.1	11.4	11.9
$6.75m/s$	15.6	15.8	13.3	14.9	15.0	12.7	17.6	17.5	17.8	17.2	18.6	17.0	16.8	14.4	12.3	16.1	12.5	12.2	11.4	13.7	15.9	16.6	19.1	21.3	21.8	19.6	19.5	18.1	21.5	19.5	19.8	20.3	18.0	17.1	15.0	14.2
$7.25m/s$	20.5	19.6	17.5	25.5	21.1	18.6	17.4	20.8	19.7	21.3	23.6	20.2	19.8	21.3	20.6	18.6	16.2	15.2	16.3	16.1	22.3	22.5	24.3	26.0	25.0	25.8	27.6	24.3	23.2	26.3	26.1	26.3	23.4	21.4	19.1	18.3
$7.75m/s$	25.0	24.2	20.8	30.9	15.4	20.3	23.0	25.1	26.6	21.1	26.4	24.7	23.2	24.6	23.6	22.8	20.8	17.0	21.7	21.3	26.5	26.1	28.4	33.2	31.1	30.5	33.4	29.6	29.4	32.1	33.6	30.5	29.2	26.6	24.4	21.0
$8.25m/s$	29.7	29.1	34.3	29.0	9.3	25.7	26.5	28.7	30.6	30.3	34.3	34.2	31.1	27.1	23.5	28.3	23.1	21.5	23.0	29.1	29.4	33.0	34.2	40.0	31.8	36.1	34.8	35.7	32.9	38.5	42.1	38.7	32.9	33.7	27.2	28.3
$8.75m/s$	38.2	33.2	41.2	29.1	32.9	28.2	30.4	30.1	35.3	40.9	41.1	39.3	32.3	31.6	27.2	30.1	25.7	24.3	32.2	32.9	35.7	38.6	39.2	42.7	42.1	41.0	42.0	50.6	36.6	37.0	48.3	44.2	39.4	40.5	36.9	34.4
$9.25m/s$	40.1	49.0	37.0	23.6	29.8	28.0	39.2	35.6	41.7	44.3	47.0	46.4	39.7	42.2	47.1	42.1	39.9	33.7	35.4	40.2	41.4	45.8	48.0	52.3	51.3	44.0	54.4	50.5	46.3	55.9	61.4	56.0	48.5	47.0	43.3	42.3
$9.75m/s$	52.8	58.5	0	42.2	33.1	41.0	44.3	45.3	48.9	51.6	53.1	53.8	50.0	46.9	52.4	40.2	38.8	43.6	39.6	45.3	51.7	50.9	56.0	59.4	54.9	51.7	53.6	57.2	71.0	68.1	58.1	63.0	57.6	53.5	54.6	47.8
$10.25m/s$	63.2	68.3	60.5	46.1	34.1	39.8	43.3	49.4	56.1	62.8	65.9	62.7	55.5	51.4	60.6	51.8	46.4	45.7	45.4	53.0	56.5	58.9	64.5	69.5	62.6	61.9	68.1	59.4	67.7	58.9	65.6	71.4	64.2	64.4	64.2	52.3
$10.75m/s$	70.6	75.6	73.2	46.6	52.5	42.1	52.3	57.5	69.0	70.7	76.3	70.2	59.0	61.5	61.4	56.1	45.2	48.4	55.8	62.3	64.8	68.1	71.5	79.7	76.1	70.1	85.5	77.3	64.0	89.2	73.6	78.3	75.8	73.4	70.2	60.0
$11.25m/s$	78.7	81.2	92.7	44.1	52.2	49.9	61.2	67.8	80.4	74.9	80.8	78.1	69.9	71.1	60.4	59.3	45.0	56.2	68.1	70.4	71.1	75.2	81.8	88.4	80.3	0	81.8	79.1	0	81.8	82.2	84.1	86.8	83.9	82.8	72.0
$11.75m/s$	91.2	95.2	0	0	62.2	70.9	67.0	78.2	85.9	80.3	87.5	88.1	79.8	83.0	76.1	64.5	63.3	57.0	75.7	79.7	77.9	77.7	86.3	88.7	84.2	0	101.0	94.2	0	86.7	87.4	90.5	93.3	89.4	88.7	83.6
$12.25m/s$	91.5	0	0	0	0	51.2	65.6	93.4	87.6	90.4	95.8	92.7	85.0	88.6	79.5	62.5	65.7	70.0	81.8	84.0	82.7	87.6	88.2	105.5	99.7	78.4	81.3	0	0	71.5	98.0	92.2	98.6	93.7	93.1	85.6
$12.75m/s$	92.3	88.0	0	0	0	61.9	88.4	88.3	91.1	94.9	99.9	98.8	91.5	92.3	87.8	0	76.3	72.7	80.5	88.9	92.2	89.5	91.6	0	0	93.0	101.5	101.9	0	0	102.2	95.7	97.7	97.4	96.3	89.7
$13.25m/s$	100.0	0	0	0	0	0	89.4	88.8	95.7	96.1	102.0	100.7	97.5	94.9	90.4	86.3	0	58.8	82.0	84.4	93.7	93.0	93.3	0	99.8	0	103.6	0	100.3	0	91.1	80.6	97.7	101.8	98.1	96.6
$13.75m/s$	104.8	0	0	0	0	0	81.2	99.1	97.3	97.2	103.2	102.8	101.1	96.5	94.8	98.5	0	78.5	94.2	88.4	94.6	95.3	92.9	0	105.4	105.5	0	0	103.2	91.6	97.0	99.4	101.1	103.7	98.9	97.9
$\geq 14m/s$	105.7	0	0	0	0	0	72.4	94.1	102.0	102.5	103.6	105.2	104.5	95.3	95.2	103.7	86.4	88.0	98.2	97.3	98.5	97.6	86.9	103.7	105.8	0	106.0	102.6	102.2	105.1	91.3	98.7	101.9	103.9	102.6	100.2

Table 7.2: Matrix containing the standard deviation relative to the average power output of the wind farm depending on the wind conditions

	0°	10°	20°	30°	40°	50°	60°	70°	80°	90°	100°	110°	120°	130°	140°	150°	160°	170°	180°	190°	200°	210°	220°	230°	240°	250°	260°	270°	280°	290°	300°	310°	320°	330°	340°	350°
$3.25m/s$	0.3	0.8	0.2	0.2	0.3	0.5	0.3	0.3	0.6	0.2	0.1	0.4	0.7	0.4	0.2	0.3	0.4	0.3	0.3	0.2	0.3	0.3	0.2	0.3	0.4	0.4	0.3	0.4	0.4	0.3	0.3	0.4	0.4	0.2	0.4	0.4
$3.75m/s$	0.3	0.8	0.6	0.4	0.8	1.2	0.4	0.6	0.7	0.6	0.8	1.1	1.1	0.7	0.7	0.4	1.0	0.8	0.5	0.5	1.0	0.7	0.9	0.8	1.2	1.1	0.8	1.2	0.9	1.0	0.9	0.9	0.6	0.7	0.7	0.6
$4.25m/s$	0.8	1.5	1.0	0.7	0.8	1.1	1.6	1.2	1.0	1.3	2.0	2.3	0.8	1.6	1.3	1.4	1.4	1.4	1.0	0.9	1.4	1.4	1.5	1.9	2.3	2.0	1.8	2.2	2.0	2.0	1.7	1.2	1.3	1.4	1.0	1.0
$4.75m/s$	1.2	2.4	1.5	2.1	0.7	1.6	2.1	2.2	0.6	2.5	2.1	2.4	2.3	2.4	2.6	2.2	2.1	1.9	1.7	1.7	1.5	1.9	2.3	2.7	2.1	2.0	2.1	2.3	5.4	2.4	2.0	1.7	1.9	1.6	1.4	1.2
$5.25m/s$	1.9	2.1	2.6	3.2	1.3	2.2	3.1	2.2	2.7	2.6	3.2	2.6	2.8	2.9	3.3	2.6	2.5	2.9	2.2	2.3	2.4	2.4	2.9	2.6	3.0	2.7	2.4	2.7	2.9	1.9	2.4	3.0	2.3	2.3	2.2	2.4
$5.75m/s$	2.6	2.7	2.0	3.9	4.6	2.3	2.4	3.6	1.6	3.9	4.2	2.9	4.1	3.1	3.4	3.6	2.7	3.3	2.4	3.4	2.9	2.8	2.9	4.5	2.2	3.1	3.0	3.7	13.5	3.9	2.6	3.2	3.3	2.5	2.8	3.0
$6.25m/s$	3.8	3.3	4.7	5.0	4.1	5.5	2.7	5.2	3.6	3.0	4.6	3.3	4.5	4.7	4.1	4.2	3.8	3.7	2.8	2.9	4.2	4.5	3.6	5.0	4.1	3.1	3.1	3.7	4.0	11.2	3.5	4.4	4.0	4.5	3.0	3.6
$6.75m/s$	2.7	3.9	3.4	2.2	3.9	3.5	0.3	4.2	4.2	4.6	6.0	4.5	6.9	6.2	3.7	4.2	5.1	5.0	5.3	4.5	5.6	4.7	3.5	3.9	4.2	4.5	4.9	4.0	12.5	3.9	4.2	5.1	4.1	4.2	3.0	3.5
$7.25m/s$	4.6	3.6	4.2	4.7	2.8	7.6	6.6	4.7	6.1	5.8	5.8	6.5	6.7	6.5	5.6	5.2	5.8	5.5	5.7	5.2	7.2	5.8	4.9	5.5	3.8	4.6	16.7	5.7	6.5	7.6	5.2	5.8	5.1	5.4	4.5	3.6
$7.75m/s$	5.4	5.9	9.0	5.5	7.6	9.0	2.1	4.5	4.2	6.7	7.1	5.6	7.4	11.2	5.7	5.8	7.0	6.4	6.1	6.5	6.6	6.0	6.4	7.0	6.2	6.4	5.0	7.2	16.3	5.5	6.0	5.0	4.9	4.7	3.8	4.1
$8.25m/s$	4.8	6.2	4.9	12.5	0.0	8.3	5.1	6.2	6.2	9.4	9.0	9.8	6.1	8.4	6.5	6.7	7.9	6.9	6.8	7.0	7.3	7.7	5.9	6.9	10.2	3.2	4.5	9.6	5.8	6.7	5.0	6.9	5.6	4.8	6.4	5.7
$8.75m/s$	6.5	11.9	6.5	12.0	0.0	5.8	6.4	8.2	11.0	11.1	10.3	9.6	10.4	9.7	7.7	7.0	8.3	8.7	8.4	10.6	8.5	9.3	7.6	7.8	7.8	8.7	9.0	12.1	7.9	9.8	10.2	9.9	7.4	8.3	8.2	6.9
$9.25m/s$	8.1	6.9	0.0	10.5	9.4	10.5	11.9	7.9	8.3	12.2	11.5	13.2	12.1	14.3	18.2	10.0	11.3	9.1	8.2	10.6	10.2	11.9	7.8	9.0	6.8	8.5	3.1	12.0	10.2	14.6	10.3	9.7	8.6	7.0	8.8	5.2
$9.75m/s$	8.7	8.2	NaN	0.0	12.9	10.9	13.8	9.8	13.4	13.3	10.8	13.6	15.2	15.3	13.2	11.2	8.5	11.9	9.3	11.2	10.0	11.9	9.8	11.3	11.3	6.7	11.3	12.7	11.6	8.6	11.4	9.9	9.7	12.3	10.3	6.5
$10.25m/s$	7.0	7.9	6.2	0.0	6.1	5.6	10.8	14.0	11.7	14.9	13.4	12.2	13.8	10.4	10.2	11.2	15.6	15.8	12.6	13.7	14.0	16.8	10.7	14.5	12.5	13.4	0.8	10.6	12.3	24.5	11.6	7.1	8.5	11.6	10.6	8.4
$10.75m/s$	10.1	12.7	12.7	0.0	25.9	5.6	11.6	12.4	15.3	16.8	13.0	9.8	17.2	13.5	13.1	14.5	3.0	13.8	15.6	16.6	14.2	15.2	12.5	8.1	11.7	10.0	0.3	7.4	0.0	0.0	9.6	8.3	10.1	10.1	11.9	12.1
$11.25m/s$	17.0	9.0	5.8	0.0	16.8	17.5	14.7	10.2	16.4	15.3	16.1	11.3	16.8	18.0	17.2	15.4	10.4	16.2	17.6	16.5	16.2	17.2	10.8	6.4	13.2	NaN	0.0	3.1	NaN	12.1	7.6	9.7	9.9	9.3	11.1	10.1
$11.75m/s$	7.5	5.6	NaN	NaN	35.1	28.6	17.8	13.0	12.4	16.8	14.0	10.0	15.6	7.8	17.8	25.9	8.9	11.3	16.7	17.7	16.1	16.7	14.8	20.9	2.3	NaN	4.3	2.8	NaN	23.2	3.6	9.7	8.8	8.6	8.3	7.8
$12.25m/s$	3.4	NaN	NaN	NaN	NaN	5.8	18.8	6.3	13.2	13.8	10.8	11.6	13.6	9.1	2.9	0.0	3.8	13.5	17.0	16.8	17.3	13.8	15.2	0.5	0.0	0.0	0.0	NaN	NaN	22.9	5.5	9.4	5.9	7.0	8.4	6.8
$12.75m/s$	4.4	0.0	NaN	NaN	NaN	12.9	15.3	11.2	9.5	14.6	9.8	8.6	10.8	5.2	3.2	NaN	5.4	14.9	15.9	15.2	13.0	13.3	13.0	NaN	NaN	16.6	0.0	0.0	NaN	NaN	2.5	11.5	6.8	9.2	7.6	8.0
$13.25m/s$	5.5	NaN	NaN	NaN	NaN	NaN	13.8	13.7	8.4	13.0	6.6	3.6	6.5	4.1	16.9	0.0	NaN	14.1	12.4	12.9	12.7	11.8	9.5	NaN	7.5	NaN	0.0	NaN	0.0	NaN	0.0	37.1	7.2	6.2	8.2	7.3
$13.75m/s$	2.4	NaN	NaN	NaN	NaN	NaN	1.1	8.2	7.1	11.3	2.9	2.8	5.4	2.8	8.5	5.8	NaN	4.7	11.6	14.0	10.5	12.2	2.8	NaN	0.0	0.0	NaN	NaN	0.8	15.6	0.0	2.4	5.0	2.6	9.0	6.2
$\geq 14m/s$	0.3	NaN	NaN	NaN	NaN	NaN	1.9	13.1	8.3	6.1	5.2	1.5	1.8	4.7	5.6	0.8	9.9	5.9	8.8	8.7	7.9	9.8	15.9	0.0	0.5	NaN	0.2	1.9	4.0	1.5	9.2	3.7	3.5	2.3	4.0	7.1

Table 7.3: Matrix containing the coefficient of variation of the average power output of the wind farm depending on the wind conditions

	0°	10°	20°	30°	40°	50°	60°	70°	80°	90°	100°	110°	120°	130°	140°	150°	160°	170°	180°	190°	200°	210°	220°	230°	240°	250°	260°	270°	280°	290°	300°	310°	320°	330°	340°	350°
$3.25m/s$	111%	140%	114%	136%	156%	124%	110%	220%	166%	90%	70%	131%	93%	123%	77%	93%	99%	91%	94%	71%	97%	86%	74%	114%	141%	133%	121%	90%	92%	78%	101%	151%	93%	67%	108%	169%
$3.75m/s$	37%	94%	97%	66%	122%	112%	107%	106%	75%	113%	86%	110%	67%	70%	78%	70%	102%	89%	75%	69%	77%	78%	77%	85%	94%	105%	72%	64%	73%	93%	91%	91%	67%	85%	67%	79%
$4.25m/s$	55%	102%	57%	63%	72%	78%	90%	151%	63%	83%	88%	68%	46%	72%	68%	78%	71%	79%	65%	61%	66%	65%	61%	66%	78%	74%	67%	48%	60%	60%	58%	48%	58%	59%	60%	62%
$4.75m/s$	37%	59%	45%	71%	39%	71%	61%	56%	16%	62%	63%	48%	54%	53%	55%	56%	55%	60%	62%	48%	43%	49%	49%	47%	34%	33%	34%	38%	88%	40%	37%	40%	49%	41%	39%	41%
$5.25m/s$	32%	40%	63%	62%	31%	40%	59%	38%	52%	41%	49%	38%	46%	41%	49%	44%	41%	53%	46%	46%	39%	34%	36%	31%	34%	30%	30%	34%	38%	23%	30%	43%	29%	32%	39%	46%
$5.75m/s$	31%	30%	30%	53%	48%	27%	30%	38%	19%	47%	47%	31%	44%	34%	34%	44%	35%	40%	33%	46%	36%	28%	28%	39%	20%	25%	25%	32%	101%	31%	22%	34%	33%	26%	35%	38%
$6.25m/s$	34%	30%	39%	44%	43%	41%	21%	47%	32%	27%	33%	31%	38%	45%	32%	34%	37%	36%	33%	28%	34%	36%	25%	29%	25%	20%	21%	24%	28%	66%	24%	32%	30%	32%	26%	30%
$6.75m/s$	17%	25%	26%	15%	26%	28%	2%	24%	24%	27%	32%	26%	41%	43%	30%	26%	41%	41%	46%	33%	35%	28%	18%	19%	19%	23%	25%	22%	58%	20%	21%	25%	23%	25%	20%	24%
$7.25m/s$	22%	18%	24%	18%	13%	41%	38%	23%	31%	27%	24%	32%	34%	31%	27%	28%	36%	36%	35%	32%	32%	26%	20%	21%	15%	18%	61%	23%	28%	29%	20%	22%	22%	25%	23%	19%
$7.75m/s$	21%	24%	43%	18%	49%	44%	9%	18%	16%	32%	27%	23%	32%	45%	24%	25%	33%	38%	28%	31%	25%	23%	23%	21%	20%	21%	15%	24%	56%	17%	18%	16%	17%	18%	15%	19%
$8.25m/s$	16%	21%	14%	43%	0%	32%	19%	22%	20%	31%	26%	29%	20%	31%	27%	24%	34%	32%	30%	24%	25%	23%	17%	17%	32%	9%	13%	27%	18%	17%	12%	18%	17%	14%	23%	20%
$8.75m/s$	17%	36%	16%	41%	0%	21%	21%	27%	31%	27%	25%	24%	32%	31%	28%	23%	32%	36%	26%	32%	24%	24%	19%	18%	18%	21%	21%	24%	22%	26%	21%	22%	19%	20%	22%	20%
$9.25m/s$	20%	14%	0%	44%	32%	38%	30%	22%	20%	28%	24%	28%	31%	34%	39%	24%	28%	27%	23%	26%	25%	26%	16%	17%	13%	19%	6%	24%	22%	26%	17%	17%	18%	15%	20%	12%
$9.75m/s$	16%	14%	NaN	0%	39%	27%	31%	22%	27%	26%	20%	25%	30%	33%	25%	28%	22%	27%	23%	25%	19%	23%	18%	19%	21%	13%	21%	22%	16%	13%	20%	16%	17%	23%	19%	14%
$10.25m/s$	11%	12%	10%	0%	18%	14%	25%	28%	21%	24%	20%	19%	25%	20%	17%	22%	34%	35%	28%	26%	25%	29%	17%	21%	20%	22%	1%	18%	18%	42%	18%	10%	13%	18%	17%	16%
$10.75m/s$	14%	17%	17%	0%	49%	13%	22%	21%	22%	24%	17%	14%	29%	22%	21%	26%	7%	29%	28%	27%	22%	22%	18%	10%	15%	14%	0%	10%	0%	0%	13%	11%	13%	14%	17%	20%
$11.25m/s$	22%	11%	6%	0%	32%	35%	24%	15%	20%	20%	20%	14%	24%	25%	28%	26%	23%	29%	26%	23%	23%	23%	13%	7%	16%	NaN	0%	4%	NaN	15%	9%	12%	11%	11%	13%	14%
$11.75m/s$	8%	6%	NaN	NaN	56%	40%	27%	17%	14%	21%	16%	11%	20%	9%	23%	40%	14%	20%	22%	22%	21%	21%	17%	24%	3%	NaN	4%	3%	NaN	27%	4%	11%	9%	10%	9%	9%
$12.25m/s$	4%	NaN	NaN	NaN	NaN	11%	29%	7%	15%	15%	11%	13%	16%	10%	4%	0%	6%	19%	21%	20%	21%	16%	17%	1%	0%	0%	0%	NaN	NaN	32%	6%	10%	6%	7%	9%	8%
$12.75m/s$	5%	0%	NaN	NaN	NaN	21%	17%	13%	10%	15%	10%	9%	12%	6%	4%	NaN	7%	20%	20%	17%	14%	15%	14%	NaN	NaN	18%	0%	0%	NaN	NaN	2%	12%	7%	9%	8%	9%
$13.25m/s$	6%	NaN	NaN	NaN	NaN	NaN	15%	15%	9%	14%	6%	4%	7%	4%	19%	0%	NaN	24%	15%	15%	14%	13%	10%	NaN	8%	NaN	0%	NaN	NaN	NaN	0%	46%	7%	6%	8%	8%
$13.75m/s$	2%	NaN	NaN	NaN	NaN	NaN	1%	8%	7%	12%	3%	3%	5%	3%	9%	6%	NaN	6%	12%	16%	11%	13%	3%	NaN	0%	0%	NaN	NaN	1%	17%	0%	2%	5%	3%	9%	6%
$\geq 14m/s$	0%	NaN	NaN	NaN	NaN	NaN	3%	14%	8%	6%	5%	1%	2%	5%	6%	1%	11%	7%	9%	9%	8%	10%	18%	0%	0%	NaN	0%	2%	4%	1%	10%	4%	3%	2%	4%	7%

Table 7.4: Greatest difference between the average power output and any of the measurements as a function of the wind conditions

	0°	10°	20°	30°	40°	50°	60°	70°	80°	90°	100°	110°	120°	130°	140°	150°	160°	170°	180°	190°	200°	210°	220°	230°	240°	250°	260°	270°	280°	290°	300°	310°	320°	330°	340°	350°
$3.25m/s$	0.6	1.6	0.5	0.3	0.8	1.1	0.6	0.8	1.1	0.4	0.2	1.1	1.5	1.2	0.4	0.6	1.4	0.8	0.7	0.3	1.0	0.8	0.4	1.4	1.2	1.3	0.8	1.0	1.4	0.7	0.9	2.0	0.9	0.4	1.4	1.7
$3.75m/s$	0.6	1.6	1.4	0.7	2.0	2.8	1.0	1.7	1.3	1.7	1.9	2.5	1.7	1.3	1.8	0.7	3.4	3.9	1.5	1.6	2.7	1.7	2.1	2.7	3.7	3.4	2.2	2.4	2.9	3.7	3.3	2.7	1.3	2.8	1.8	1.6
$4.25m/s$	1.4	3.0	2.6	1.8	2.6	2.5	3.3	3.3	3.4	2.9	5.6	4.4	1.5	4.4	4.9	2.9	3.9	4.5	2.0	3.0	4.5	5.3	3.9	5.0	6.1	3.6	4.6	4.1	3.9	4.0	3.9	2.5	4.5	4.7	2.2	3.0
$4.75m/s$	2.3	4.6	2.8	3.2	1.2	3.2	4.2	6.0	1.0	5.5	4.8	5.2	5.5	9.1	5.4	4.5	5.0	7.1	5.7	4.0	3.7	5.2	5.0	5.7	4.8	4.1	4.4	5.7	35.8	5.4	4.5	4.5	3.7	3.5	3.0	2.3
$5.25m/s$	4.1	4.5	3.5	4.5	2.4	5.0	5.3	5.0	3.8	5.7	10.1	5.8	9.1	6.4	7.0	5.7	8.1	8.7	4.6	6.6	7.6	5.5	6.2	7.0	5.8	6.7	5.9	5.2	7.0	4.4	6.1	6.8	6.5	4.9	6.1	8.3
$5.75m/s$	6.1	7.2	2.6	4.3	5.1	3.8	4.9	7.8	3.3	10.8	9.0	8.2	7.8	7.4	8.3	10.7	5.9	9.6	4.8	12.9	6.6	6.3	7.8	9.3	5.1	6.0	9.2	8.9	72.6	8.7	7.2	6.9	10.0	5.3	5.8	6.6
$6.25m/s$	9.7	7.4	8.1	6.8	5.7	8.9	4.4	8.8	8.5	7.7	10.6	6.1	10.6	11.5	11.0	11.9	9.2	10.0	5.6	6.5	14.2	10.0	7.4	12.0	14.3	8.1	6.8	8.3	9.4	67.7	8.2	11.4	12.3	11.3	7.8	8.2
$6.75m/s$	5.9	6.7	6.0	3.0	7.5	4.9	0.2	7.2	11.7	9.1	17.8	9.2	16.6	13.8	8.4	8.6	9.6	11.0	14.0	11.2	14.0	12.3	7.5	7.2	10.4	8.6	9.7	8.9	67.2	11.3	9.1	11.7	13.5	8.7	9.7	9.3
$7.25m/s$	8.9	6.8	5.9	5.4	3.1	10.7	15.7	13.1	11.6	10.1	13.7	17.2	15.4	12.7	15.1	14.2	12.2	10.2	13.1	11.3	17.3	17.9	9.9	15.4	8.3	8.2	67.2	11.4	13.4	16.7	11.8	17.6	11.7	14.4	9.1	8.7
$7.75m/s$	10.8	10.8	13.3	6.0	9.3	13.3	6.3	8.6	8.7	15.8	18.7	13.6	16.3	18.9	10.6	10.7	16.4	18.5	15.5	16.9	18.0	18.7	17.8	18.9	13.7	15.8	7.6	11.9	67.0	11.4	13.4	10.7	11.6	10.7	9.5	8.6
$8.25m/s$	9.1	9.4	3.5	15.5	0.0	13.6	9.7	9.6	11.6	20.7	17.4	24.7	16.3	15.7	15.8	14.7	15.2	17.3	16.1	18.6	17.9	18.1	15.4	15.7	17.2	7.8	7.3	17.2	8.6	15.3	10.4	16.5	12.5	9.6	12.1	13.6
$8.75m/s$	16.0	20.3	9.6	12.6	0.0	10.5	11.0	18.0	20.1	21.6	21.6	21.9	24.3	19.1	12.8	11.4	16.3	19.7	26.7	26.2	28.0	21.2	17.9	20.0	14.2	21.7	16.9	14.2	16.2	20.0	21.2	23.2	14.9	22.1	17.7	31.0
$9.25m/s$	19.4	10.3	0.0	12.1	11.5	15.4	27.6	13.0	16.9	23.7	20.4	21.8	28.3	30.7	23.6	12.7	23.2	16.2	19.6	27.9	25.0	22.6	21.8	20.8	12.0	21.4	6.1	16.4	11.8	18.9	18.2	22.5	22.2	18.2	19.3	10.6
$9.75m/s$	15.6	12.3	NaN	0.0	12.6	15.9	32.8	22.8	33.4	29.7	28.3	24.9	26.6	28.4	20.7	14.9	14.6	21.4	24.8	32.4	23.1	31.4	19.8	25.9	19.1	10.2	12.7	14.6	23.6	10.9	17.5	25.0	23.4	32.8	24.2	15.3
$10.25m/s$	16.9	18.3	6.9	0.0	7.2	7.2	18.9	30.7	32.8	28.8	27.1	32.1	31.0	18.5	12.6	20.3	19.7	31.0	33.2	28.3	35.0	32.7	35.3	40.0	26.8	34.4	0.6	14.3	16.4	27.0	18.9	20.8	21.3	38.0	35.2	15.4
$10.75m/s$	26.0	39.9	17.5	0.0	24.3	8.0	24.3	27.4	26.3	37.3	27.1	29.7	32.3	21.5	18.8	20.4	2.1	25.0	30.6	34.7	33.3	33.0	33.3	24.1	29.4	11.5	0.2	7.8	0.0	0.0	22.3	17.6	26.4	38.8	37.8	24.3
$11.25m/s$	51.9	10.4	6.5	0.0	43.1	46.4	30.8	16.3	29.6	25.3	30.8	25.5	30.0	35.0	22.7	20.1	19.7	31.8	39.3	33.6	32.7	36.9	23.1	12.2	33.0	NaN	0.0	2.2	NaN	18.1	18.4	24.1	31.7	30.6	29.1	23.2
$11.75m/s$	19.5	6.4	NaN	NaN	24.8	32.0	35.2	29.6	25.4	38.7	31.6	30.4	32.0	15.9	26.6	29.9	10.0	21.2	41.9	36.8	37.3	33.8	42.5	46.8	1.6	NaN	3.0	1.9	NaN	26.6	4.7	32.7	26.2	31.4	27.3	17.0
$12.25m/s$	6.5	NaN	NaN	NaN	NaN	12.4	36.6	11.0	29.1	33.1	33.5	23.6	32.8	19.0	4.4	0.0	4.8	28.9	35.4	33.4	39.7	33.0	31.1	0.4	0.0	0.0	0.0	NaN	NaN	16.2	5.9	14.1	17.7	21.2	29.2	13.4
$12.75m/s$	9.0	0.0	NaN	NaN	NaN	24.7	16.7	16.1	21.4	45.4	46.1	27.2	34.2	13.5	3.1	NaN	6.4	26.4	43.0	32.8	38.9	42.8	26.7	NaN	NaN	11.7	0.0	0.0	NaN	NaN	1.8	20.1	21.3	33.6	18.7	15.7
$13.25m/s$	11.2	NaN	NaN	NaN	NaN	NaN	19.6	18.8	20.4	37.5	23.8	9.7	11.3	5.9	11.9	0.0	NaN	18.2	17.3	27.4	39.0	29.3	22.9	NaN	8.4	NaN	0.0	NaN	0.0	NaN	0.0	42.7	20.9	23.4	22.9	21.1
$13.75m/s$	9.1	NaN	NaN	NaN	NaN	NaN	1.2	15.3	13.8	39.0	7.8	8.6	15.9	5.9	9.8	6.3	NaN	5.3	30.3	37.2	38.9	38.3	3.3	NaN	0.0	0.0	NaN	NaN	1.2	21.3	0.0	2.8	11.9	10.7	33.0	16.0
$\geq 14m/s$	0.6	NaN	NaN	NaN	NaN	NaN	3.1	24.0	37.2	40.3	23.4	6.9	8.1	5.7	8.8	0.9	13.3	7.4	25.9	26.9	37.2	33.3	18.3	0.0	0.5	NaN	0.1	3.2	11.6	1.7	19.3	4.7	8.5	8.4	25.0	29.5

The results shown in Table 7.1 are indicating the power production of the wind farm in MW. The cases in which the power is reported to be equal to 0 represent those particular conditions of wind speed and direction that never occurred during the 6 months considered for the creation of the empirical power model. The data with wind speed $\geq 14m/s$ has been collected all in one single bin because in the vast majority of the directions all the turbines should be working at or close to the nominal wind speed. Also, given the short period of time available to be used it was thought that using a higher number of velocity bins would only have created additional empty slots.

In addition to these results, the standard deviation σ relative to each wind condition has also been estimated. The results relative to σ are reported in Table 7.2, where the standard deviation is reported in MW. In this case, the boxes indicating a 0 are the ones in which the data reported in Table 7.1 was the average of a single number and therefore the number itself. On the other hand, the ones displaying NaN identify the wind conditions that never happened in the time interval analysed. By comparing the global power output and the relative standard deviation it can be noted how in some cases the value of σ is extremely elevated (sometimes even more than the power output itself).

To better analyse this aspect, σ was divided by the power output to which it refers in order to find the coefficient of variation. The outcome of these calculations is shown in Table 7.3. The value of the coefficient of variation seems to be higher for lower power outputs, while for higher values it is not as high and actually acceptable. Another way to study the variability of the power production depending on the wind conditions is to check the value of the greatest difference between the average condition (the one indicated in Table 7.1) and any of the power measurements for that wind speed and that direction. These differences are exposed in Table 7.4, where again the values are reported in MW. It can be seen how the difference increases almost constantly with the wind speed, but if compared to the average value the lower velocities have a higher relative value. These last three tables are used to highlight once again the strong variability of the wind within a limited amount of time, like 10 minutes.

7.2 Results of the Predictions

Since this model does not allow to make any comparison relative to the wind field, the only possibility to check its validity is through the prediction of the remaining 3 months. When making the predictions, the model was able to recognise when the conditions used as input were some that never occurred during the training. In case of such an occurrence, the time slot was neglected because it would have been impossible to predict. The time slots here analysed are the same as in Section 5.8, while in Appendix D the prediction of the entire 3 months is reported. The error used to check the validity of the prediction is again the Mean Absolute Error (MAE), defined previously in Section 5.8 in equation (5.6).

In Figure 7.1, the results of the prediction relative to the first week of October 2016 are shown. These results do not look as good as the ones of the empirical model (Figure 5.5), especially when the power output is higher. However, the empirical power model seems to be pretty accurate at the lower power outputs. The MAE of the empirical model is lower than the one estimated for the empirical power model, and the reason is the better accuracy at high outputs. The values of the two MAEs are similar, though.

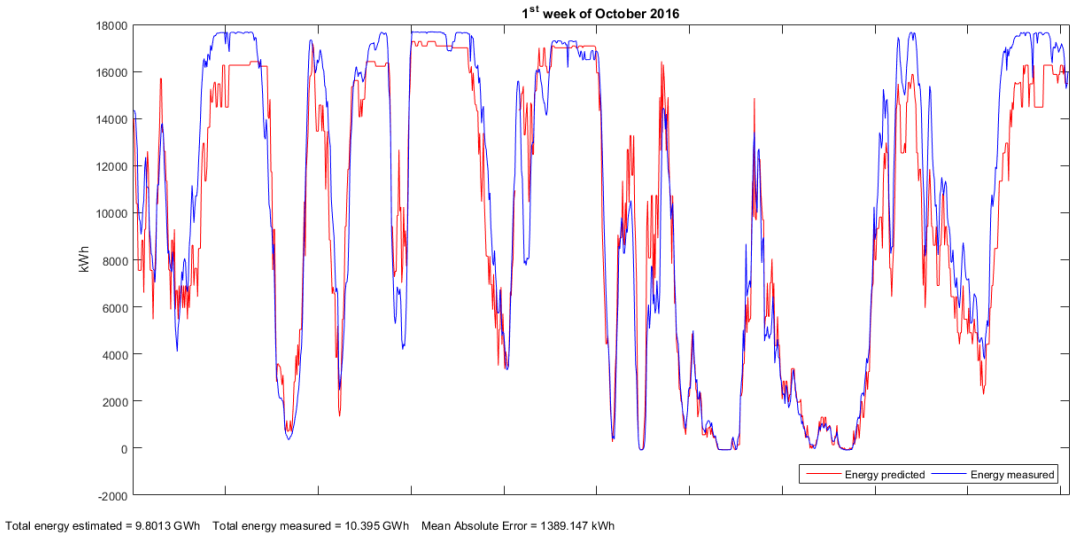

Figure 7.1: Comparison between measurements and results of the empirical power model relative to the power output during the 1^{st} week of October 2016

The comparison between the prediction and the measurements collected on $26/10/2016$ is reported in Figure 7.2. The date is the same as the one predicted in Figure 5.6 and by comparing the two it is possible to note that in this case the prediction is more accurate and the MAE is lower for the empirical power model. This happened because the power output is pretty low and, as mentioned before, in this case the empirical power model seems to perform better than the empirical one.

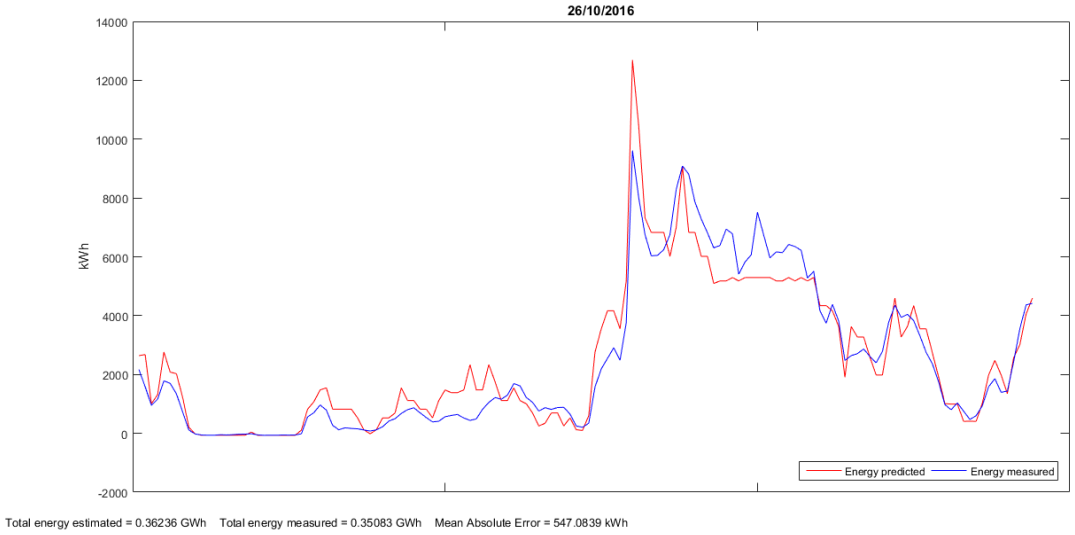

Figure 7.2: Comparison between measurements and results of the empirical power model relative to the power output on $26/10/2016$

In Figure 7.3, the prediction from the empirical power model is compared with the actual data for the day $27/11/2016$. The prediction seems pretty satisfactory and better than the one obtained with the empirical model (Figure 5.7). Again, the Mean Absolute Error is lower ($804.9377kWh$ vs $1072.1154kWh$). From the comparison of the two predictions, it seems that the empirical model is better at forecasting

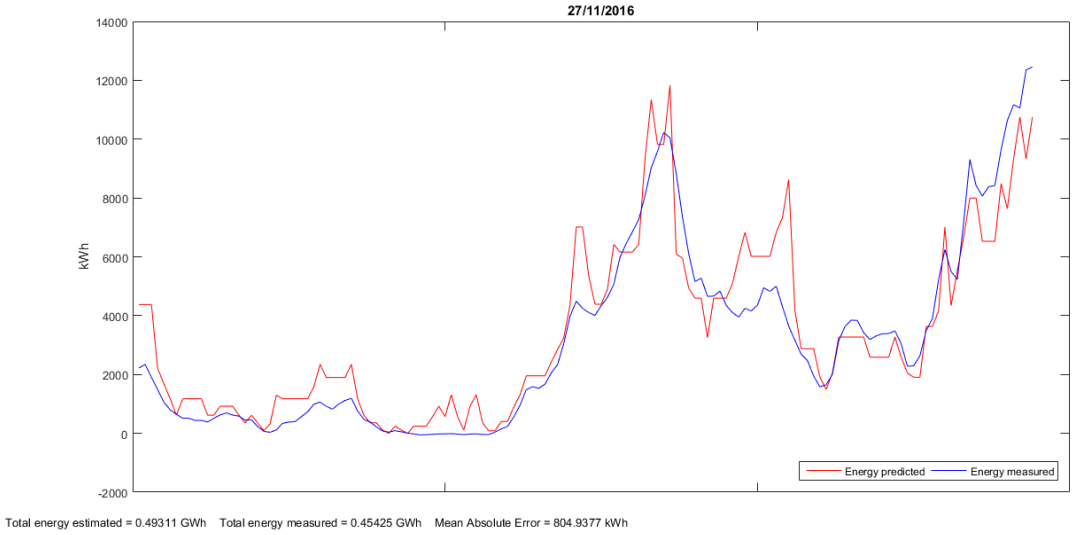

Figure 7.3: Comparison between measurements and results of the empirical power model relative to the power output on $27/11/2016$

the fluctuations. This probably happens because the empirical model actually uses the value of the maximum wind speed in the calculations, while the empirical power model uses it only to select a value within a matrix. Because of this reason, if the maximum wind speed and the wind direction do not vary much, the empirical power model might easily predict the same value as in the previous time slot. From the sole analysis of this time slot, the empirical power model model seems to be better at not overpredicting the spikes in power production.

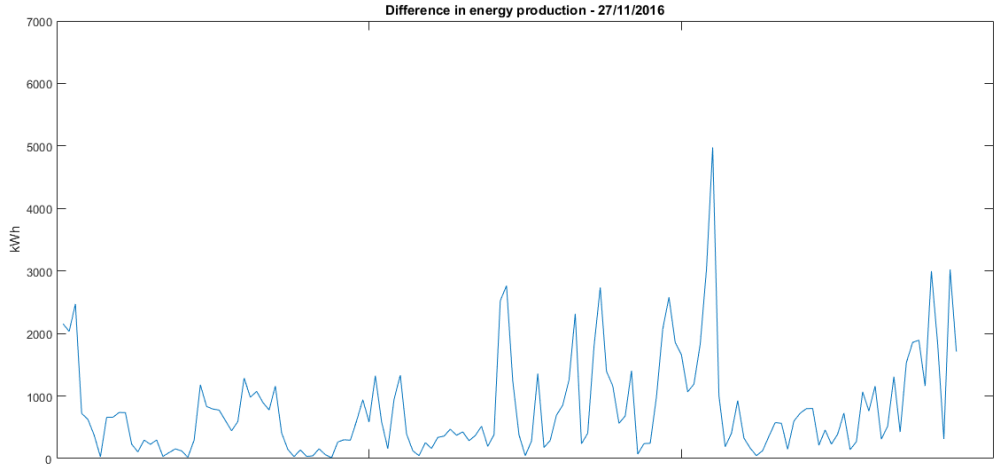

Figure 7.4: Difference between the prediction of the empirical power model and the measurements on $27/11/2016$

Like in Section 5.8, in addition to the comparisons between prediction and measurements the evolution of the absolute value of the difference between the two during one day is analysed. The day that has been chosen is the same as before ($27/11/2016$) so that it is possible to see the differences between

the two models. The comparison between Figure 7.4 and Figure 5.8 perfectly highlights the problem of the empirical model with the overprediction of spikes. The first thing that is noted is the great difference in the spike, which is significantly lower in Figure 7.4 and therefore for the empirical power model. However, the lower difference between results of the empirical power model and the measurements can be easily seen for the vast majority of the day. Nonetheless, the better performance of the empirical model during the last hours of the day $27/11/2016$, when the output increases, can be easily noted. Comparing the two graphs highlights once more how the empirical power model is better for lower outputs, while the empirical one performs better when the power produced is higher.

By comparing the global results of the empirical model and of the empirical power model (Appendix C and Appendix D, respectively) it can be seen how the MAEs of the latter are lower during all of the 3 months. Therefore it looks like the empirical power model might perform better than the empirical one. However, this might happen because of the season forecasted. Maybe, if winter months had been predicted the results of the empirical model would have been the better ones because of higher wind speeds and consequently, higher power outputs.

7.3 Possible Improvements

The possible way to improve this model are mainly the same ones as for the empirical model (Section 5.11). One of the possible improvements is to recreate this model when more data will be available. It will be possible to have an average value that better represents the actual conditions and also all the possible combinations of wind speed and direction will most probably have occurred. By having a higher amount of data available, the fluctuations typical of the seasons will not affect the results of the model in a significant way.

The other ways to improve the model and its results are relative to the variability of the wind. A way to have it to less influence the results is to include it in the model in a statistical way, perhaps based on the wind conditions of the previous time slots. The other possibility is to use shorter time intervals. In such a case, the mean wind speed would better represent the temporal evolution of the wind during the time gap and therefore, the variable and stochastic nature of the wind would affect less the final results.

7.4 Conclusions to the Chapter

In this chapter a third and final model was exposed: the empirical power model. In this model, a database of possible scenarios based on wind speed and direction was built. If a specific situation happened again, the power output would be assumed to be the same. This model can be applied in an easier way as the final result is a matrix reporting the average power output depending on the wind speed and the wind direction. Also, the standard deviation, the coefficient of variability and the highest measured difference are reported in order to highlight once again the variability of the wind and explain one of the reasons why the model did not predict the output more accurately. Afterwards, three separate time slots are predicted and analysed. The results of these predictions are compared with the outcomes of

the simulations using the empirical model and the main differences between them are highlighted. By analysing the values of the coefficients of variability and the Mean Absolute Errors it can be noted how these values could be used even when not all the turbines are operating, as the error introduced by this aspect should be significantly smaller than the one that already happens. The main differences between the models are the tendency of the empirical model at predicting spikes in the power production even though they do not happen, its better performance when the output is higher and at reproducing small fluctuations and the better forecasts by the empirical power model when the production is low. In the end, a few possible ways to improve the model are suggested. This last model, on the contrary of the others, thanks to the creation of Table 7.1 allowed to produce something that could turn out to be useful for the wind farm management team.

Chapter 8

Conclusions

The work conducted in this project included several different subjects and topics and it allowed to improve the relative skills and learn new ones. Unfortunately, the results obtained were not completely satisfactory as for the vast majority of the times they lacked consistency. Among the main topics studied in the project, the ones that led to the best outcomes are the study of the empirical and empirical power model. In some cases, they presented good results however, in others the difference between the outcomes of the models and the measurements was significant. For this reason, it can be stated that the models as they are are not good enough to precisely predict the output of the wind farm.

The creation of the physical model was the topic that obtained the poorest results. In this case, the model failed significantly in predicting the wind speed experienced by the turbines because the only aspect considered was the interception between wakes and rotors. Because of this lack of aspects considered, the deficits obtained were often underestimated or not present at all. Because of this failure, the empirical model was formulated using a completely different approach. As it has already been stated, the empirical model obtained better results compared to the ones of the physical model. Another aspect which failed to reach its goal is the creation of a set of equations that would have allowed the wind farm management team to know the output of each turbine knowing the conditions of the wind entering the wind farm. Probably, one of the main causes of this failure is the presence of too many points to reproduce with the equations. If the number of angular sectors had been lower, probably it would have been possible to find a pattern between the parametres and the direction. However, the results obtained from this set of equations would have been worse than the outcome of the model because a further step in the creation of the model had been introduced.

In an attempt to decrease the error in the results of the model, a third model directly predicting the power output based on wind speed and direction was formulated. The product of the empirical power model was a table (Table 7.1) indicating the power output in MW according to the wind velocity (which identifies the row) and direction (which indicates the column). The results of this model were better than the ones of the empirical model for low power output, but worse when the value is higher. Comparing the results of the two models in Appendix C and Appendix D, the empirical power model obtains lower MAEs in all of the 3 months.

One interesting aspect highlighted by the work exposed in this thesis is represented by the shortcomings of the Jensen model. Even though it is still widely used in the industry, it fails to predict the velocity deficit at the location of the turbines. Therefore, it is not suitable to predict the output of the wind farm if working on its own without considering further phenomena. If included in a wider model incorporating several other aspects it might work, but not as used in this project. However, another reason why the Jensen model failed might be the layout of the wind farm. In fact, usually the wake models work better in case of a regular layout.

A small achievement of the project is the one of having identified the wind turbines that fail to collect correct measurements and the main aspect where they fail at. Fixing the anemometers present on those turbines would allow to have a bigger and more reliable set of data for possible future work. Also, if these measurements are currently used in any way, being able to correct possible errors might translate into more stable operating conditions.

In spite of the partial lack of results in the main topics exposed in the thesis, there is still a good potential to find a proper model to predict the output of the wind farm with a higher accuracy. As exposed previously, the approach that seems to be the best one in the case of this wind farm is the statistical one using empirical data from the turbines themselves. Using some additional aspects typical of statistics, it would be possible to have the results of the models exposed in Chapter 5 and Chapter 7 vary depending on some of the conditions in the previous time slots. Also, it could be possible to include other inputs to the model in order to make it more precise. However, this possibility would add complexity to the model and maybe to the creation of the set of equations or of the table as well.

The use of a set of equations to predict the output instead of a power curve for the whole wind farm might seem an improvement as it allows not to consider the wind turbines that at the moment are not working for different reasons. However, analysing the table obtained from the empirical power model, it was noted that the variability of and the error in the results are higher than the ones that would be added by not considering a turbine. Consequently, the results obtained for all the turbines might be used also to predict the output when a single turbine is not working. Related to this fact, it is important to add that being the models based on predictions, which will never be absolutely precise, the error will always be present and it will not be possible to avoid it.

Bibliography

[1] N. O. Jensen. A note on wind generator interaction. Technical report, Risø National Laboratory for Sustainable Energy, Technical University of Denmark, 1983.

[2] I. Katic, J. Højstrup, and N. O. Jensen. A simple model for cluster efficiency. *European Wind Energy Association and Exhibition*, 1986.

[3] L. Parada, C. Herrera, P. Flores, and V. Parada. Wind farm layout optimization using a gaussian-based wake model. *Renewable Energy*, 2017.

[4] A. Peña, P. E. Réthoré, and M. P. V. D. Laan. On the application of the jensen wake model using a turbulence-dependent wake decay coefficient: The sebierum case. *Wind Energy*, 2016.

[5] N. G. Nygaard. Wakes in very large wind farms and the effect of neighbouring wind farms. *Journal of Physics: Conference Series*, 2014.

[6] L. J. Vermeer, J. N. Sørensen, and A. Crespo. Wind turbine wake aerodynamics. *Progress in Aerospace Sciences*, 2003.

[7] M. L. Thøgersen, T. Sørensen, P. Nielsen, A. Grötzner, and S. Chun. Introduction to wind turbine wake modelling and wake generated turbulence. *EMD International A/S*, 2005.

[8] J. F. Ainslie. Calculating the flowfield in the wake of wind turbines. *Journal of Wind Engineering and Industrial Aerodynamics*, 1988.

[9] D. R. VanLuvanee. Investigation of observed and modeled wake effects at horns rev using windpro. Master's thesis, Denmarks Tekniske Universitet, 2006.

[10] G. C. Larsen. A simple wake calculation procedure. Technical report, Risø National Laboratory for Sustainable Energy, Technical University of Denmark, 1988.

[11] G. Larsen, J. Højstrup, and H. A. Madsen. Wind field in wakes. *European Wind Energy Conference and Exhibition*, 1996.

[12] G. C. Larsen. A simple stationary semi-analytical wake model. Technical report, Risø National Laboratory for Sustainable Energy, Technical University of Denmark, 2009.

[13] S. Frandsen, R. Barthelmie, S. Pyror, O. Rathmann, S. Larsen, J. Højstrup, and M. Thøgersen. Analytical modelling of wind speed deficit in large offshore wind farms. *Wind Energy*, 2006.

[14] D. J. Renkema. Validation of wind turbine wake models. Master's thesis, Delft University of Technology, 2007.

[15] M. Bastankhah and F. Porté-Agel. A new analytical model for wind-turbine wakes. *Renewable Energy*, 2014.

[16] B. Lange, H. P. Waldl, A. G. Guerrero, D. Heinemann, and R. J. Barthelmie. Modelling of offshore wind turbine wakes with the wind farm program flap. *Wind Energy*, 2003.

[17] E. Machefaux, G. C. Larsen, and J. P. M. Leon. Engineering models for merging wakes in wind farm optimization applications. *Journal of Physics: Conference Series*, 2015.

[18] K. Gunn, C. Stock-Williams, M. Burke, R. Willden, C. Vogel, W. Hunter, T. Stallard, N. Robinson, and S. R. Schmidt. Limitations to the validity of single wake superposition in wind farm yield assessment. *Journal of Physics: Conference Series*, 2016.

[19] M. Samorani. The wind farm layout optimization problem. *PowerLeeds School of Business*, 2010.

[20] G. C. Larsen, H. A. Madsen, F. Bingöl, J. Mann, S. Ott, J. N. Sørensen, V. Okulov, N. Troldborg, M. Nielsen, K. Thomsen, T. J. Larsen, and R. Mikkelsen. Dynamic wake meandering modeling. Technical report, Risø National Laboratory for Sustainable Energy, Technical University of Denmark, 2007.

[21] G. C. Larsen. From solitary wakes to wind farm wind fields a simple engineering approach. Technical report, Risø National Laboratory for Sustainable Energy, Technical University of Denmark, 2009.

[22] W.-Y. Chang. A literature review of wind forecasting methods. *Journal of Power and Energy Engineering*, 2014.

[23] M. Milligan, M. Schwartz, and Y. Wan. Statistical wind power forecasting models: results for u.s. wind farms. Technical report, National Wind Technology Center, National Renewable Energy Laboratory, 2003.

[24] S. S. Soman, H. Zareipour, O. Malik, and P. Mandal. A review of wind power and wind speed forecasting methods with different time horizons. *Proceedings of the 2010 North American Power Symposium*, 2010.

[25] Y. K. Wu and J. S. Hon. A literature review of wind forecasting technology in the world. *Proceedings of the IEEE Conference of Power Tech*, 2007.

[26] L. Ma, S. Y. Luan, C. W. Jiang, H. L. Liu, and Y. Zhang. Review on the forecasting of wind speed and generated power. *Renewable and Sustainable Energy Review*, 2009.

[27] J. W. Taylor, P. E. McSharry, and R. Buizza. Wind power density forecasting using ensemble predictions and time series models. *IEEE Transactions on Energy Conversion*, 2009.

[28] M. C. Alexiadis, P. S. Dokopoulos, H. S. Sahsamanoglou, and I. M. Manousaridis. Short-term forecasting of wind speed and related electrical power. *Solar Energy*, 1998.

[29] A. M. Foley, P. G. Leahy, A. Marvuglia, and E. J. McKeogh. Current methods and advances in forecasting of wind power generation. *Renewable Energy*, 2012.

[30] P. Milan, M. Wächter, and J. Peinke. Stochastic modeling and performance monitoring of wind power production. *Journal of Renewable and Sustainable Energy*, 2014.

[31] N. J. Cutler, H. R. Outhred, and I. F. MacGill. Using nacelle-based wind speed observations to improve power curve modeling for wind power forecasting. *Wind Energy*, 2012.

[32] A. Llombart, S. J. Watson, D. Llombart, and J. M. Fandos. Power curve characterization i: improving the bin method. *Proceedings of the International Conference of Renewable Energies and Power Quality (ICREPQ),*, 2005.

[33] D. Cabezon, I. Marti, J. S. Isidro, and I. Perez. Comparison of methods for power curve modelling. *Proceedings of Global Windpower*, 2004.

[34] https://uk.mathworks.com, .

[35] S. J. Andersen, J. N. Sørensen, S. Ivanell, and R. F. Mikkelsen. Comparison of engineering wake models with cfd simulations. *Journal of Physics: Conference Series*, 2014.

[36] A. Peña and O. Rathmann. Atmospheric stability-dependent infinite wind-farm models and the wake-decay coefficient. *Wind Energy*, 2013.

[37] G. Mosetti, C. Poloni, and B. Diviacco. Optimization of wind turbine positioning in large windfarms by means of a genetic algorithm. *Journal of Wind Engineering and Industrial Aerodynamics*, 1994.

[38] T. Ishihara, A. Yamaguchi, and Y. Fujino. Development of a new wake model based on a wind tunnel experiment. *Global Wind Power*, 2004.

[39] A. Mittal, L. Taylor, K. Sreenivas, and A. Arabshahi. Investigation of two analytical wake models using data from wind farms. *Volume 6: Fluids and Thermal Systems; Advances for Process Industries, Parts A and B*, 2011.

[40] E. Politis, J. Prospathopoulos, D. Cabezon, K. S. Hansen, P. K. Chaviaropoulos, and R. J. Barthelmie. Modeling wake effects in large wind farms in complex terrain: the problem, the methods and the issues. *Wind Energy*, 2012.

[41] L. Tian, W. Zhu, W. Shen, Y. Song, and N. Zhao. Prediction of multi-wake problems using an improved jensen wake model. *Renewable Energy*, 2017.

[42] M. Gaumond, P. E. Réthoré, A. Bechmann, S. Ott, G. C. Larsen, A. Peña, and K. S. Hansen. Benchmarking of wind turbine wake models in large offshore wind farms. *The Science of Making Torque from Wind Conference*, 2012.

[43] http://fitteia.ist.utl.pt/.

[44] https://systatsoftware.com/.

[45] https://www.curveexpert.net.

[46] https://uk.mathworks.com/matlabcentral/fileexchange/38043-five-parameters-logistic-regression-there-and-back-again?requesteddomain=www.mathworks.com, .

[47] L. Tian, W. Zhu, W. Shen, N. Zhong, and Z. Shen. Development and validation of a new two-dimensional wake model for wind turbine wakes. *Journal of Wind Engineering and Industrial Aerodynamics*, 2015.

Appendix A

Finding of the Point T

Figure A.1 is the general case of Figure 3.5 and it can help in understanding the calculations. In this case the two turbines do not experience wind blowing from the same direction and therefore, the rotors are not parallel.

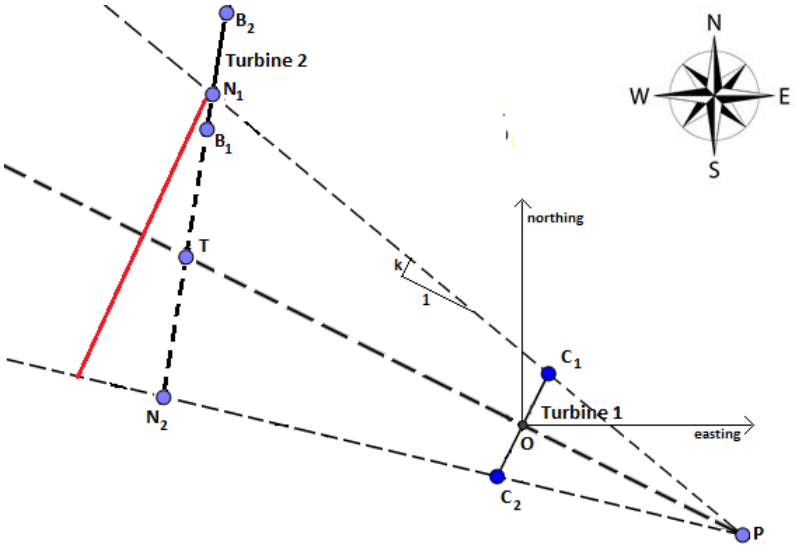

Figure A.1: Graphical simplification of the general case of interception between wake and rotor

Point T is found as the interception between the line of the rotor of Turbine 2 and the line indicating the wind direction. The angular coefficient m_x is used to indicate the direction of the wind at the turbine x, which therefore in this case in equal to either 1 or 2. The coordinates x_2 and y_2 indicate the location of the nacelle of turbine 2 in the $2D$ coordinate system centred at the hub of turbine 1.

$$\begin{cases} y - y_2 = -\frac{1}{m_2}(x - x_2) \\ y = m_1 \cdot x \end{cases} \tag{A.1}$$

$$-\frac{1}{m_2}(x - x_2) + y_2 = m_1 \cdot x_1 \tag{A.2}$$

$$-\frac{x}{m_2}+\frac{x_2}{m_2}+y_2=m_1\cdot x \tag{A.3}$$

$$x\left(m_1+\frac{1}{m_2}\right)=\frac{x_2}{m_2}+y_2 \tag{A.4}$$

$$\begin{cases} x_T=\frac{\frac{x_2}{m_2}+y_2}{m_1+\frac{1}{m_2}} \\ y_T=m_1\cdot x_T=m_1\cdot\frac{\frac{x_2}{m_2}+y_2}{m_1+\frac{1}{m_2}} \end{cases} \tag{A.5}$$

The two equations in (A.5) allow to locate point T in the coordinate system. In the case of the physical model (explained in Chapter 3) the wind blows always in the exact same direction for all the turbines and therefore there is just a single angular coefficient m. By substituting m_1 and m_2 with m, the equations in (3.2) are obtained.

The red line in Figure A.1 represent the distance at which the deficit should be calculated in case the assumption of parallel rotors is not valid anymore. A system of equations able to find the interception between the red line and the direction of the wind passing through turbine 1 would be much more complicated and tough to implement in the whole model as all the particular cases should have been taken into account.

Appendix B

2D_k Jensen Model

The traditional Jensen model has been found to have two major limitations, the top-hat profile and the constant value of the wake decay parametre. About the former aspect, it has been found that the deficit does not depend only on the downwind distance (it is therefore not a $1D$ model), but also on the crosswind one. Along this direction, the velocity deficit varies following a Gaussian or trigonometric distribution. On the other hand, the latter issue is raised because the wake decay coefficient k should be related to the overall turbulence (dependent on the roughness length), which is equal to the sum of both the ambient and turbine-added turbulences.

The 2D_k Jensen model [47] is implemented in two different steps. Initially, the speed deficit is estimated using the original Jensen model and then its value is corrected depending on the crosswind distance from the centreline. In order to do so, the value of the wake decay coefficient has to be previously estimated using equation (B.1):

$$k = k_0 \frac{\varepsilon_{wake}}{\varepsilon_0} \tag{B.1}$$

where ε_0 is the ambient turbulence, ε_{wake} is the effective turbulence and k_0 is the constant value of the wake decay coefficient, 0.04 for offshore sites and 0.075 for onshore ones [4]. Since the effective turbulence is greater than the ambient one, the resulting wake is wider and characterised by a faster recovery than the one obtained using the original Jensen model.

According to the most-widely used turbulence models, ε_{wake} is given by the combination of the atmospheric turbulence and the turbine-added turbulence, ε_0 and ε_{add} respectively.

$$\varepsilon_{wake} = \sqrt{\varepsilon_0^2 + \varepsilon_{add}^2} \tag{B.2}$$

The turbine-added turbulence ε_{add} is best defined according to the Larsen model [11]. The definition given in (B.3) is valid for distances greater than $2D$, which does not create problems as the 2D_k Jensen model is also valid for the far wake region.

$$\varepsilon_{add} = 0.29 \left(\frac{x}{D} \right)^{-\frac{1}{3}} \sqrt{1 - \sqrt{1 - C_T}} \tag{B.3}$$

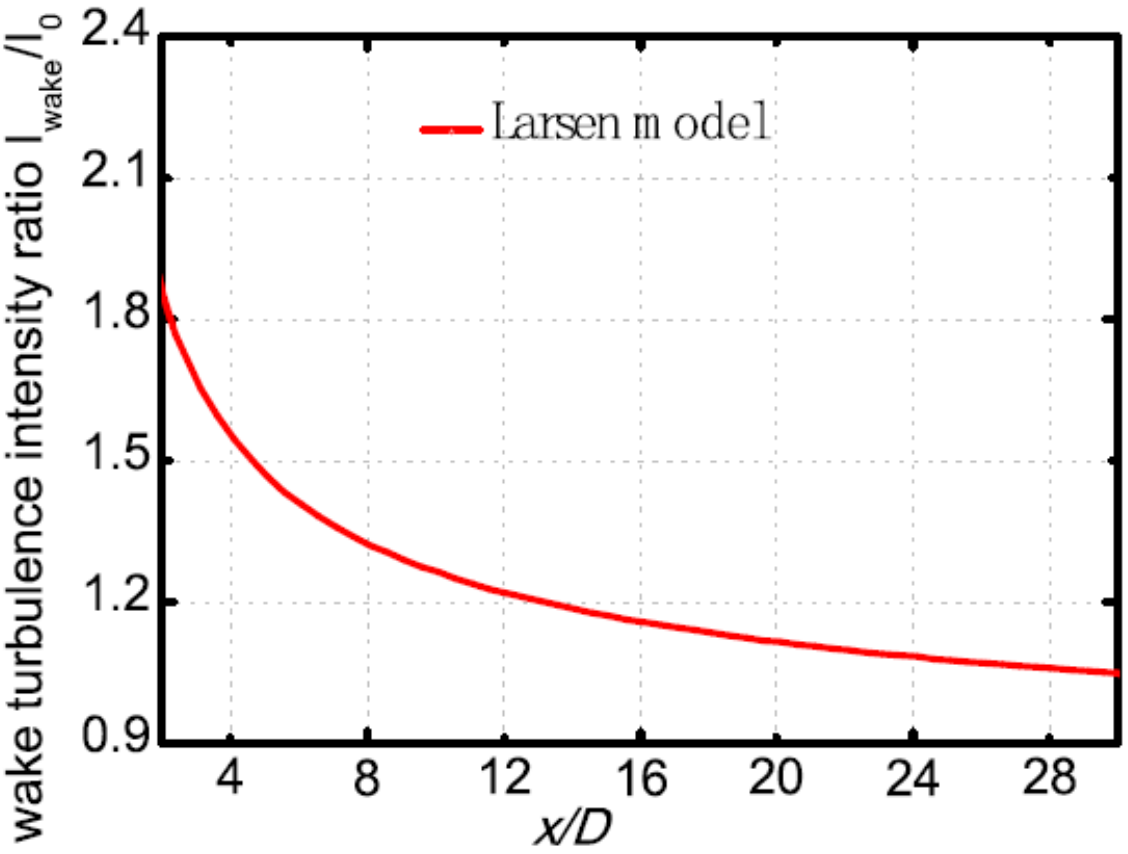

Figure B.1: Behaviour of the wake turbulence intensity ratio downstream of the rotor according to the Larsen model [41]

In Figure B.1, the ratio between ε_{wake} and ε_0 in case of an initial value for ε_0 equal to 8% and $C_T = 0.78$ is shown. From Figure B.1 it can be noted how for the first several diameters of downstream distance the turbine-added turbulence affects the value of ε_{wake}. Towards the end it can be seen how the value of ε_0 decreases to 0 and consequently the effective turbulence reaches the same value of the ambient turbulence.

After having estimated the wake decay coefficient k, the wind speed according to the original Jensen model, indicated as u^*, is calculated. As a next step, the wind speed at the required location can be computed taking into account the crosswind distance from the centreline. According to the 2D_k model, the distribution along the crosswind direction follows the behaviour of a cosine. The wind velocity at the required location is found according to equation (B.4):

$$u = (U_\infty - u^*) \cdot \cos\left(\frac{\pi}{r_x} \cdot r + \pi\right) + u^*\,, \tag{B.4}$$

where r is the distance from the centreline and r_x is the radius of the wake at the downstream distance x calculated using k found with equation (B.1).

$$r_x = R + k \cdot x \tag{B.5}$$

In Figure B.2 the expansion of the wake and the behaviour of the velocity deficit behind the rotor of

the turbine is shown. The difference in results from the original Jensen model can be clearly seen by comparing Figure B.2 with Figure 2.1.

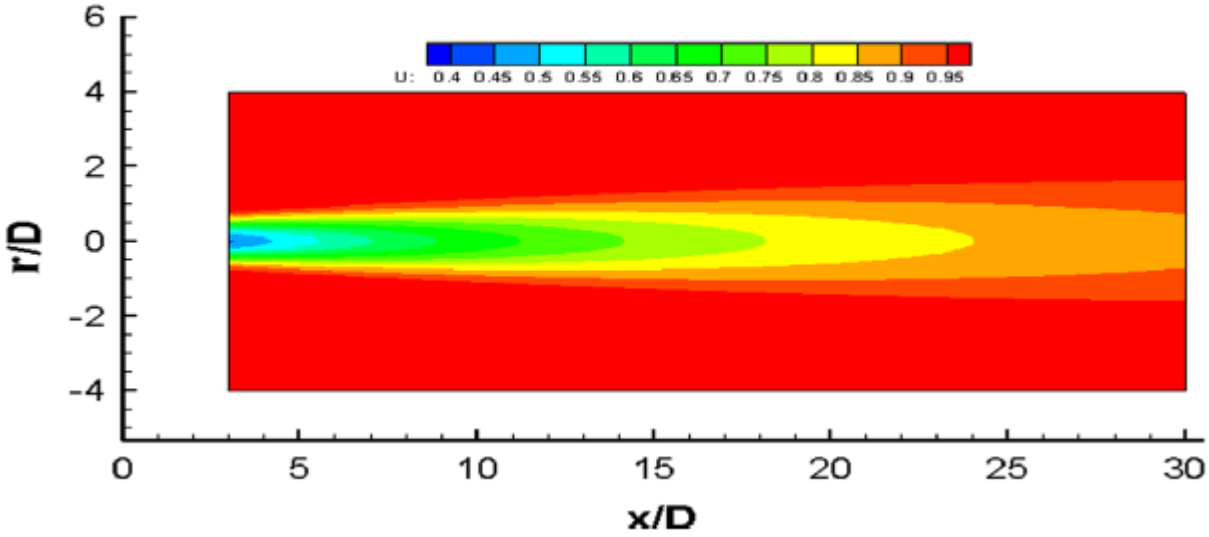

Figure B.2: Expansion of the wake behind the turbine according to the 2D_k Jensen model [47]

Appendix C

Results of the Energy Production Prediction for the Empirical Model

In this appendix, the results relative to the 3 months simulated with the empirical model and their comparisons with the measurements are shown. Also, the evolutions of the absolute value of the difference between the measurements and the results of the empirical model are exposed.

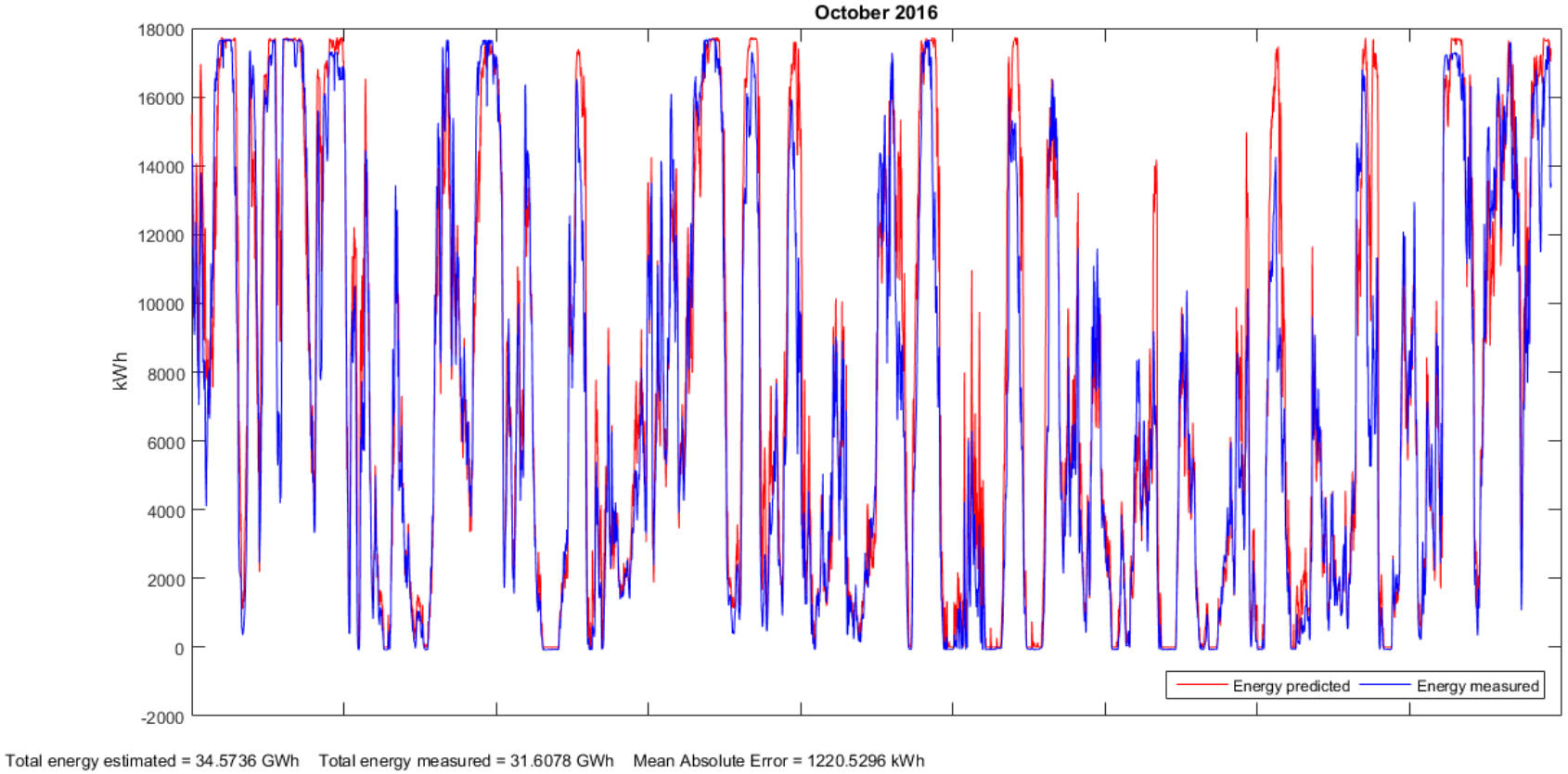

Figure C.1: Comparison between the results of the model and the measurements for October 2016 according to the empirical model

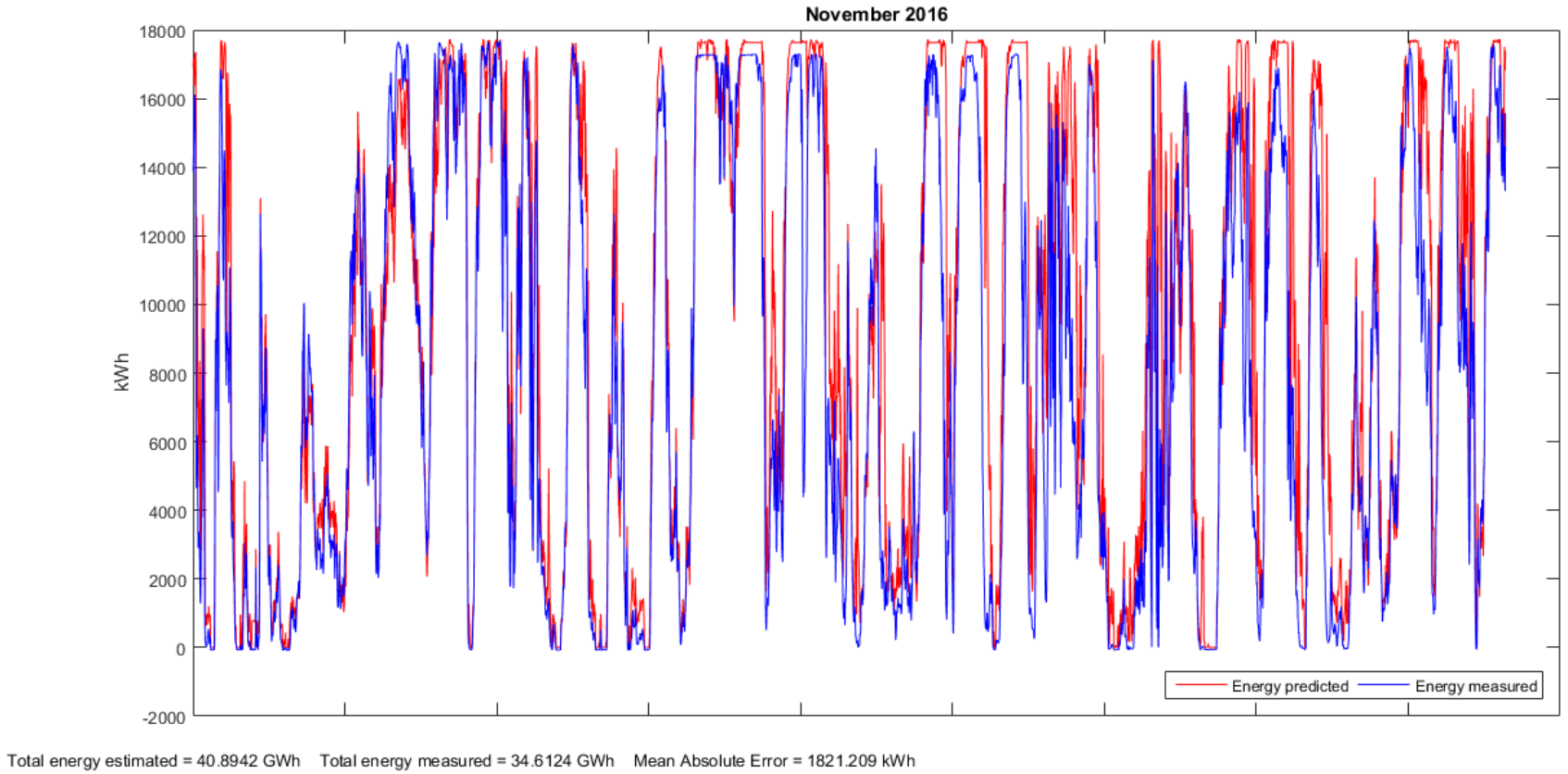

Figure C.2: Comparison between the results of the model and the measurements for November 2016 according to the empirical model

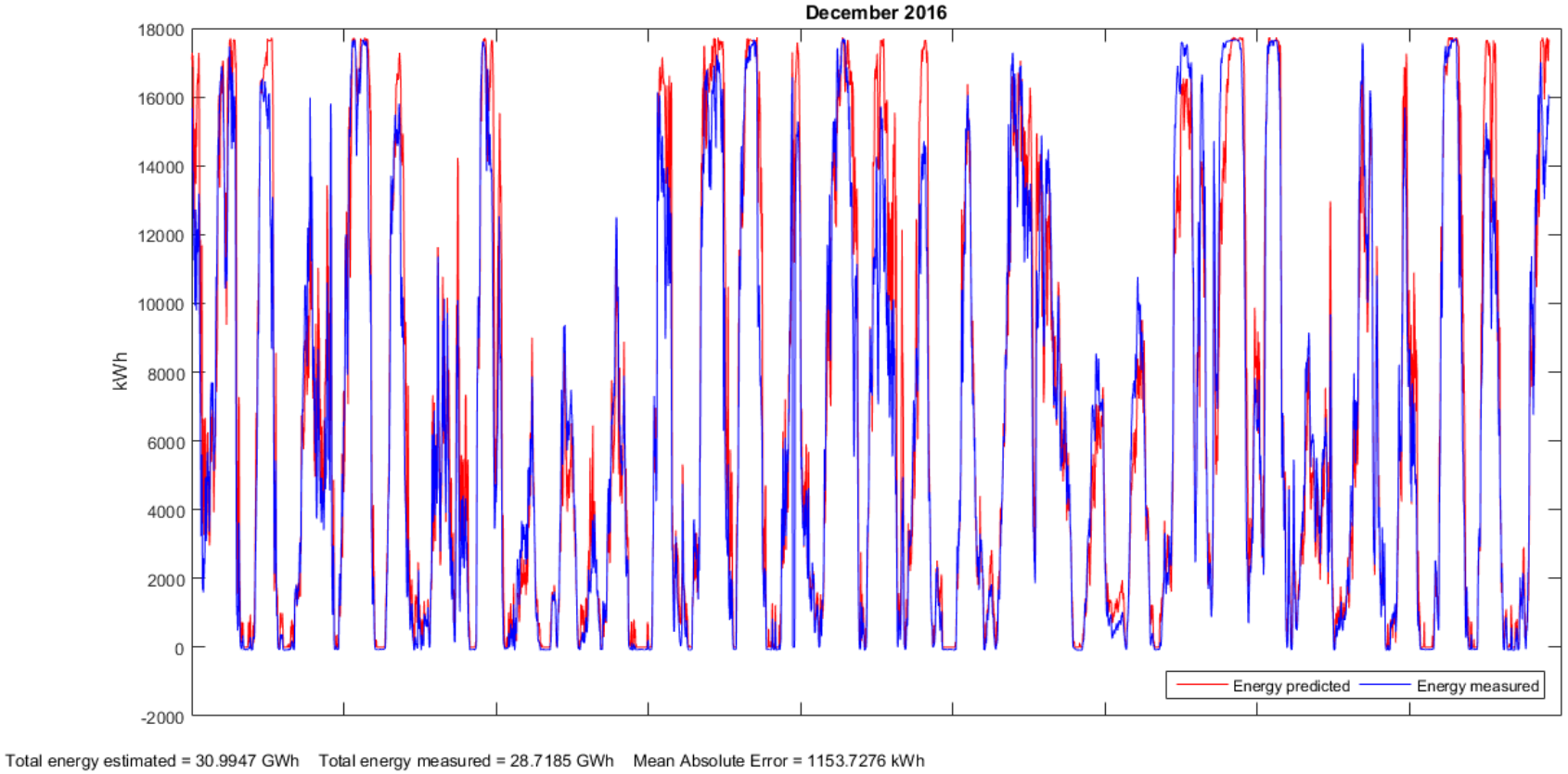

Figure C.3: Comparison between the results of the model and the measurements for December 2016 according to the empirical model

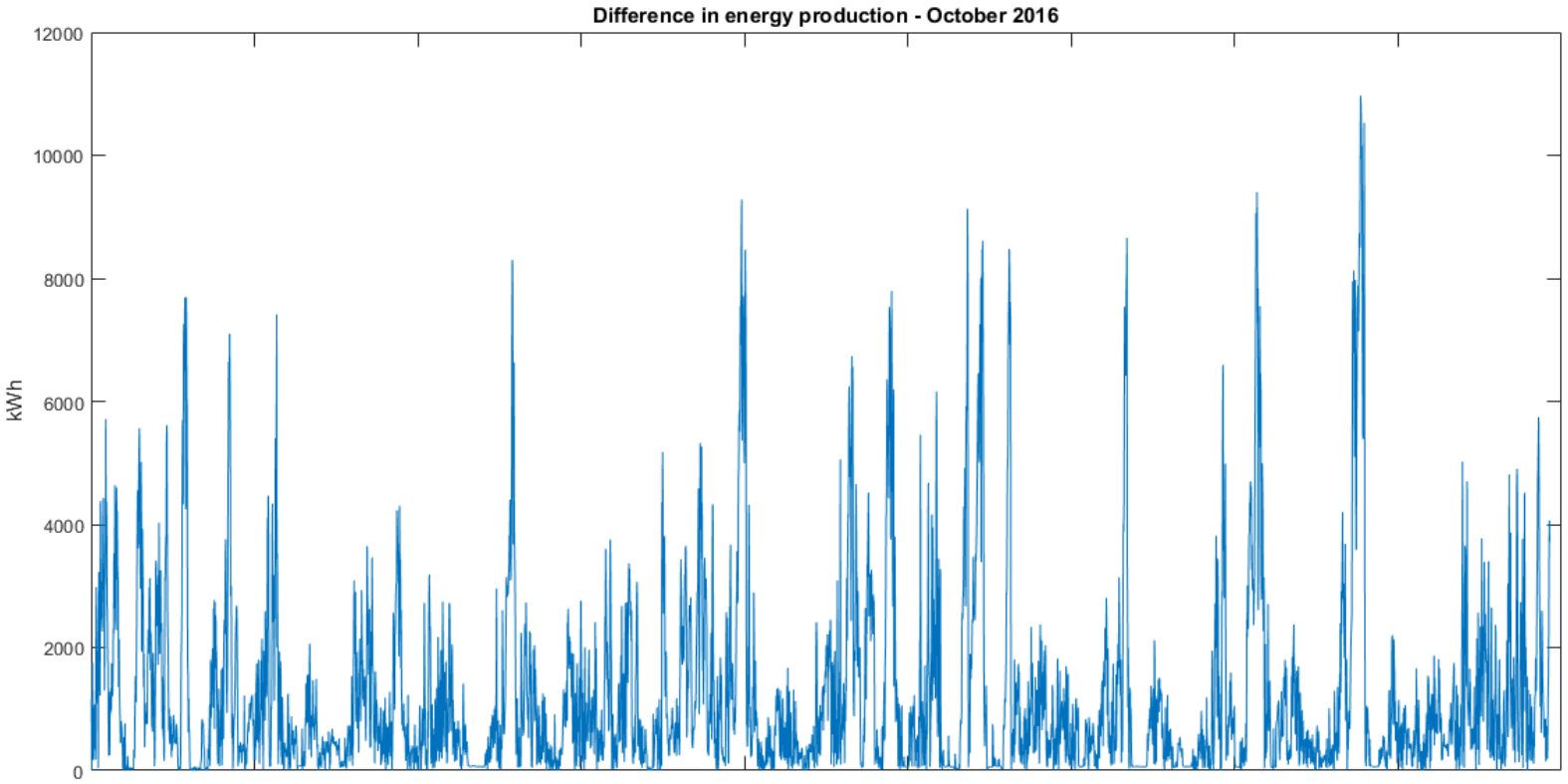

Figure C.4: Difference in absolute terms between the prediction and the measurements for October 2016 according to the empirical model

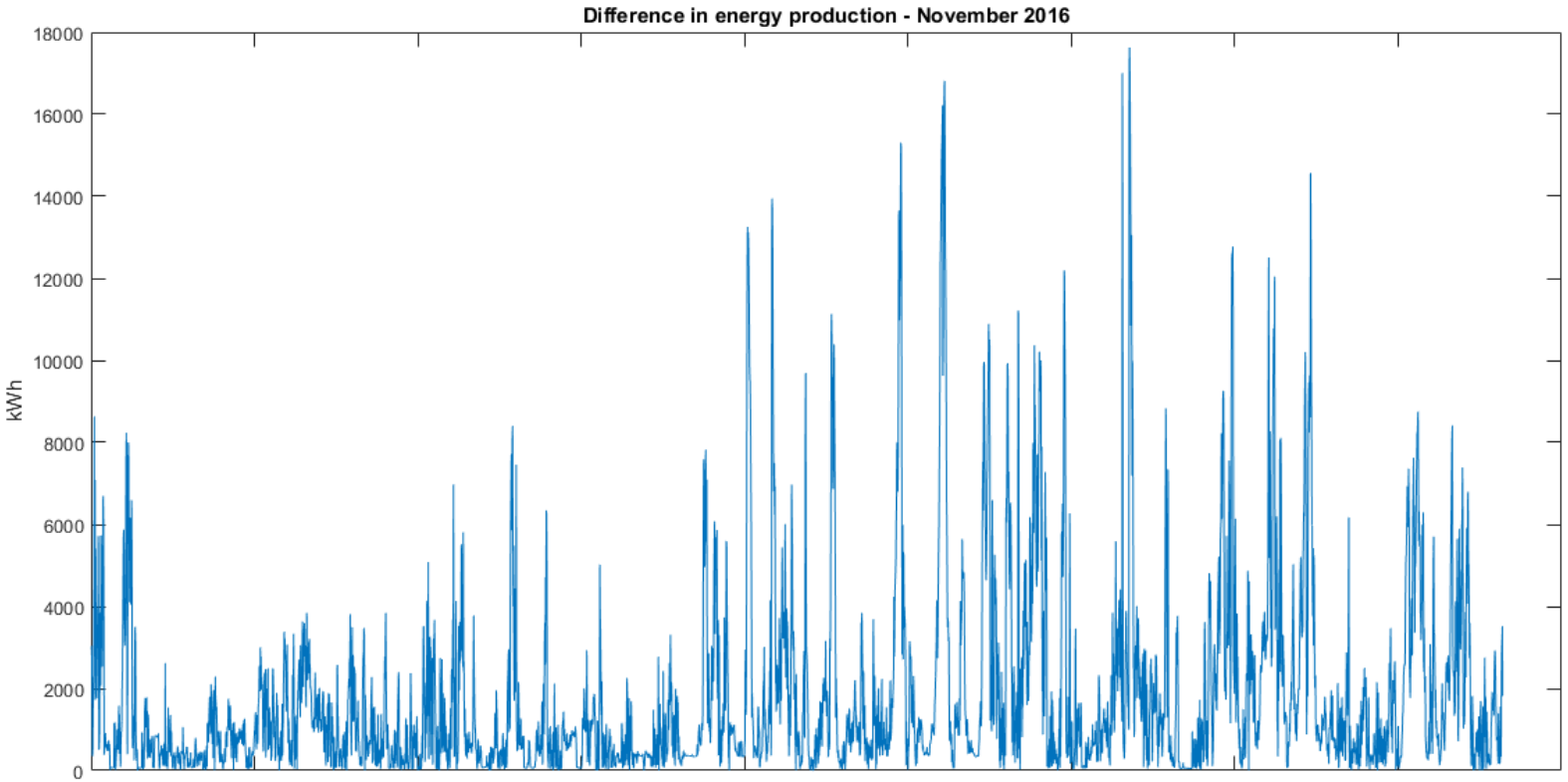

Figure C.5: Difference in absolute terms between the prediction and the measurements for November 2016 according to the empirical model

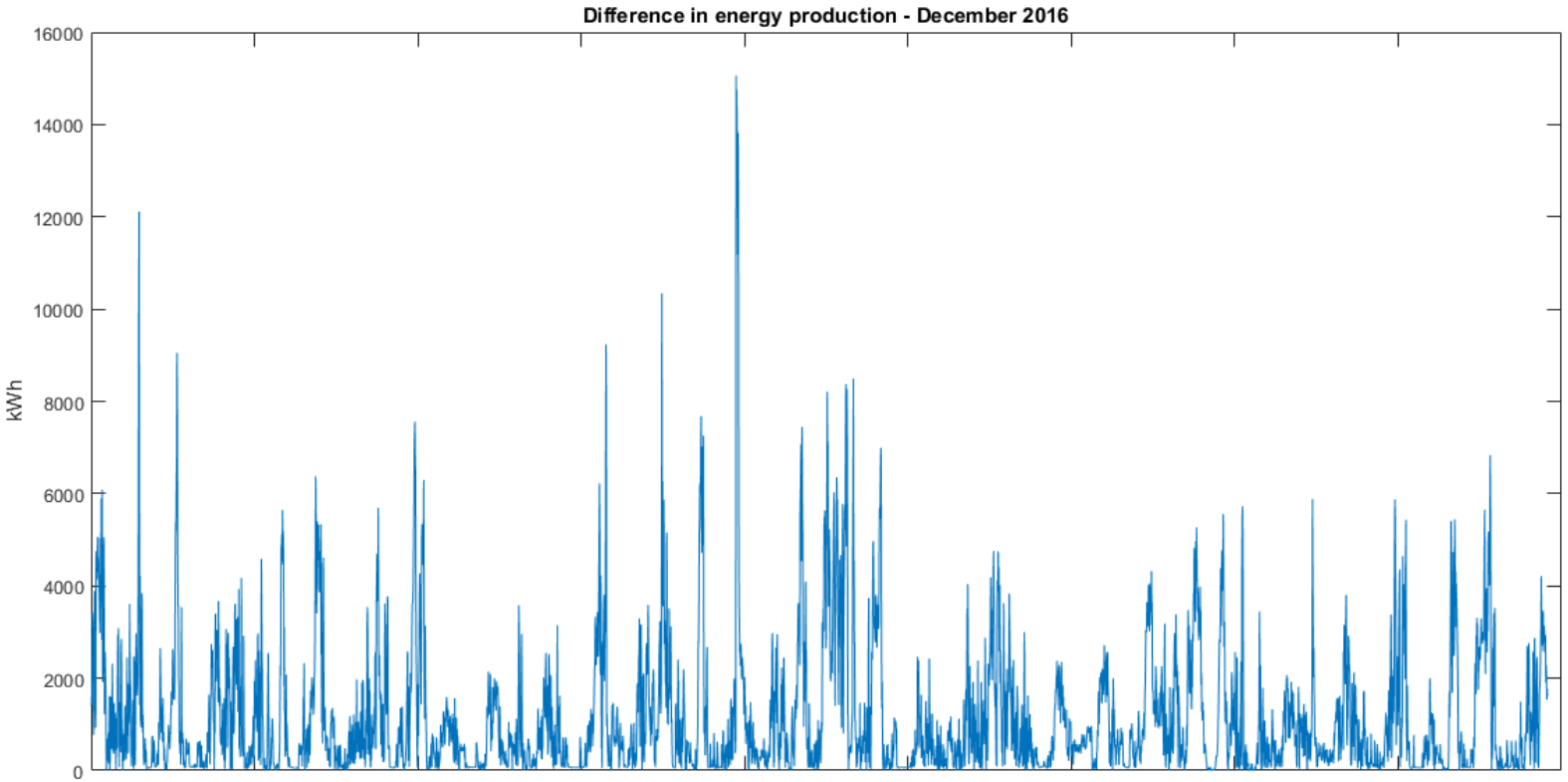

Figure C.6: Difference in absolute terms between the prediction and the measurements for December 2016 according to the empirical model

Appendix D

Results of the Energy Production Prediction for the Empirical Power Model

In this appendix, the results relative to the 3 months simulated with the empirical power model and their comparisons with the measurements are shown. In addition to this, the differences between the value predicted and the measurement throughout each month are reported

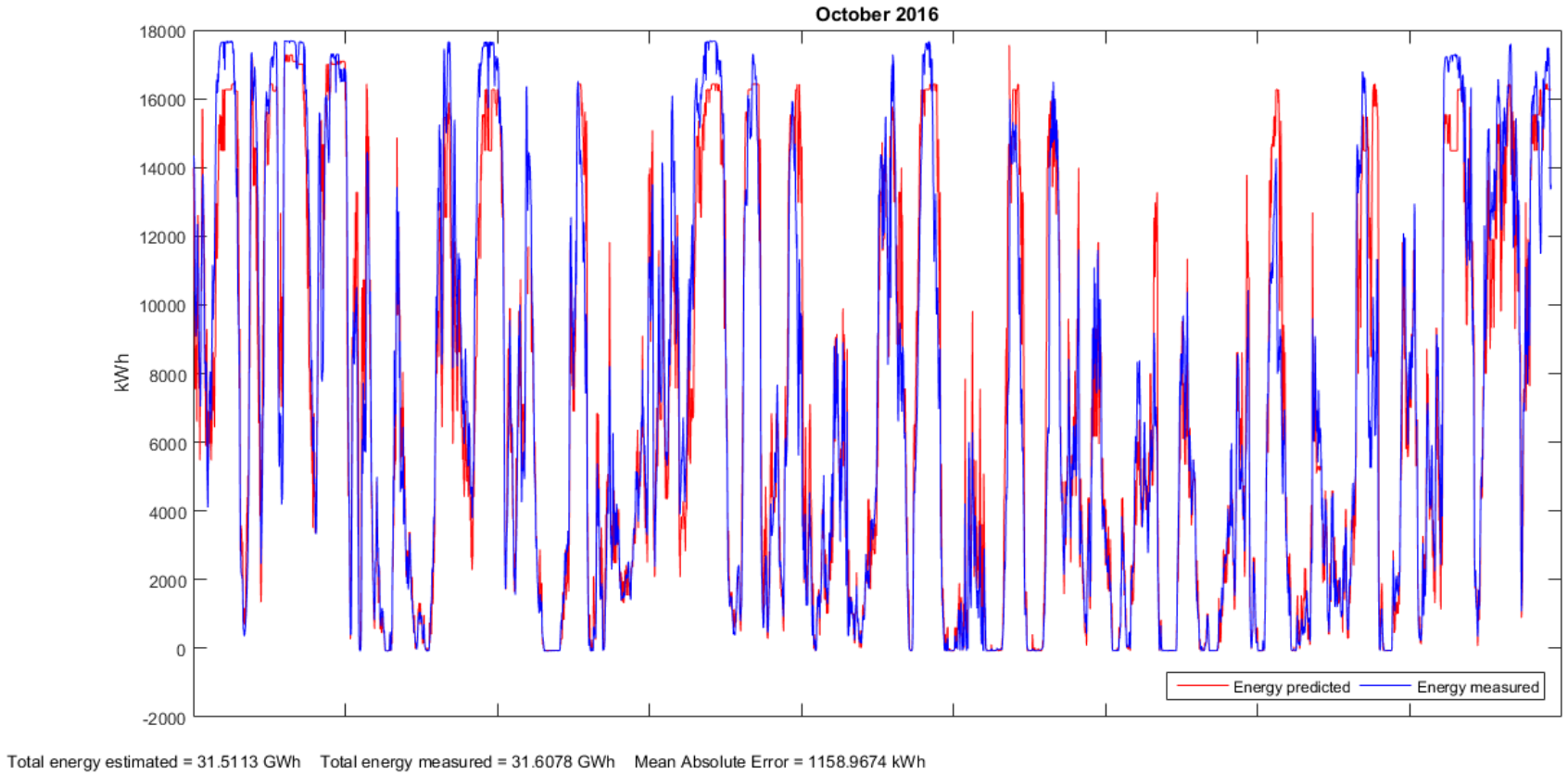

Figure D.1: Comparison between the results of the model and the measurements for October 2016 according to the empirical power model

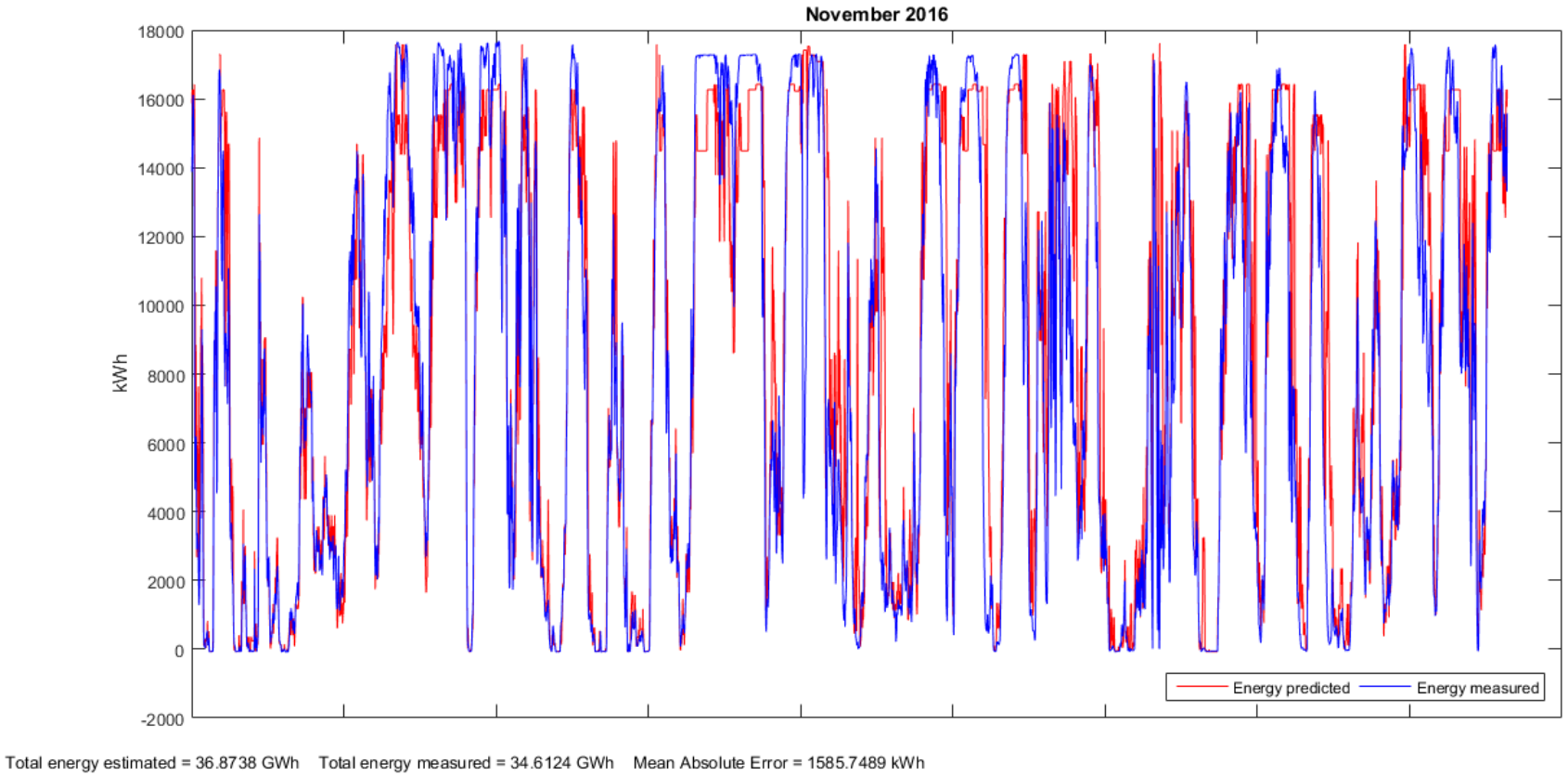

Figure D.2: Comparison between the results of the model and the measurements for November 2016 according to the empirical power model

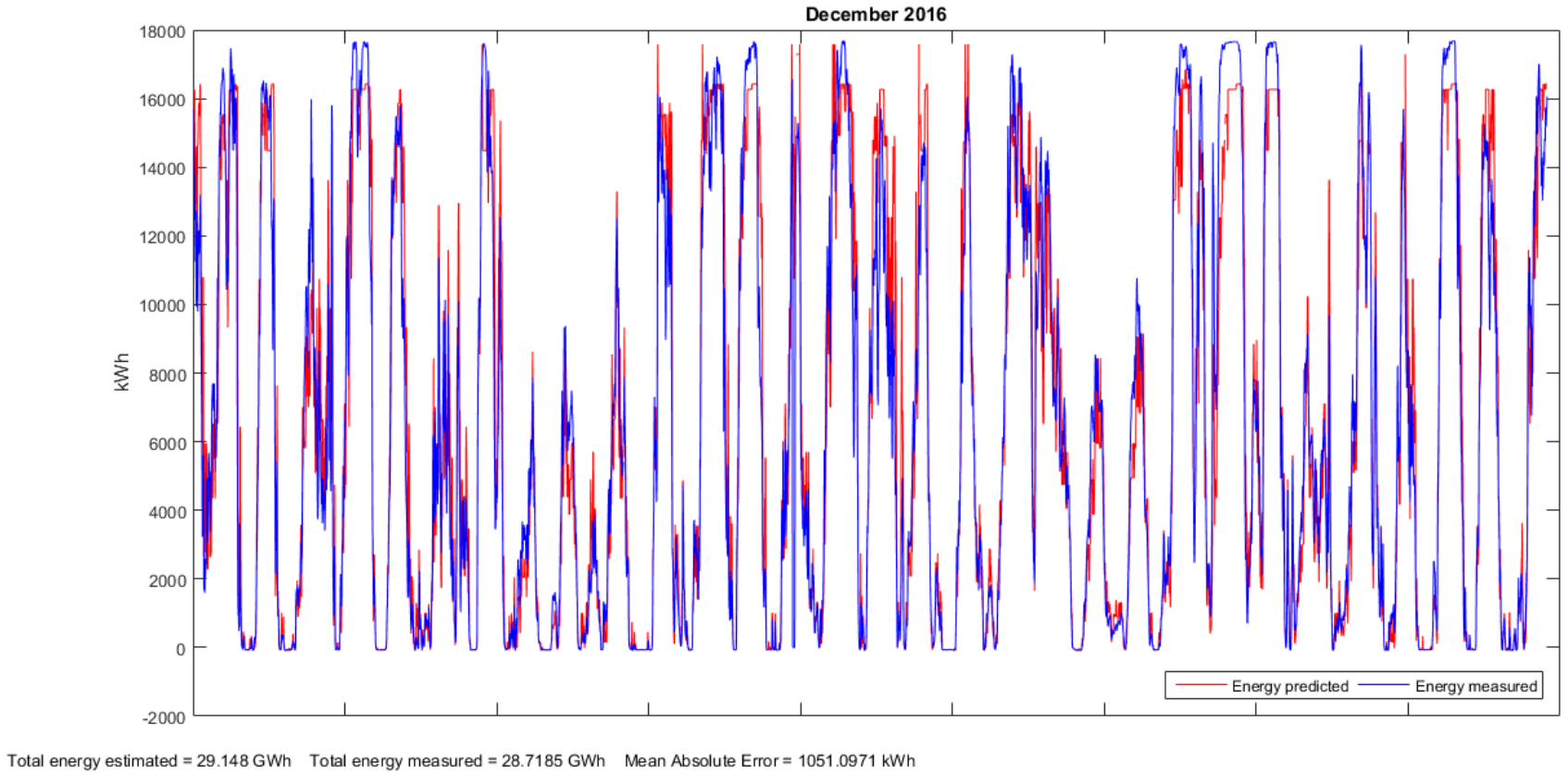

Figure D.3: Comparison between the results of the model and the measurements for December 2016 according to the empirical power model

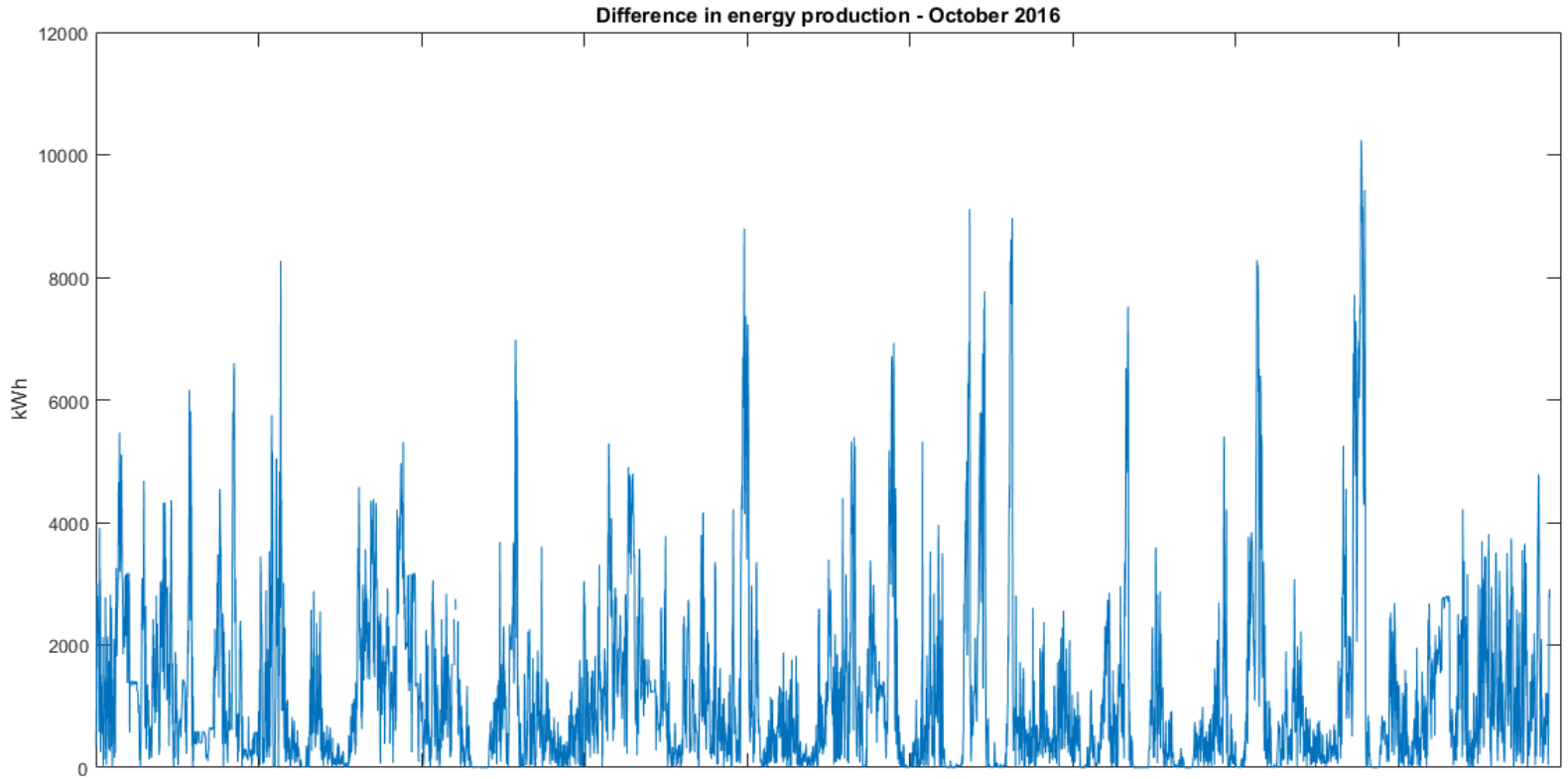

Figure D.4: Difference in absolute terms between the prediction and the measurements for October 2016 according to the empirical power model

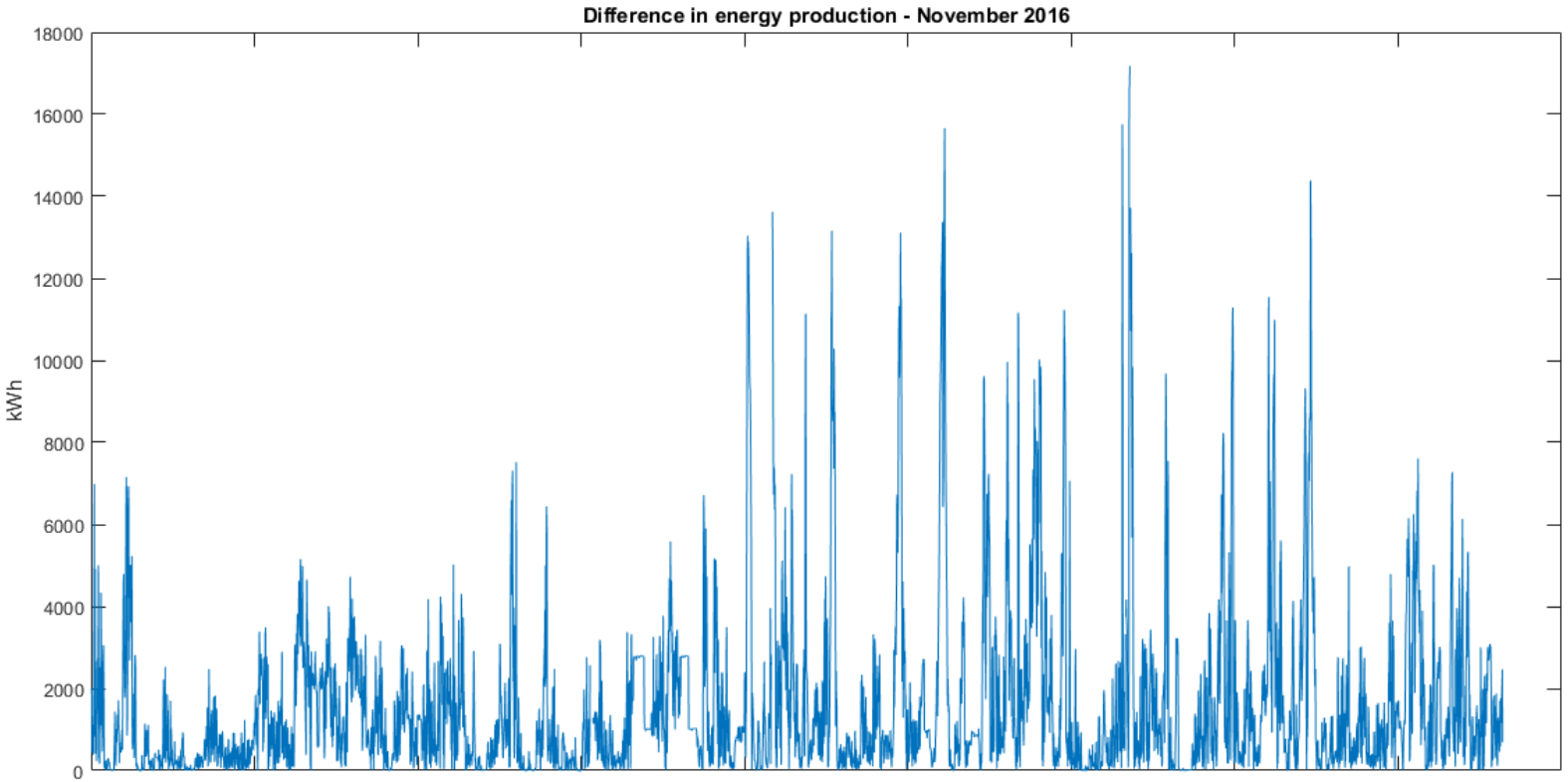

Figure D.5: Difference in absolute terms between the prediction and the measurements for November 2016 according to the empirical power model

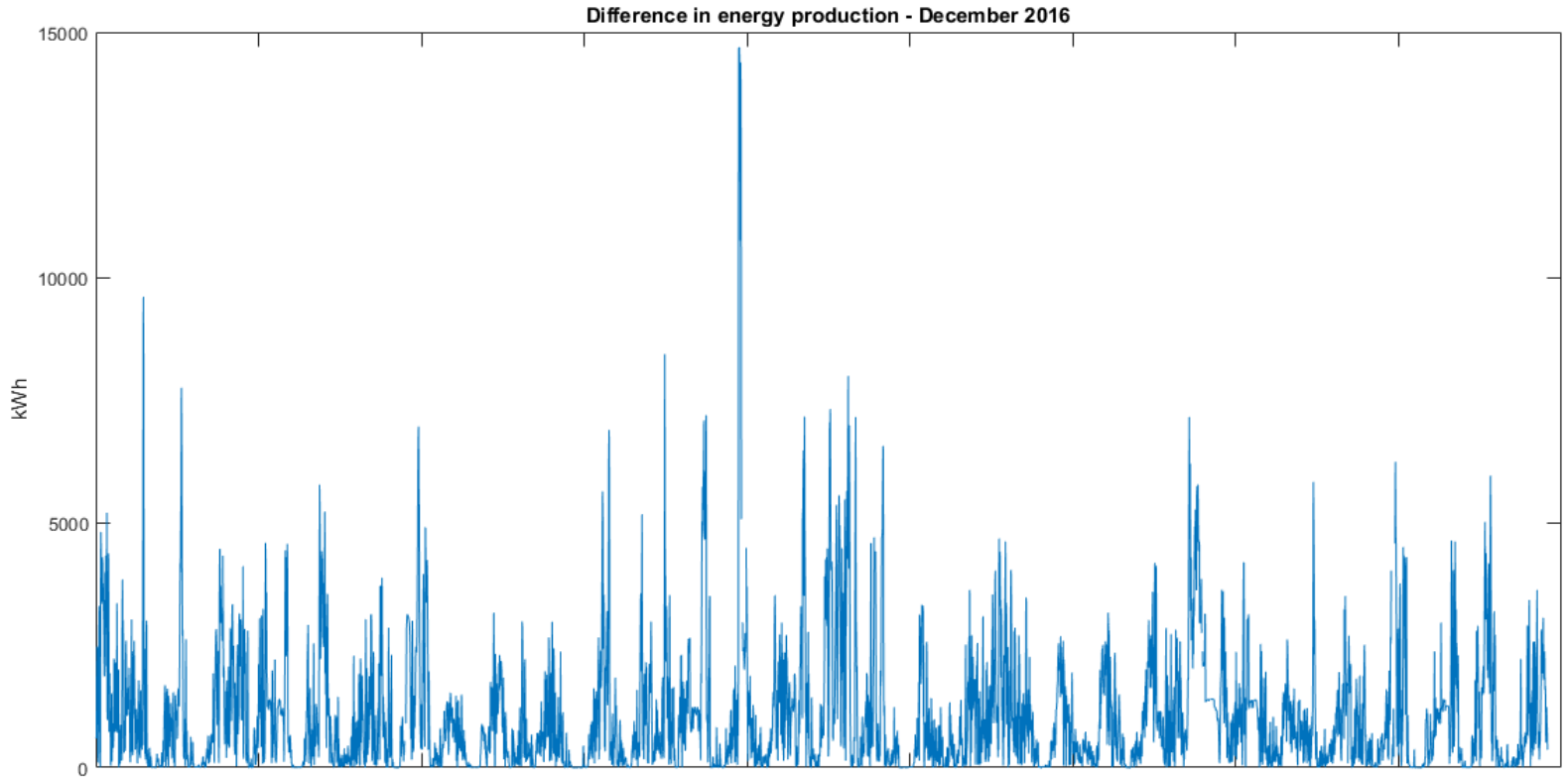

Figure D.6: Difference in absolute terms between the prediction and the measurements for December 2016 according to the empirical power model